REGULATED microRNA BIOGENESIS GENERATES SPECIFICITY IN PRO-GROWTH NEURONAL GENE EXPRESSION

By Claudia Roxana Ruiz

A dissertation submitted to the Johns Hopkins University in conformity with the requirements for the degree of Doctor of Philosophy

Baltimore, Maryland

March 2014

Abstract

Control of translation is a fundamental source of regulating gene expression. Brain-derived neurotrophic factor (BDNF) is a critical activity-dependent modulator of gene expression, which can regulate both transcription and translation. Several functions of BDNF, including the induction of dendrite outgrowth and long-term synaptic plasticity, depend upon the ability of BDNF to regulate protein synthesis. Although BDNF modestly increases total neuronal protein synthesis, substantial evidence indicates that BDNF induces translation of only a small subset of expressed mRNAs and demonstrates an extraordinary degree of transcript specificity. The mechanism by which BDNF selectively upregulates the translation of only a discrete group of mRNAs is of intrinsic importance to its trophic function in promoting neuronal growth and plasticity, but how BDNF selects only a minority of expressed mRNAs is poorly understood. My thesis work addressed this question and led to the finding that BDNF rapidly elevates Dicer, increasing mature microRNA (miRNA) levels and inducing mRNA repression. BDNF also rapidly induces Lin28, an RNA binding protein, causing selective loss of Lin28-regulated miRNAs and a corresponding upregulation in translation of their target mRNAs. Loss of Lin28, or expression of a Lin28-resistant Let-7 precursor miRNA, inhibits BDNF translation specificity and BDNF-dependent dendrite arborization.

The finding that Lin28 could be upregulated in mature neurons and was required for the specificity of BDNF-induced protein synthesis, led to the second portion of my thesis research, which investigates the molecular mechanism responsible for rapid transcription-independent induction of Lin28 by BDNF. This portion of my doctoral work demonstrated that TAR-RNA-binding protein (TRBP), a critical miRNA biogenesis

component and Dicer binding partner, is required for the induction of Lin28 by BDNF and revealed that TRBP is a novel Lin28 binding partner.

My dissertation sheds light on novel mechanisms of specificity in stimulus-dependent gene expression and offers a mechanistic understanding of how neuronal protein composition is controlled through induction of Lin28 in mature neurons. In addition, my thesis work elucidated cellular pathways underlying plasticity and established molecular links between neuronal pro-growth pathways and pluripotency, which may help us understand the dysregulated translation associated with cognitive disorders and diseases of the central nervous system.

Advisor: Mollie K. Meffert, M.D., Ph.D.

Acknowledgements

I have always said that the journey towards a Ph.D. is like a roller coaster ride. The ups and downs are both frightening and thrilling. Sometimes you want to throw your hands up in the air in pure delight and joy, while other times your stomach is in knots and you want to close your eyes and pretend you were somewhere else. Whichever the case, it is always nice to have someone sitting next to you to help you get through the ride. Luckily, countless individuals have accompanied me on this journey and helped me reach the end of this exhilarating ride.

First, this journey would not have been made possible without the unconditional love and support from my family. My parents, Silvia and Pedro, have always emphasized the importance and value of a strong education. They have encouraged me to follow my dreams wherever they may lead. My brother, Pedro, was also supportive and has shown a genuine interest in a wide range of scientific topics, which I've enjoyed discussing with him. I am grateful that my family has been able to visit me often in Baltimore and provided a continuous outpouring of support and inspiration throughout my Ph.D. training. My parents would often ask me, "So when will you be done? How is your thesis?" Finally, I can proudly say, "It's done. I did it!"

I must also express my profound gratitude for my brilliant advisor, Mollie Meffert, who gave me the opportunity to receive superior training in basic science research. Her door was literally always open and I am happy that I took full advantage of that. Starting out I had a new question every single day (often multiple times a day) and every day she would provide a careful and sophisticated answer and always do so with a smile. With her superb guidance, I have been able to tackle interesting questions and

acquire the skills necessary to make exciting discoveries. Mollie helped me believe in myself and in my scientific skills, which gave me the confidence to persevere and take on new challenges. Without a doubt Mollie has been an extraordinary role model for me, and I hope that in my career I will be able to exhibit the same level of sharp analytical skills and love for mentoring that she demonstrates everyday.

I am also grateful for the highly interactive and collaborative environment Mollie has created in the laboratory. I was fortunate to work alongside and learn from many talented scientists. For my first project in the lab I worked closely with Alvin Huang and Elizabeth Eyler. They were extremely friendly and willing to drop whatever they were doing to assist me with an experiment. My fondest memories of my Ph.D. training were the countless hours we spent discussing our data and refining our manuscript for publication. It was a magical moment when all the puzzles pieces started coming together and as a team we were able to contribute to the creation of a new body of work. I would also like to thank Matt Boersma, Anca Mihalas, and Erica Dresselhaus who have always been willing help out in any way possible and helped establish the collegial atmosphere in the lab.

As the lab grew in size I had the chance to work with several new and talented colleagues. For my second project I worked closely with Alexandra Amen and Jay Shi. Alex was one of my first rotation students and then became my lab baymate and one of my best friends. I truly admire her sharp scientific insight and careful attention to detail. With her strong work ethic and advanced technical skills she has helped move our project forward at a rapid pace. Jay Shi joined the lab as my undergraduate student and I quickly recognized the talent he had to become a highly skilled scientist. He was quick to master

any task he was given, and I have thoroughly enjoyed training him and witnessing his transformation into a superb independent scientist. I have cherished the opportunity to work with both Alex and Jay, and I will deeply miss our stimulating discussions about science, life, and everything in between.

I would like to thank another labmate, Daniel Pham, for being a constant source of positive energy and creative insight. His enthusiasm and dedication to science is apparent and contagious. He has a relentless and fiercely determined attitude, which has enabled him to establish and optimize new techniques in the lab. I am grateful for his optimistic spirit, which helps makes the lab environment a fun place to conduct science. I would like to thank Joshua Schwartz and Leonardo Hagmann for also helping make the laboratory a friendly and pleasant environment and for their helpful scientific insight. In addition I want to thank my "little sib" Megha Subramanian. Her tremendous work ethic and passionate personality has been a valuable addition to the lab. She is a highly conscientious worker with impressive analytical skills and a remarkably friendly disposition, which makes her a complete joy to be around. I would like to also thank Laurel Oldach for always having a smile on her face and possessing the power to cheer anyone up by consistently having something thoughtful and positive to say.

I would also like to thank the members of my thesis committee: David Ginty, Richard Huganir, Geraldine Seydoux, and Dwight Bergles. Their insight and valuable advice helped me to understand and appreciate what it takes to design well-controlled and informative experiments. I deeply appreciate their perspective and constructive criticisms, which have had a positive impact on my scientific training.

I would like to also thank Rita and Beth in the Neuroscience office who work incredibly hard to make sure that all of us stay on track during our Ph.D. training. They are always there to answer all our questions, and I am extremely grateful for their kindness and patience. In addition, I want to thank Brenda and Marvin who work diligently to keep our laboratory space clean and organized. Their friendly and positive personalities help brighten our day. They go above and beyond what is asked of them and I've enjoyed getting to know them and chatting with them at the end of each day. I would like to also thank former staff members Clif, Liz, and Carol for taking excellent care of our lab equipment. They performed their job efficiently and carefully and always with a smile.

Finally, I would like to thank my soon-to-be husband, Tomás Garzón-Muvdi. He has been there from the start of my Ph.D. journey and has done more than he will ever know to help me attain my goals, both scientific and personal. He was consistently there to remind me of my capabilities and really pushed me to succeed when at times I felt that it was nearly impossible. He has remained steadfast in his faith in me and has helped me become a better person by showing me the true value of hard work and sacrifice. I will be eternally grateful for his unfailing love and encouragement, as I know he will continue to drive me to succeed for the rest of our lives together.

Table of Contents

Abstract..... ii

Acknowledgements..... iv

Table of Contents..... viii

List of Figures..... xi

Chapter I: Introduction..... 1

Translational regulation and synaptic plasticity..... 1

Requirement for BDNF-regulated protein synthesis in synaptic plasticity, learning and memory..... 2

BDNF regulates the translation of a subset of neuronal mRNAs..... 3

Post-transcriptional regulatory mechanisms underlying translational specificity of BDNF..... 5

The role of miRNA biogenesis regulation in BDNF signaling..... 9

The Lin28 / Let-7 Axis in post-transcriptional control of pro-growth gene expression programs..... 10

Figures and Legends..... 15

Chapter II: Dual regulation of miRNA biogenesis generates target specificity in neurotrophin-induced protein synthesis..... 17

Background..... 17

Results..... 18

BDNF increases neuronal P-body number..... 18

Loss of GW182 prevents BDNF regulation of target protein synthesis..... 20

The role of miRNA-mediated repression in BDNF regulation of target protein synthesis…….. 21

Rapid enhancement of mature miRNA biogenesis by BDNF……. 23

BDNF confers selectivity to miRNA biogenesis through Lin28a…… 27

Loss of miRNA-mediated regulation prevents BDNF-enhanced dendrite arborization……..... 32

Discussion……. 33

Figures and Legends…… 38

Experimental Methods…… 69

Chapter III: TRBP mediates differential induction of Lin28 paralogs by neurotrophin signaling……... 81

Background……. 81

Results…….. 83

BDNF induces rapid posttranscriptional upregulation of Lin28a protein but has no effect on its paralog Lin28b…… 83

BDNF modulates TRBP phosphorylation to stabilize Lin28a…… 85

Lin28a, but not Lin28b, exists in a protein complex with TRBP and Dicer...87

Lin28a and TRBP are regulated by ubiquitin modifications……..88

Discussion…….91

Figures and Legends……93

Experimental Methods……..103

Chapter IV: Conclusions and Perspectives…….120

References…….. 125

Curriculum Vitae…….. 135

List of Figures

Figure 1.1 Model: BDNF regulation of miRNA biogenesis mediates mRNA target specificity..... 15

Figure 1.2 Lin28a blocks the processing of mature Let-7 miRNAs..... 16

Figure 2.1 BDNF increases P-body formation in soma and dendrites of hippocampal neurons..... 39

Figure 2.2 Composition of neuronal P-bodies..... 43

Figure 2.3 miRNA-mediated repression is enhanced by BDNF and associated with BDNF target specificity..... 46

Figure 2.4 Loss of P-bodies in neurons lacking either GW182 or LSm5 leaves other cellular responses to BDNF intact..... 50

Figure 2.5 The transcription inhibitor Actinomycin-D does not alter BDNF-induced protein synthesis under the assayed conditions..... 51

Figure 2.6 Control experiments supporting involvement of the miRNA pathway in BDNF-regulation of protein synthesis..... 53

Figure 2.7 BDNF increases Dicer levels and the biogenesis of mature miRNAs..55

Figure 2.8 BDNF induces Lin28, selectively diminishes Lin28-regulated miRNAs, and specifically upregulates a heterologous reporter containing Let-7 binding sites..... 58

Figure 2.9 Lin28 is required for relief of miRNA-mediated repression and selective induction of BDNF-upregulated mRNA targets..... 60

Figure 2.10 Lin28-mediated degradation of Let-7 precursors is required for induction of BDNF-upregulated targets and neuronal outgrowth..... 62

Figure 2.11 Binding sites for Lin28-regulated miRNAs (let-7, miR-143, and miR-107) in the 3'UTRs of example BDNF-upregulated targets, CaMKIIα and GluA1.64

Figure 2.12 Loss of P-bodies in neurons expressing dominant-negative form of GW182 (DNGW182) inhibits BDNF-induced dendritic arborization..... 66

Figure 2.13 Proposed model for the determination of mRNA target specificity in BDNF-mediated translation..... 68

Figure 3.1 Lin28a, but not its paralog Lin28b, is regulated by BDNF in a rapid, transcription-independent manner.....94

Figure 3.2 BDNF modulates TRBP phosphorylation to induce Lin28a..... 96

Figure 3.3 TRBP is sufficient to induce Lin28a protein and reduce Let-7 miRNAs..... 98

Figure 3.4 Dicer and TRBP can co-associate in a protein complex with Lin28a but not Lin28b..... 100

Figure 3.5 Lin28a and TRBP are rapidly turned over and subject to modification by ubiquitin.....102

Chapter I: Introduction

Translational regulation and synaptic plasticity

The complement of proteins expressed in neurons fundamentally shape brain function and are ultimately the determining factor in the enduring changes of synaptic responses that underlie learning and memory. The selective strengthening and weakening of synapses in response to neuronal activity is termed synaptic plasticity. Stimuli that generate persistent forms of synaptic plasticity critically regulate gene expression by acting at the level of transcription, translation, or both. In each case, specificity is a key feature in ensuring the correct cellular response. Elements enabling transcriptional specificity have been under investigation for many years and key components, such as transcription factors, co-activators, and chromatin modifiers have been identified. In contrast, our knowledge of general pathways enabling specificity in protein synthesis is lacking and results in failures to understand or predict the mechanisms and consequences of defects in these pathways. While dysregulated translation is known to impair cognition and is associated with disorders including Fragile X syndrome, Autism Spectrum Disorders, and Parkinson's disease (Bassell and Warren, 2008; Gehrke et al., 2010), the mechanisms by which translation selectivity is normally specified in neurons remain unclear.

BDNF is a potent regulator of synapse development, plasticity, and neuronal survival in the mammalian nervous system, which is known to mediate many of its physiological effects by regulating protein synthesis. Although BDNF leads to a general stimulation of the translational machinery, BDNF is a highly selective regulator of protein synthesis. This extraordinary degree of pro-growth target specificity is critical to

the function of BDNF in the nervous system. Our lab chose to study the post-transcriptional mechanisms enabling gene target specificity of BDNF as a model system. We set out to establish a paradigm for how specificity in stimulus-dependent neuronal protein synthesis might be controlled by investigating the molecular mechanism underlying the remarkable gene target specificity of BDNF-induced translation.

Requirement for BDNF-regulated protein synthesis in synaptic plasticity, learning and memory

The neurotrophin BDNF is widely expressed in both the developing and mature mammalian brain where it serves as a crucial regulator of neuronal survival, growth, and activity-dependent synaptic plasticity. Many of the well-known pro-growth functions of BDNF rely upon its ability to enhance the production of ensembles of proteins that support neuronal growth and excitatory synaptic function. This thesis focuses on the physiological function of BDNF-regulated protein synthesis and how BDNF achieves the gene target specificity for pro-growth mRNAs that are required for enhanced synaptic function and plasticity. Multiple lines of evidence indicate that novel protein synthesis is required for long-lasting forms of synaptic plasticity associated with learning and memory. The importance of BDNF in supporting synaptic plasticity and memory formation stems, at least in part, from its capacity to regulate protein synthesis. BDNF has been shown to increase total cellular translation by signaling through its tropomyosin-related kinase B (TrkB) receptor leading to the activation of the PLCγ, P13K, and the MAPK pathways (Huang and Reichardt, 2003).

Multiple forms of BDNF-mediated plasticity depend upon the regulation of protein synthesis by BDNF. The enhancement of dendritic arborization in response to BDNF has been shown to require the regulation of translation (Jaworski et al., 2005). Likewise, BDNF-dependent structural plasticity of dendritic spines, specifically spine head enlargement, was also shown to depend upon protein synthesis in rat brain slices (Tanaka et al., 2008). Additional protein-synthesis dependent effects of BDNF include enhanced abundance of GluA1 association with the postsynaptic plasma membrane (Caldeira et al., 2007a). BDNF also upregulates both the abundance and plasma membrane-association of NMDA receptor subunits NR1, NR2A, and NR2B in a protein synthesis-dependent manner, and this was shown to correlate with an increase in NMDA receptor activity (Caldeira et al., 2007b). Multiple reports support a critical role for BDNF-regulated protein synthesis in *in-vitro* assays of long-term use-dependent synaptic plasticity. BDNF was shown to enhance the induction of early phase LTP (E-LTP) and late-phase LTP (L-LTP) in hippocampal slices, and BDNF-mediated stimulation of *de novo* protein synthesis is essential for the maintenance of L-LTP (Kang and Schuman, 1996; Korte et al., 1995; Pang and Lu, 2004; Patterson et al., 1996; Poo, 2001; Tyler et al., 2002) These findings are consistent with *in-vivo* studies showing that secretion of BDNF is crucial for the persistence of long-term memory storage in the hippocampus (Bekinschtein et al., 2007).

BDNF regulates the translation of a subset of neuronal mRNAs

While the capacity of BDNF to modestly enhance global cellular translation has been readily appreciated, accumulated evidence has also revealed that only select proteins

are increased in response to BDNF. Multiple investigations examining small numbers of transcripts suggested that BDNF could induce the translation of plasticity-related proteins (such as CaMKIIα, Staufen, Arc, Homer2, NR1, GluA1) while leaving the levels of other proteins unaffected (Aakalu et al., 2001; Jourdi et al., 2009; Kanhema et al., 2006; Kelleher et al., 2004; Takei et al., 2004; Yin et al., 2002; Ying et al., 2002). High-throughput approaches examining gene target selectivity on a more global scale have helped to elucidate the truly impressive extent of gene target specificity in BDNF-regulated protein synthesis. 2D electrophoresis of radiolabeled proteins from isolated synapses demonstrated that only specific proteins were enhanced by BDNF, while most proteins show no change, and a subset of proteins were decreased in response to BDNF (Yin et al., 2002). In 2004, Schratt and colleagues provided compelling evidence for the transcript selectivity of BDNF-induced protein synthesis using polysome profiling. In this study conducted in cortical neurons, BDNF was shown to induce a transcription-independent recruitment of a specific subset of mRNAs, less than 4 % of the total expressed transcripts, to polysomes (Schratt et al., 2004). This selective regulation was sensitive to inhibition of mTOR. Intriguingly, BDNF not only upregulates translation of a discrete group of mRNAs, but in some cases BDNF mediates the transcription-independent downregulation of specific transcripts and their corresponding proteins, such as the potassium co-transporter KCC2 and potassium channel Kv1.1 (Raab-Graham et al., 2006; Rivera et al., 2002; Wardle and Poo, 2003). Using multidimensional protein identification technology (MudPIT) to analyze several thousand proteins, the selective downregulation of significant numbers of proteins by BDNF, in addition to upregulated proteins, was also observed in isolated cortical synapses (synaptoneurosomes) (Liao et al.,

2007). Components of the translational machinery, including translation factors, ribonucleoproteins, ribosomal proteins, as well as proteins known to regulate synaptic function and dendritic spine morphology were among the protein classes upregulated by 30 minutes of BDNF treatment (Liao et al., 2007).

These investigations illustrate not only the effects of BDNF in promoting the synthesis of many proteins that support neuronal growth and synaptic plasticity, but also collectively underscore the high degree of selectivity in the regulation of target transcripts by BDNF. In the context of BDNF's known roles in the brain, it is perhaps not surprising that this growth factor would need to selectively regulate only certain proteins in order to achieve a net pro-growth or pro-plasticity function. Nonetheless, this striking specificity for both up- and down-regulated gene targets is a feature of BDNF control of protein synthesis that has sometimes been overlooked in favor of the simplified understanding that BDNF enhances total cellular protein synthesis.

Post-transcriptional regulatory mechanisms underlying translational specificity of BDNF

How does BDNF selectively regulate the translation of only a discrete group of mRNAs? In addition to acting on initiation factors of protein synthesis machinery, BDNF also modulates several more selective post-transcriptional regulators of gene expression. Multiple modes of exerting transcript selectivity in the post-transcriptional regulation of gene expression have been described, including cis-regulatory elements such as internal ribosome entry sites (IRES) and cytoplasmic polyadenylation elements (CPEs), and trans-regulatory factors such as RNA-binding proteins, and microRNAs (miRNAs).

RNA-binding proteins have been shown to modulate the synthesis of several plasticity-related proteins that are also targets of BDNF. The Cytoplasmic Polyadenylation Element Binding protein (CPEB) (Huang et al., 2003; Huang et al., 2002) and the Fragile-X Mental Retardation Protein (FMRP) (Vanderklish and Edelman, 2005; Zalfa et al., 2006) function in both localizing and regulating translation of mRNAs. Cytoplasmic polyadenylation, and likewise translation, can be regulated in certain mRNAs that contain sequence-specific binding sites for CPEB. CPEB is phosphorylated in an activity-dependent manner which enhances translation initiation by promoting the recruitment of poly(A) polymerase and causing the dissociation of eIF4E from an inhibitory protein, Maskin. BDNF may promote the activity-dependent polyadenylation of several CPE-containing neuronal RNAs (Du and Richter, 2005; Wu et al., 1998).

The translation of mRNAs interacting with the RNA-binding protein Fragile X mental retardation protein (FMRP) may also undergo activity-dependent regulation (Brown et al., 2001; Miyashiro et al., 2003). BDNF has been shown to downregulate *FMR1* mRNA expression in cultured hippocampal neurons as well as to decrease FMRP protein levels in the hippocampus of transgenic mice overexpressing TrkB receptors *in vivo* (Castren et al., 2002). In addition, BDNF treatment has been reported to post-translationally regulate FMRP by activating calcineurin-mediated FMRP dephosphorylation in hippocampal neurons (Wang et al., 2012). Dephosphorylation of FMRP has been suggested to activate mRNA translation (Ceman et al., 2003; Narayanan et al., 2007). By decreasing FMRP levels and promoting dephosphorylation of FMRP, BDNF may induce the translation of a subset of plasticity-related genes. Indeed, BDNF treatment elicits an increase in protein synthesis from several mRNAs, CaMKIIα, Arc,

Map1B, and APP, that are known to be targets of FMRP (Napoli et al., 2008). FMRP may also modulate translation of mRNAs through interaction with the cytoplasmic FMRP interacting protein 1 (CYFIP1), which binds to eIF4E and forms a complex with FMRP-target mRNAs (Napoli et al., 2008). BDNF stimulation in cultured primary hippocampal neurons and cortical synaptoneurosomes was shown to decrease co-immunoprecipitation of CYFIP1 and eIF4E leading to activation of target mRNA translation (Napoli et al., 2008).

Recent evidence indicates that miRNAs may play an important role in the capacity of BDNF to selectively regulate specific mRNA targets. miRNAs are small 22-24 nucleotide non-coding endogenous RNAs that regulate post-transcriptional translational by binding to partially complementary sites in target mRNAs. Perfect complementarity of a miRNA seed sequence (miRNA nucleotides 2-8) for the mRNA has been shown to be a strong predictor of miRNA binding and functional regulation of a given mRNA target (Bartel, 2009; Grimson et al., 2007; Nielsen et al., 2007). Binding of an mRNA by a miRNA can lead to translational repression of the mRNA which may be accompanied by degradation of the target mRNA.

Hundreds of miRNAs are expressed in the mammalian brain and there is strong evidence that brain-specific miRNAs are crucial for synaptic plasticity and neuronal function (Bonev et al., 2011; Schratt et al., 2006; Yu et al., 2008). An initial report implicating miRNAs in the regulation of protein synthesis by BDNF involved the brain-specific miRNA, miR-134. miR-134 was found to negatively regulate dendritic spine size by inhibiting the translation of an mRNA encoding Limk1 (Schratt et al., 2006). Limk1 mRNA undergoes enhanced translation in response to BDNF (Schratt et al., 2004),

and loss of Limk1 protein produces deficits in spatial learning and hippocampal LTP (Meng et al., 2002; Sarmiere and Bamburg, 2002). BDNF was shown to relieve translational suppression of Limk1 by inactivating miR-134 and permitting increased protein synthesis of synaptic Limk1 and spine growth (Schratt et al., 2006); the mechanism by which BDNF relieved miR-134 dependent suppression was not elucidated. This study highlighted the concept that BDNF could regulate gene expression through altering the function of a specific miRNA to relieve suppression.

Additional evidence for reversal of miRNA-mediated silencing in neurons came from Ashraf and colleagues' demonstration that loss of an RNA-induced silencing complex (RISC) component, Armitage, released translational repression of a synaptic mRNA, CaMKII, in drosophila (Ashraf et al., 2006). MOV10, the mammalian homolog of Armitage, was subsequently shown to undergo activity-dependent proteasomal degradation that lead to the relief in translational silencing of a several mRNAs (Banerjee et al., 2009). While MOV10 degradation was never explicitly linked to BDNF, these studies drew attention to the concept that reversal of miRNA-mediated silencing could present a mechanism for the regulation of synaptic protein synthesis important for neuronal plasticity and memory formation. MOV10 degradation was found to require NMDA receptor activation, and many studies have positively linked BDNF to NMDA signaling. BDNF increases mRNA and protein levels of NMDA receptor subunits NR1, NR2A, and NR2B (Caldeira et al., 2007b) and also enhances the phosphorylation of NR1 and NR2B in hippocampal and cortical neurons (Lin et al., 1998) which contributes to increased glutamatergic transmission (Alder et al., 2005). BDNF also increases the open probability of NMDAR channels (Levine et al., 1998; Levine and Kolb, 2000). In

contrast to modulation of miR-134, the regulation of Armitage or MOV10 might be expected to produce more 'global', rather than miRNA-specific, changes in relief of miRNA-mediated repression. While the effects of loss of MOV10 were not assayed in a high-throughput manner, a candidate-based screen did reveal multiple candidate mRNAs, including CaMKIIα and Lypla1, that underwent enhanced translation upon loss of MOV10 (Banerjee et al., 2009).

The role of miRNA biogenesis regulation in BDNF signaling

Since the discovery of miRNAs twenty years ago (Lee et al., 1993), nuclear and cytoplasmic steps have been elucidated which are necessary for the processing of miRNA precursors to mature functional miRNAs. Regulatory mechanisms that impact and control the biogenesis of miRNAs at these steps continue to be revealed. Given that miRNAs are predicted to regulate more than 60% of mRNAs, the control of cellular miRNA composition holds significant potential for post-transcriptional gene regulation. New insights into the effects of BDNF on post-transcriptional regulators, including RNA-binding proteins and miRNAs, has shed light on mechanisms that contribute to the specificity of BDNF translational control. The physiological effects of BDNF in promoting neuronal growth, survival, and plasticity arise from *selective* regulation of mRNA translation; the investigations of myself and others in our laboratory indicate that BDNF can achieve this selectivity through both positive and negative regulation of the production of miRNAs (Figure 1.1). As detailed in the following chapters, the translation of pro-growth or plasticity-related mRNAs is selectively enhanced by BDNF through the induction of an RNA-binding protein, Lin28. My thesis work highlights the importance

of Lin28 and its effects on the Let-7 miRNA family and suggests that the Lin28/Let-7 axis may be essential to the physiological impact of BDNF on brain function.

The Lin28 / Let-7 Axis in post-transcriptional control of pro-growth gene expression programs

There is considerable precedence for a prominent role of Let-7 family miRNAs in the repression of genes controlling growth, proliferation, and pluripotency. In mammals, the cellular abundance of mature Let-7 miRNAs can be controlled, at least in part, in a post-transcriptional manner by Lin28 (Newman et al., 2008; Viswanathan et al., 2008). Lin28 selectively recognizes and binds to pre-miRNAs that contain a 'GGAG' sequence motif in their terminal loop; this class of precursors includes the Let-7 miRNAs. Lin28 then recruits a udridinylase, TUT4, which causes uridylation and blocks processing of the Let-7 miRNAs leading to a subsequent decline in mature Let-7 miRNA levels which can occur through exonuclease action of Dis3l2 (Chang et al., 2013) (Figure 1.2). Lin28 was first discovered in C. elegans as a heterochronic gene and regulator of developmental timing (Ambros and Horvitz, 1984; Moss et al., 1997). Recent evidence from genome-wide association studies (GWAS) indicates that Lin28 may retain its heterochronic function in humans and play a critical role in coordinating growth and development. Genetic variation near and within Lin28 (*LIN28B* loci) has been correlated with human age at onset of puberty and height (Ong et al., 2009; Perry et al., 2009). Work from the Daley lab further substantiated these findings with transgenic mice overexpressing Lin28a, which exhibited increased body size and delayed onset of puberty. Increased glucose metabolism and insulin sensitivity, phenotypes that recapitulated human

developmental traits identified in GWAS studies, were also observed in mice overexpressing Lin28 (He et al., 2009; Lettre et al., 2008; Ong et al., 2009; Sulem et al., 2009; Zhu et al., 2010). Subsequently, Zhu and colleagues showed that Lin28 regulates mammalian glucose metabolism in an mTOR-dependent manner in part through derepression of metabolic genes, including INSR, IGF1R, and IRS2, which are targets of Let-7 miRNAs (Zhu et al., 2011).

While Let-7-independent functions for Lin28 are known, the role of Lin28 in managing growth and metabolism is most well-established through its regulation of the Let-7 family miRNAs that can coordinately repress many pro-growth genes. As a consequence of these broad effects, Let-7 family miRNAs are often classified as tumor suppressor genes. Lin28, which blocks Let-7 miRNA production, is believed to be overexpressed in up to 15 % of all cancers (Viswanathan et al., 2009). Dysregulated reduced expression of Let-7 miRNAs is frequently found in lung cancer cell lines and patient tumor samples, and Let-7 miRNA overexpression has been used to inhibit proliferation of lung cancer cells (Takamizawa et al., 2004). Other cancers exhibiting low levels of Let-7 miRNAs include glioblastoma multiforme, chronic myelogenous leukemia, B cell lymphoma, breast, colon, esophageal, ovarian, liver, kidney, prostate cancer. Several studies have identified oncogenes including Ras, Myc, and HMGA2, as Let-7 targets providing molecular insight into how aberrant reductions in Let-7 miRNAs could contribute to tumorigenesis (Calin et al., 2004; Johnson et al., 2007; Johnson et al., 2005; Kumar et al., 2008; Shell et al., 2007; Yu et al., 2007a; Yu et al., 2008). In healthy tissue, a major role of the Let-7 miRNA family is in the control of target genes that regulate cellular proliferation and differentiation, as required for proper development. Let-7 levels

are progressively elevated during development, across many species, and function to promote differentiation and represses self-renewal by decreasing the expression of target genes that induce proliferation and inhibit differentiation such as c-Myc, Pax6, Ascl1, and the transcription factors HBL-1 and DAF-12 (Abrahante et al., 2003; Grosshans et al., 2005; Lin et al., 2003; Ramachandran et al., 2010; Sampson et al., 2007) Let-7 levels are low or absent in a variety of stem cell or progenitor cell populations of normal tissue (Thomson et al., 2004; Wulczyn et al., 2007). High Let-7 expression is detected late in embryonic development and in adult tissues (Sempere et al., 2004; Thomson et al., 2004). It is now firmly established that Let-7 functions as a key developmental timing switch in the transition from stem cell to differentiated cell fate across multiple organisms from *C. elegans* to vertebrates.

Why might the reduction in Let-7 family miRNAs by BDNF have a profound effect on the translation of neuronal mRNAs containing binding sites for Let-7 family miRNAs? This is an interesting consideration, particularly given that miRNAs are sometimes viewed as mediators that serve only to fine-tune gene expression. There are several reasons why targeting Let-7 miRNA levels may be particularly effective in allowing BDNF to promote the synthesis of an ensemble of neuronal proteins with roles in growth and synaptic plasticity. Several high-throughput studies have been conducted to quantitatively assess brain region-specific miRNA expression patterns, and by multiple approaches the Let-7 family of miRNAs appears to be highly abundant in the adult mammalian brain. A miRNA profiling study using deep sequencing (Illumina Genome analyzer) of bilateral rat hippocampal CA3 regions reported that the Let-7 family of miRNAs represent nearly 50% of small RNA sequences (Shinohara et al., 2011). In the

adult mouse frontal cortex and hippocampus, miRNA expression was quantitatively compared using methods of both miRNA-Seq (Illumina Genome analyzer) and miRNA microarray (Affymetrix) (Juhila et al., 2011). This study found that the Let-7 family of miRNAs was collectively by far the most abundant class of miRNAs in both the hippocampus (59%) and frontal cortex (47%). Remarkably, individual members of the Let-7 family represented 7 of the 15 most abundant miRNAs in the hippocampus (Juhila et al., 2011). These studies exemplify why mRNAs containing seed-matched sites for Let-7 miRNAs might be anticipated to be repressed by these miRNAs under basal conditions, and to undergo significantly enhanced translation when a BDNF stimulus leads to relief from miRNA-mediated repression by a substantial and selective decline in the highly abundant Let-7 family miRNAs.

While a foundation of previous research has illuminated the mechanisms of bulk regulation of protein synthesis by BDNF, the first portion of my doctoral work has focused on how selectivity of BDNF-induced protein synthesis is achieved. My doctoral work demonstrates that mRNA transcript selectivity in protein synthesis can be achieved through BDNF-mediated control of miRNA biogenesis, and this project will be discussed in chapter two. The second bulk of my thesis work investigates neurotrophin-induced regulation of Lin28a in differentiated tissue and unveils key steps responsible for the transcription-independent upregulation of Lin28a in hippocampal neurons, and these findings are described in chapter three.

Note: During my doctoral research, I have worked within and as a leader of a team investigating different aspects of miRNA biogenesis in mature neurons. Contributions

that have been made by other team members are denoted in each figure legend. I participated in the writing of publications and in all intellectual aspects of the work presented in this thesis.

Figures and Legends

Figure 1.1 Model of BDNF regulation of mRNA target specificity mediated through control of miRNA biogenesis

(Left) Dicer and TRBP process precursor miRNAs (pre-miRNAs) in blue and Lin28-regulated pre-miRNAs in red into mature miRNAs. These mature miRNAs then go on to repress target mRNAs. (Right) BDNF stimulation leads to rapid upregulation of Dicer/TRBP, which enhances processing of pre-miRNAs into mature miRNAs. This leads to increased miRNA biogenesis and gene repression and explains why the majority of mRNAs are excluded from translation in response to BDNF. BDNF simultaneously elevates Lin28a levels, which leads to the specific downregulation of Let-7 miRNAs. This selectively enhances the translation of a subset of mRNAs that undergo a relief of translational repression by Let-7 miRNAs.

Figure 1.1

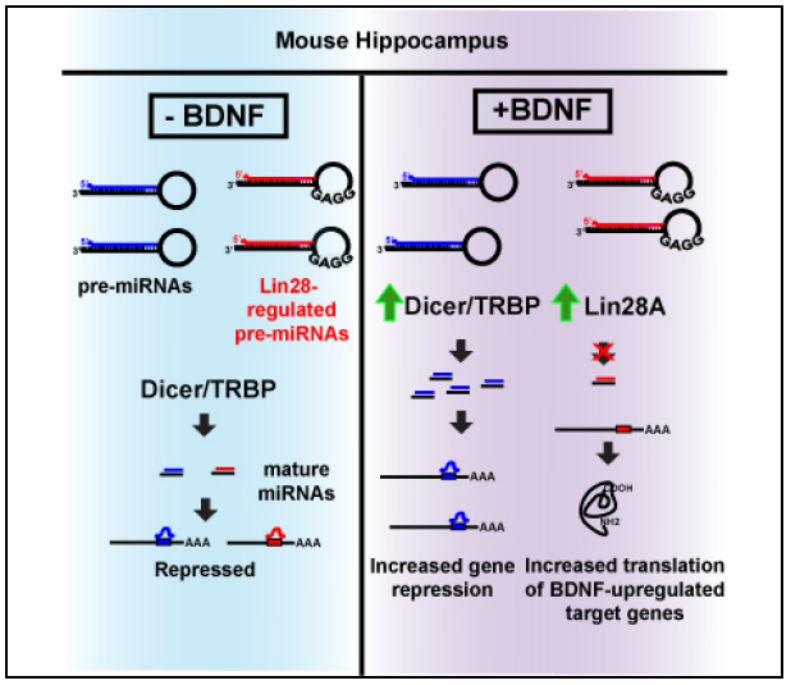

Figure 1.2 Lin28a blocks the processing of mature Let-7 miRNAs

Lin28a recognizes and binds to the GGAG sequence motif in the terminal loop of pre-Let-7 miRNAs. Upon binding to the precursor miRNA loop region, Lin28a recruits a terminal uridyltransferase that leads to the uridylation of the pre-Let-7 miRNA. This blocks processing by Dicer and prevents the biogenesis of mature Let-7 miRNAs. Dis3L2 is the exonuclease that specifically targets and degrades uridylated pre-Let-7.

Figure 1.2

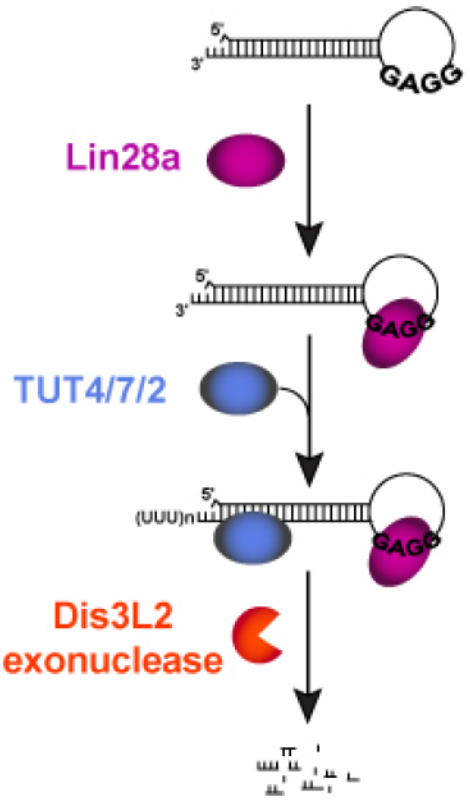

Chapter II: Dual regulation of miRNA biogenesis generates target specificity in neurotrophin-induced protein synthesis

Background

The control of gene expression at the level of translation is vital to neuronal function and synaptic plasticity. Dysregulated translation has been linked to cognitive disorders, including Fragile X syndrome, Autism, and Parkinson's disease. The regulation of translation plays a key role in the neuronal response to multiple stimuli, including synaptic activity (Huber et al., 2000; Raab-Graham et al., 2006; Wang et al., 2009), depolarization (Schratt et al., 2004), retinoic acid (Aoto et al., 2008), and neurotrophins (Aakalu et al., 2001; Jaworski et al., 2005; Schratt et al., 2004). While most of these stimuli enhance total cellular protein synthesis, their responses demonstrate marked transcript specificity. This has been best defined for the brain-derived neurotrophic factor (BDNF), which is broadly expressed in the mammalian brain, plays pivotal roles in neuronal survival, structure, and synapse function. The effects of BDNF on protein synthesis, while physiologically important, are quite selective with an estimated 4% or less of expressed mRNAs undergoing enhanced translation (Schratt et al., 2004; Yin et al., 2002) despite a general enhancement of cap-dependent initiation and elongation by BDNF (Takei et al., 2009). Mechanisms conferring specificity to post-transcriptional control of gene expression are incompletely defined. mRNA regulatory elements and binding proteins provide significant examples of control for specific transcripts, but explanations for concerted changes in groups of mRNAs are largely lacking. While subcellular restriction of stimulus-dependent signals in neurons likely

imparts some transcript selectivity, target specificity remains inadequately explained since hundreds of mRNAs populate discrete cellular compartments such as dendrites.

We suspected that global regulatory mechanisms for mRNA translation, storage, or degradation might be enlisted to impart specificity to BDNF control of protein synthesis. RNA processing bodies (P-bodies or GW-bodies) are RNA granules that depend upon RNA for their formation (Teixeira et al., 2005), and harbor translationally repressed mRNAs that may be degraded or stored and released for subsequent translation (Brengues et al., 2005). In this work, we demonstrate that BDNF induces the rapid appearance of P-bodies in neurons, and determine that the function of miRNA biogenesis pathways is required for BDNF-mediated regulation of translation as well as the induction of P-bodies. Remarkably, BDNF induces widespread changes in miRNA biosynthesis through enhancement of the general miRNA processing enzyme, Dicer, and elevation of levels of Lin28a, a protein that prevents the processing of a subset of miRNAs. The combined action of BDNF on Dicer and Lin28a mediates target-specificity of BDNF-induced translation by dictating the profile of neuronal miRNAs that target mRNAs for translational repression.

Results

BDNF increases neuronal P-body number

To investigate whether changes in RNA processing might be induced by BDNF, we first used live cell imaging to examine BDNF effects on neuronal P-body abundance as a readout of potential broad effects on RNA regulatory mechanisms. P-bodies were monitored by expression of GFP-tagged Dcp1a (GFP-Dcp1a), a decapping enzyme and

specific P-body marker (Anderson and Kedersha, 2006) that colocalized with endogenous Dcp1a (Figure 2.2A) and other P-body components, including the RNA-binding protein GW182 (neuronal dendrites, Figure 2.1A; Figure 2.2A-F). BDNF-stimulated hippocampal pyramidal neurons responded with a rapid and robust increase in the number of both dendritic and somatic P-bodies, compared to mock-stimulated neurons, as assessed by live imaging of GFP-Dcp1a (Figure 2.1B-D) or endogenous staining (Figure 2.2G). Neurons were pre-incubated and imaged in the presence of the transcription inhibitor, Actinomycin-D, indicating that the rapid increase in P-bodies can be mediated post-transcriptionally. BDNF induces P-body complex formation rather than synthesis of components since protein levels of endogenous Dcp1a or GW182, or GFP-Dcp1a were not altered by BDNF (Figure 2.2H), and BDNF enhanced the total co-localization of two tagged P-body components, Dcp1a and Pat1b, without altering their expression (Figure 2.2F,I). Immunoprecipitation of GW182 demonstrated that BDNF increased the association of P-body components Argonaute 2 (Ago2) and Dcp1a with GW182 (Figure 2.1E, F) and, as anticipated since P-bodies require RNA for formation, BDNF induced a more than two-fold increase in the total co-immunoprecipitated RNA (Figure 2.1G). Exclusion of ribosomal protein S6 (RPS6) was used to corroborate immunopurification purity (Figure 2.1E). Collectively, these data show that the formation of P-bodies, containing non-translating RNA targeted for repression or degradation, is increased by BDNF, a stimulus known to enhance the activity of general translation factors and total cellular translation.

Loss of GW182 prevents BDNF regulation of target protein synthesis

Despite modestly enhancing total cellular translation, BDNF modulation of protein synthesis is highly selective with increases or decreases only in the levels of specific target proteins. To examine whether RNA-processing or repression might factor in this target specificity, we tested the effect of loss of GW182 function by either knockdown of GW182 or by expression of a GFP-tagged dominant negative GW182 (GFP-DNGW182) (Jakymiw et al., 2005). Both manipulations resulted in the loss of visible P-bodies (Figure 2.4A-C), as previously reported by Jakymiw and colleagues. Loss of GW182 function did not alter the modest enhancement of total translation mediated by BDNF (Figure 2.3A), and also did not interfere with BDNF-regulation of another pathway, CREB-dependent transcription (Figure 2.4D).

In contrast, GW182 knockdown or DNGW182 expression both strikingly eliminated the mRNA target specificity of BDNF-regulated protein synthesis. The AMPA glutamate receptor subunit GluA1, calcium calmodulin-dependent protein kinase II (CaMKIIα), and Homer2 normally undergo enhanced protein synthesis in response to BDNF (Narisawa-Saito et al., 1999; Schratt et al., 2004), while synthesis of the potassium-chloride co-transporter, KCC2, is decreased by BDNF (Rivera et al., 2002). GW182 knockdown (Figure 2.3B) or DNGW182 expression (Figure 2.3C) in hippocampal neurons elevated the basal levels of proteins normally upregulated by BDNF (GluA1, CaMKIIα, and Homer2) and prevented their further induction by BDNF. In contrast, the basal protein level of BDNF-downregulated target (KCC2) was unchanged by loss of GW182 function, but KCC2 protein level was no longer reduced by BDNF. b-tubulin III was unchanged by BDNF and used for normalization. These

experiments were performed in the presence of Actinomycin-D; similar effects were seen without Actinomycin-D (Figure 2.5). Effective GW182 knockdown was achieved using lentiviral transduction and verified by imunoblotting for GW182 (serum 18033, M.Fritzler, Figure 2B, and Abcam Figure 2.4B)

Quantitative real time PCR (RT-qPCR) showed that mRNA levels of BDNF-upregulated targets were unchanged by loss of GW182 function (Figure 2.4E), suggesting that the observed changes in basal protein levels could result from altered target translation. As previously reported, BDNF stimulation reduced mRNA levels of the gene (*SLC12A5*) encoding the down-regulated target, KCC2, in control neurons (Rivera et al., 2002). In neurons deficient in GW182, however, BDNF no longer significantly reduced the level of mRNA for KCC2 (Figure 2.4E). These results indicated that GW182 function is required for both baseline translational repression of BDNF-upregulated targets and for BDNF-induced mRNA degradation of a downregulated target. The composite effects implied a role for GW182 in the process that allows BDNF to differentially regulate specific mRNA targets.

The role of miRNA-mediated repression in BDNF regulation of target protein synthesis

Several RNA processing events are associated with P-body formation, including multiple RNA decay mechanisms, mRNA suppression by RNA binding proteins, and RISC-mediated repressive functions. Previous reports demonstrated that P-body disruption through targeting of discrete P-body protein components, such as GW182, can differentially block distinct RNA processing events (Liu et al., 2005a). To test whether

functions associated with GW182 in particular were required for translational specificity of BDNF, we compared the effects of loss of GW182 with loss of another P-body component, LSm5. We focused initially on assessing RISC-mediated functions, in contrast to decay pathways, since transcript levels of BDNF-upregulated targets appeared unchanged by loss of GW182 (Figure 2.4E). The functions of miRNA and siRNA pathways were tested by a reporter assay consisting of co-expression of a hairpin precursor shRNA (shCXCR4) and a luciferase reporter containing 3'UTR binding sites with either perfect (siRNA reporter) or mismatched (miRNA reporter) complementarity for the CXCR4 shRNA (Doench et al., 2003; Wang et al., 2006). Expression of either reporter without the shRNA exhibited full luciferase activity (Figure 2.3D); a control reporter lacking CXCR4 binding sites was unaffected by shCXCR4 co-expression (Figure 2.6).

P-body disruption by loss of GW182 function produced a preferential miRNA pathway deficit, as shown by failure of coexpressed shRNA to repress the miRNA reporter, with no effect on siRNA-dependent inhibition (Figure 2.3D). Loss of GW182 has been previously reported to impair miRNA-mediated translational repression (Jakymiw et al., 2005; Liu et al., 2005a). In contrast, P-body disruption by LSm5 knockdown (Figure 2.4F,G) did not significantly alter reporter suppression through siRNA or miRNA pathways in comparison to controls (shRNA-1, shRNA-2, or GFP; Figure 2.3D), indicating that these pathways remain intact.

The finding that loss of GW182, but not LSm5, disrupted miRNA-mediated repression, presented the opportunity to probe the importance of miRNA function in determining the specificity of BDNF-regulated translation. In contrast to the loss of

specificity in BDNF-regulated protein synthesis produced by GW182 deficiency (Figure 2.3B,C), loss of LSm5 did not alter translation specificity (Figure 2.3E) even though LSM5 knockdown also disrupted P-bodes (Figure 2.4F,G). LSm5 knockdown, like loss of GW182, also did not affect BDNF-enhancement of total cellular translation (Figure 2.4H). Comparing the effects of loss of GW182 or LSm5 function suggested the involvement of miRNA-mediated functions in conferring target specificity to BDNF-regulated protein synthesis.

Rapid enhancement of mature miRNA biogenesis by BDNF

To further investigate the role of miRNA in the specificity of BDNF-regulated translation, we asked whether BDNF might itself affect the miRNA pathway. Intriguingly, BDNF stimulation of cells co-expressing the shCXCR4 and miRNA reporter greatly enhanced miRNA-mediated suppression. Titration of shCXCR4 in this assay revealed that a low dose that did not suppress the reporter in the absence of BDNF generated maximally effective suppression after cellular stimulation with BDNF (Figure 2.3F). This effect was independent of new transcription as stimulation was carried out in the presence of Actinomycin-D. CXCR4 shRNA resembles endogenous pre-miRNA and requires Dicer cleavage to generate mature duplex RNA. We reasoned that BDNF could enhance miRNA-mediated repression in the reporter assay by two potential general mechanisms: first, BDNF might increase the efficacy of the RISC complex or, second, BDNF might increase the generation of functional mature duplex miRNA from transfected CXCR4 shRNA. A mechanism invoking BDNF-enhanced mature miRNA biogenesis was congruent with our earlier findings since elevated levels of miRNA can

deliver additional mRNAs targeted for repression to P-bodies and increase P-body number (Liu et al., 2005b).

We addressed the potential for global regulation of miRNA biogenesis by BDNF using miRNA arrays that selectively measure mature miRNA, as opposed to pre-miRNA. Hippocampal neurons were treated with BDNF for 30 min in the presence of Actinomycin-D to assess changes due to processing of existing pre-miRNAs rather than new pre-miRNA production. Each array (TaqMan) contained 375 rodent miRNA targets of which 195 were detectable in hippocampus in three independent paired experiments. Remarkably, of detectable endogenous miRNAs with levels significantly altered by BDNF, 89.4% were increased more than 2-fold by BDNF, while only 10.6% were decreased to < 50% (Figure 2.7A, left panel). Many more miRNA species showed smaller, less than 2-fold, posttranscriptional changes in abundance in response to BDNF. While absolute changes in individual miRNAs were not reproducible between paired array experiments, the qualitative effect of a predominantly increased abundance of many miRNA species in response to BDNF was reproducible on this platform as well as an initial analysis using Geniom miRNA biochips (Febit Inc., data not included). An expression analysis of fold change for each detectable miRNA species from the arrays illustrates an overall trend toward higher miRNA quantities in BDNF compared to mock-treated primary neurons (Figure 2.7A, right panel).

Widespread post-transcriptional upregulation of mature miRNA production suggested that BDNF might regulate an essential component of miRNA biogenesis, such as the Dicer processing complex. To assess this, we examined Dicer protein levels in BDNF-stimulated neurons. BDNF elicited a marked transcription-independent increase

in Dicer levels that peaked between 5 – 20 min after stimulation (Figure 2.7B). The binding of BDNF to TrkB receptors triggers signaling pathways promoting growth and survival, including activation of PI3K/AKT and MAPK/ERK pathways. Previous work in tumor cell lines revealed that a component of the Dicer complex, HIV-1 TAR RNA-binding protein (TRBP), could undergo Erk-dependent phosphorylation and that phospho-mimetic TRBP stabilized and enhanced Dicer levels (Paroo et al., 2009); mutations resulting in decreased TRBP protein also destabilize Dicer (Melo et al., 2009). Accordingly, we evaluated the effect of BDNF on TRBP levels and phosphorylation status in neurons. BDNF rapidly induced phospho-ERK and a multiple-banding pattern of TRBP (Figure 2.7C, upper panel) that was collapsed by phosphatase treatment (Figure 3C, lower panel). Total TRBP protein levels were also rapidly elevated and reached significance by 5 min after BDNF (2.61 fold increase +/- 0.86).

To evaluate a requirement for Dicer activity and miRNA biogenesis in BDNF-induced recruitment of non-translating mRNA to P-bodies, we depleted Dicer by RNAi. Dicer knockdown completely prevented a BDNF-induced increase in P-body numbers (Figure 2.7 D, E) in hippocampal pyramidal neurons. Neurons expressing control non-target shRNA responded to BDNF similarly to wildtype neurons (Figure 2.7E, Figure 2.1D). The requirement for Dicer in BDNF induction of P-bodies indicated a role for Dicer in targeting some mRNAs to the non-translating pool in response to BDNF.

We next asked whether Dicer activation, and by implication an increase in mature miRNAs, was sufficient to generate P-bodies in neurons. The fluoroquinolone, enoxacin, was previously shown to promote pre-miRNA processing by the Dicer/TRBP complex while a structurally similar derivative, oxolinic acid, did not significantly increase

miRNA biogenesis(Shan et al., 2008). Enoxacin, but not equimolar oxolinic acid, rapidly and robustly increased P-body numbers in neuronal soma and dendrites (Figure 2.7F). In comparison to BDNF, the time course of P-body induction by enoxacin was slightly more rapid, consistent with a more direct signaling mechanism. In accordance with a role for miRNA in regulating mRNA target selection, but not bulk translation, enoxacin did not alter basal or BDNF-induced total protein synthesis (Figure 2.6B). These results defined a potential mechanism for regulation of miRNA biogenesis by BDNF and linked BDNF-upregulation of Dicer activity to rapid changes in mRNA repression.

To test whether Dicer is also required for the regulation of BDNF-target genes, we examined the response of representative up- and down-regulated BDNF targets in the presence or absence of Dicer. Hippocampal pyramidal neurons from mice with a conditional *Dicer* allele ($Dicer^{flox/flox}$, 3A8 line) (Andl et al., 2006) were infected with lentivirus expressing 4-hydroxy tamoxifen (OHT)-inducible Cre recombinase and subsequently mock- or BDNF-stimulated with or without OHT. Targets that are normally low at baseline and upregulated by BDNF, including GluA1, CaMKIIα, and Homer2, were each elevated at baseline in Dicer-deficient neurons, consistent with basal de-repression in the absence of Dicer, and failed to be further upregulated by BDNF. A representative target normally downregulated by BDNF, KCC2, was non-responsive to BDNF in Dicer-deficient neurons (Figure 2.7G). Collectively, these results demonstrate that BDNF lacks specificity for up- or down-regulated targets in the absence of Dicer, consistent with a critical role for Dicer in BDNF-induced sequestration of mRNAs in P-bodies and in the mechanism determining the selective regulation of target mRNAs by BDNF.

BDNF confers selectivity to miRNA biogenesis through Lin28a

Widespread upregulation of miRNA production and consequent removal of mRNAs from the translating pool by targeted repression provides a viable negative selection mechanism to account for the low proportion of mRNAs reported to undergo BDNF-enhanced translation (Schratt et al., 2004). We next asked whether the miRNA biogenesis pathway might also be regulated to generate positive selection of BDNF-upregulated targets in protein synthesis. By miRNA array analysis, a small number of miRNAs were observed to decrease in response to BDNF; the decreases were more apparent in some individual experiments than in the collective averaged array data. Among these decreased miRNAs were several members of the Let-7 family. miRNA biogenesis can be regulated at multiple steps by trans-acting factors, including the Lin28 RNA-binding proteins (Heo et al., 2009; Newman et al., 2008; Viswanathan et al., 2008) which target Let-7 family members. Lin28 binding and subsequent pre-miRNA uridylation suppresses processing of targeted pre-miRNA to mature miRNA (Hagan et al., 2009; Heo et al., 2009), and could provide a mechanism for decreasing select mature miRNAs even in the context of Dicer elevation. Consistent with this possibility, we found a robust and rapid transcription-independent increase in Lin28a, but not Lin28b, protein in mature neurons by 5 min following BDNF exposure (Figure 2.8A).

Analysis of the terminal loop region of the Let-7, miR-107, and miR-143 pre-miRNAs showed that each has a putative or previously functionally confirmed 'GGAG' sequence motif that can permit recognition by Lin28 (Hagan et al., 2009; Heo et al., 2009). Individual RT-qPCR assays showed significant and reproducible BDNF-induced decreases in abundance of all tested members of the Let-7 family, as well as miR-107,

and miR-143 (Figure 2.8B), even though not all were reproducibly detected through the less sensitive miRNA arrays. Significant decreases in each of these miRNAs were apparent by 5 min post-BDNF stimulation (Figure 2.8B). In accordance with the expected effects of Lin28, Northern blotting for a member of the Let-7 family (Let7-a) showed significant decreases in both pre-Let7 and mature Let-7 miRNA levels in BDNF-treated neurons (Figure 2.8C). A control mature miRNA, miR-17, is modestly increased by BDNF, consistent with enhanced Dicer processing (Figure 2.8C).

If Lin28 positively selects BDNF-upregulated targets by decreasing specific miRNAs, an mRNA containing functional binding sites for a Lin28-downregulated miRNA would be predicted to undergo BDNF-enhanced translation. To test this prediction, we compared the response to BDNF of luciferase reporters whose 3'UTR contained either wildtype or mutated Let-7 miRNA binding sites, or no miRNA binding sites, under conditions of transcription blockade. As predicted, the reporter containing Let-7 binding sites was significantly induced by BDNF, while levels of the control reporters were unchanged (Figure 2.8D). This result indicates that downregulation of Let-7 family members by BDNF is sufficient to relieve repression and mediate positive target selection for BDNF-enhanced translation.

To examine the extent to which this mechanism could generalize to known BDNF targets, we evaluated the presence of binding sites for Lin28-regulated miRNAs in the 3'UTRs of mRNAs known to undergo upregulated, downregulated, or unchanged translation in response to BDNF. Positive scores (pink boxes, (Figure 2.8E)) were restricted to sites in which the miRNA seed sequence (nucleotides 2 - 7) paired as a perfect or G-U wobble-containing match; similar miRNA seed sequence pairing was

previously found important for target recognition (Guo et al., 2010). Thirteen representative BDNF-upregulated targets were all found to contain two or more sites for a Lin28-regulated miRNA (example sites in Figure 2.11), while targets known to be downregulated by BDNF (KCC2, KV1.1) (Raab-Graham et al., 2006; Rivera et al., 2002) or unregulated by BDNF (eEF1A, eIF4E, MAP2, β-tubulin III) (Schratt et al., 2004; Wang et al., 2009) did not contain such sites (Figure 2.8E).

We next directly tested the role of Lin28a in BDNF target mRNA selection. Depletion of Lin28a through RNAi, but not expression of a control hairpin, prevented the decline in mature Let-7 miRNAs in hippocampal neurons responding to BDNF (Figure 2.9A). Lin28a knockdown also prevented the increased translation of representative mRNA targets normally upregulated by BDNF (Figure 2.9B). In accordance with basal mRNA repression by miRNAs that are diminished through Lin28, protein levels of these normally upregulated targets (CaMKIIα, GluA1, and Homer2) remained at low basal levels even in the presence of BDNF under Lin28a knockdown conditions (Figure 2.9B, left and top right panels). Lin28a knockdown did not prevent the increased association of P-body protein and RNA components in response to BDNF (Figure 2.9C), which instead requires Dicer (Figure 2.7).

Targets normally de-repressed and upregulated by BDNF remained repressed in Lin28a-deficient neurons, in contrast with the effects of loss of GW182 (Figure 2.3B,C) or Dicer (Figure 2.7G) which both resulted in de-repression of BDNF-induced targets at baseline and occlusion of further upregulation by BDNF. Notably, targets normally downregulated by BDNF, represented by KCC2 and KV1.1, remained responsive to BDNF in the presence of Lin28a knockdown. BDNF effects on target mRNA levels

were unaffected by loss of Lin28a (Figure 2.9B, bottom right panel). These findings are consistent with translation specificity in response to BDNF being generated by a two-part regulation of the miRNA biogenesis pathway: 1) general upregulation of miRNA biogenesis that is required for repression of mRNAs whose protein products are decreased in response to BDNF, 2) downregulation of select miRNAs whose processing is blocked by the BDNF-induced Lin28a, resulting in de-repression and enhanced translation of mRNAs containing binding sites for Lin28-regulated miRNAs.

We further examined the role of Lin28a in BDNF-regulated translation by evaluating its effects on specific target mRNA repression in association with GW182. GW182-associated RNA was immunopurified, as in Figure 1E, under control shRNA and Lin28a knockdown conditions and the effects of BDNF on mRNA recruitment to GW182 were assessed by individual RT-qPCR assays. mRNAs undergoing regulated translation were enriched in overall association with GW182 in comparison to a 'housekeeping' *GAPDH* mRNA (Figure 2.9D). Under control shRNA conditions, BDNF reduced the GW182-association of representative mRNAs for targets whose translation is upregulated by BDNF (GluA1, CaMKIIα, and Homer2); in contrast, BDNF promoted the GW182-association of representative mRNAs for targets (KCC2 and Kv1.1) whose translation is downregulated by BDNF (Figure 2.9D). Translation of mRNA for b-tubulin III is unchanged by BDNF (Schratt et al., 2004) and was used for normalization; 18s rRNA is absent from P-bodies and served as a control for immunopurification purity (Figure 2.9D).

As expected if Lin28 regulates only selection of BDNF-upregulated targets, Lin28a knockdown altered only the GW182 enrichment profile of mRNAs for representative targets (CaMKIIα, GluA1, and Homer2) that undergo BDNF-enhanced

translation (Figure 2.9D). mRNAs for BDNF-upregulated targets remained equivalently repressed and associated with GW182 in Lin28a knockdown neurons in the presence or absence of BDNF, and protein levels of these targets were no longer enhanced by BDNF. In contrast, mRNAs for representative BDNF-downregulated targets (KCC2 and Kv1.1) remained enriched in association with GW182 at baseline and their enrichment was equivalently increased by BDNF in both control and Lin28 knockdown neurons (Figure 2.9D). A target not regulated by BDNF (GAPDH) was not enriched in GW182-association at baseline, did not change in response to BDNF, and was also unaffected by Lin28 loss (Figure 2.9D). These findings indicate that Lin28a, induced by BDNF, is required to suppress the processing of specific pre-miRNAs and selectively decrease levels of these mature miRNAs, concomitant with a general BDNF-induced upregulation in the biogenesis of most miRNAs by enhanced Dicer levels. The negative regulation of miRNA biogenesis by Lin28 presents a mechanism for the selection of upregulated targets in BDNF-induced protein synthesis.

To further test the mechanism by which Lin28 mediates induced translation of BDNF-upregulated targets, we constructed a Let-7 pre-miRNA that would be resistant to Lin28-mediated degradation through mutation of the pre-miRNA terminal loop residues from GGAG to GUAU. This mutation prevents Lin28-induced uridinylation and degradation of Let-7 pre-miRNA (Heo et al., 2009), but does not alter the target specificity of the Let-7 miRNA. Lentiviral-mediated expression of either wildtype (Let-7^{WT}) or Lin28-resistant Let-7 (Let-7^{LR}) in hippocampal cultures enhanced mature Let-7 levels in a dose-dependent manner that could be titrated to achieve equivalent and low levels of exogenous Let-7 expression (Figure 2.10A). Co-expression of Let-7^{LR} with

reporters harboring the 3'UTR from either of two BDNF-upregulated targets (GluA1 or CaMKIIα) completely prevented their induction by BDNF. In contrast, co-expression of Let-7^{LR} with a reporter harboring the 3'UTR from a BDNF-downregulated target (KCC2) had no effect on the BDNF-mediated depression of this reporter (Figure 2.10B). These results supported a selective role for Lin28 in mediating the specificity of BDNF for its upregulated targets.

While alternative mechanisms for selectivity could co-exist, our collective results strongly indicate that dual control by BDNF of the miRNA biogenesis pathway through Lin28a and Dicer critically contributes to determining both up- and down-regulated target specificity in BDNF-mediated protein synthesis. These findings prompted us to investigate the effects of loss of Lin28a on a physiological response requiring BDNF-regulated protein synthesis.

Loss of miRNA-mediated regulation prevents BDNF-enhanced dendrite arborization

Induction of dendrite outgrowth in excitatory neurons both in culture and *in-vivo* is a well-characterized BDNF function requiring the regulation translation (Jaworski et al., 2005). Since inhibiting new translation blocks BDNF-induction of dendrite growth, we reasoned that BDNF-upregulated targets, selected by Lin28, might be particularly important for this process. We tested the physiological relevance of selective mRNA translation by release from Lin28-targeted miRNAs using low-dose BDNF to stimulate proximal dendrite growth in developing hippocampal pyramidal neurons expressing Let-7^{LR}, or Let-7^{WT} as a control. Based on our previous results (Figures 2.9, 2.10A,B) and

the distribution of sites for Lin28-targeted miRNAs (Figure 2.8E, 2.9), Let-7^{LR} expression could be expected to function as a dominant negative to repress mRNA targets despite BDNF-mediated elevation of Lin28. Analysis of dendrite complexity (experimental methods), showed that Let-7^{LR} expression prevented BDNF enhancement of dendrite outgrowth (Figure 2.10C), without significantly altering basal dendrite complexity (mock condition) in comparison to control neurons expressing either Let-7^{WT} (Figure 2.10C) or GFP (Figure 2.12B, $p = 0.78$, one-way ANOVA), or cell soma size and total dendritic length, which were also unaffected by BDNF (Figure 2.10D). Loss of GW182 function, which would be expected to inhibit miRNA-mediated repression by both Lin28-regulated and non-Lin28-regulated miRNAs, also prevented BDNF-induced dendrite growth without altering basal dendrite complexity or total protein synthesis (Figures 2.12, 2.3A). These experiments highlight the importance of miRNA-mediated target selection in a neuronal response to BDNF requiring the induction of protein synthesis. We conclude that Lin28-induced degradation of pre-miRNAs is specifically required for the appropriate specification of mRNA targets for BDNF-upregulated translation and is required for BDNF-dependent growth of neuronal dendrites.

Discussion

The capacity to rapidly alter the abundance of effector proteins through regulating translation is critical to the biological actions of multiple stimuli. However, the pathways that mediate stimulus-dependent selection of specific mRNAs for enhanced translation have remained poorly understood. We have defined a novel coordinated mechanism for

genome-wide control of translation specificity that involves stimulus-dependent positive and negative regulation of miRNA biogenesis (model, Figure 2.13). We provide direct evidence that BDNF achieves translation target specificity by elevating levels of both Dicer and Lin28a proteins in a rapid and transcription-independent manner. The resultant action of Dicer and Lin28a on the cellular profile of miRNAs in response to BDNF effectively determines which mRNAs will participate in translation or be excluded through GW182-associated repression.

Our results provide the following insights into specificity for BDNF up- and down-regulated protein synthesis: First, upregulation of an mRNA's translation by BDNF requires the target mRNA to be repressed and enriched in association with P-body component GW182 under basal conditions. Interference with Dicer or GW182 function prevents this basal repression and therefore occludes stimulus-dependent induction of translation. Second, interference with Dicer or GW182 blocks the downregulation of target mRNA translation by BDNF. Third, the presence of seed-matched sites for a Lin28-regulated miRNA within the 3'UTR are predictive of an upregulated BDNF-target mRNA. Interference with selective Lin28-mediated pre-miRNA degradation blocks the induction of targets upregulated by BDNF. Fourth, the stimulus-induced association of an mRNA with GW182 is reciprocally related to its level of translation. BDNF diminishes the GW182 association of mRNA for translationally upregulated targets and enhances the GW182 association for downregulated targets.

Collective evidence indicates that GW182 interaction with miRNAs and RISC components can trigger the formation of P-bodies as sites where repressed mRNAs accumulate (Eulalio et al., 2007; Liu et al., 2005b). It seems plausible that the miRNA-

dependent repression induced by BDNF typically employs P-bodies, consistent with the striking Dicer-dependent increase in P-body number in response to BDNF. However, loss of visible P-bodies by LSm5 knockdown produced no apparent interference with the specificity of BDNF-induced protein synthesis, and our data could also be consistent with a model in which the mRNA repression does not occur in P-bodies per se, but elsewhere in a GW182- and miRNA-dependent manner.

BDNF-induced repression of mRNAs involves the rapid Dicer-dependent appearance of P-bodies in neuronal cell soma and dendrites that can occur independently of new transcription and, as reported in other cell types (Teixeira et al., 2005) appears to result from coalescence of existing P-body components. Consistent with these results, both Dicer and pre-miRNAs are present in dendrites and isolated synapses (Lugli et al., 2008), suggesting that trafficking might not be required for rapid responses; whether BDNF regulates neuronal miRNA biogenesis on a subcellular level remains to be investigated.

Recent work indicates that many miRNAs can turnover more quickly in neurons than in other cell types. miRNAs from brain or from hippocampal cultures have variable estimated half-lives of 0.5 – 6 hr (Krol et al., 2010; Sethi and Lukiw, 2009), compared with half-lives $\geq$ 24 hr in non-neuronal cells. This property might allow degradation of a pre-miRNA species in neurons to rapidly lower the corresponding mature miRNA level, as supported by our finding of rapid Lin28-mediated decline in mature Let-7 miRNAs. When miRNA precursors are not depleted by BDNF-induced Lin28, the available precursors (i.e. pri- and pre-miRNAs) appear sufficient to replenish mature Let-7 levels even when transcription is blocked for 1 – 2 hr.

miRNAs have been reported to repress target mRNA by inhibition of translation or by degradation. We observed miRNA-dependent degradation of target mRNA for representative mRNA targets that underwent decreased translation in response to BDNF; these findings are consistent with studies citing mRNA destabilization as a predominant source of miRNA-dependent reductions in protein (Guo et al., 2010; Hendrickson et al., 2009). However, our data also suggest that miRNAs can function by translation suppression in neurons under basal conditions. Specifically, BDNF-upregulated targets were repressed and associated with GW182 prior to BDNF stimulation. Disruption of this basal repression (by deficiency of GW182 or Dicer) increased protein production from BDNF-upregulated targets with no detectable elevation of their mRNA levels, consistent with reports of miRNA function by inhibition of translation (Chendrimada et al., 2007; Mathonnet et al., 2007; Petersen et al., 2006). In addition to its established role in tuning protein levels, our data highlight a role for miRNA-mediated repression in determining the specificity of stimulus-induced protein synthesis through both translation inhibition and mRNA degradation.

Mammalian Lin28 is reported to be downregulated during development with little or no expression in differentiated cells such as neurons (Moss and Tang, 2003). Our data similarly indicate low basal Lin28 expression in mature neurons, but show that BDNF induces rapid transcription-independent upregulation of Lin28a, which alters levels of Lin28-targeted miRNAs and might also perform additional functions. Lin28 expression has been associated with oncogenesis and, in conjunction with other modulators, can also induce pluripotent stem cells from differentiated tissues (Viswanathan et al., 2009; Yu et al., 2007b). This underscores the concept that the reprogramming of gene expression

accompanying both neoplastic transformation and induced pluripotency states may, at least in part, be additionally shared by the induction of plasticity in the adult nervous system.

Collectively, our data indicate that miRNA biogenesis undergoes dynamic post-transcriptional regulation in neurons to impart mRNA selection for BDNF-dependent protein synthesis. Our findings also reveal a role for mRNA repression in association with the P-body component GW182 in conferring specificity to basal as well as stimulus-dependent translation through miRNA-dependent regulation. It is likely that other stimuli use distinct or overlapping regulatory mechanisms in the miRNA biogenesis pathway to generate specificity in the post-transcriptional regulation of gene expression.

Figures and Legends

Figure 2.1 BDNF increases P-body formation in soma and dendrites of hippocampal neurons.

(A) Endogenous GW182 (top panel, red) colocalizes with GFP-Dcp1a (middle panel, green) in neuronal dendrites; overlay (bottom panel). (B) P-body formation in dendrites of hippocampal pyramidal neurons following mock- (top panels) or BDNF-stimulation (bottom panels, 100 ng/mL). (C) P-body formation in cell somas following mock- (top panels) or BDNF-stimulation (bottom panels). t = min post-stimulation. (D) Quantification and time course of percent change in GFP-Dcp1a P-body numbers in neuronal dendrites following mock- (open circles) or BDNF-stimulation (closed circles) in the presence of Actinomycin D (0.5 μg/ml) to isolate changes due to translation. * = $p<0.05$ by one-way ANOVA with Bonferroni correction. (E) Lysates from mock (-) or BDNF (+, 1 hour) stimulated neuronal cultures immunoprecipitated (IP) with GW182 antiserum (IP-GW) or isotype-control serum (IP-Ctrl). Input is 20% of IP'd protein. (F) Densitometric quantification from 9 independent experiments, as in (E); mock condition (open bars) set as 1.0. (G) Total RNA, measured by A_{260}, recovered by GW182 IP from equal lysate inputs; mock (open bar) set as 1.0. BDNF increased GW182-associated RNA 2.62 ± 0.29 fold. All error bars represent SEM. * = $p<0.05$ by unpaired Student's t-test. Scale bars represent 10μm.

The experiments performed in A of this figure were performed by Elizabeth Eyler and also published in her thesis; E-G were performed by Alvin Huang and also published in his thesis.

Figure 2.1

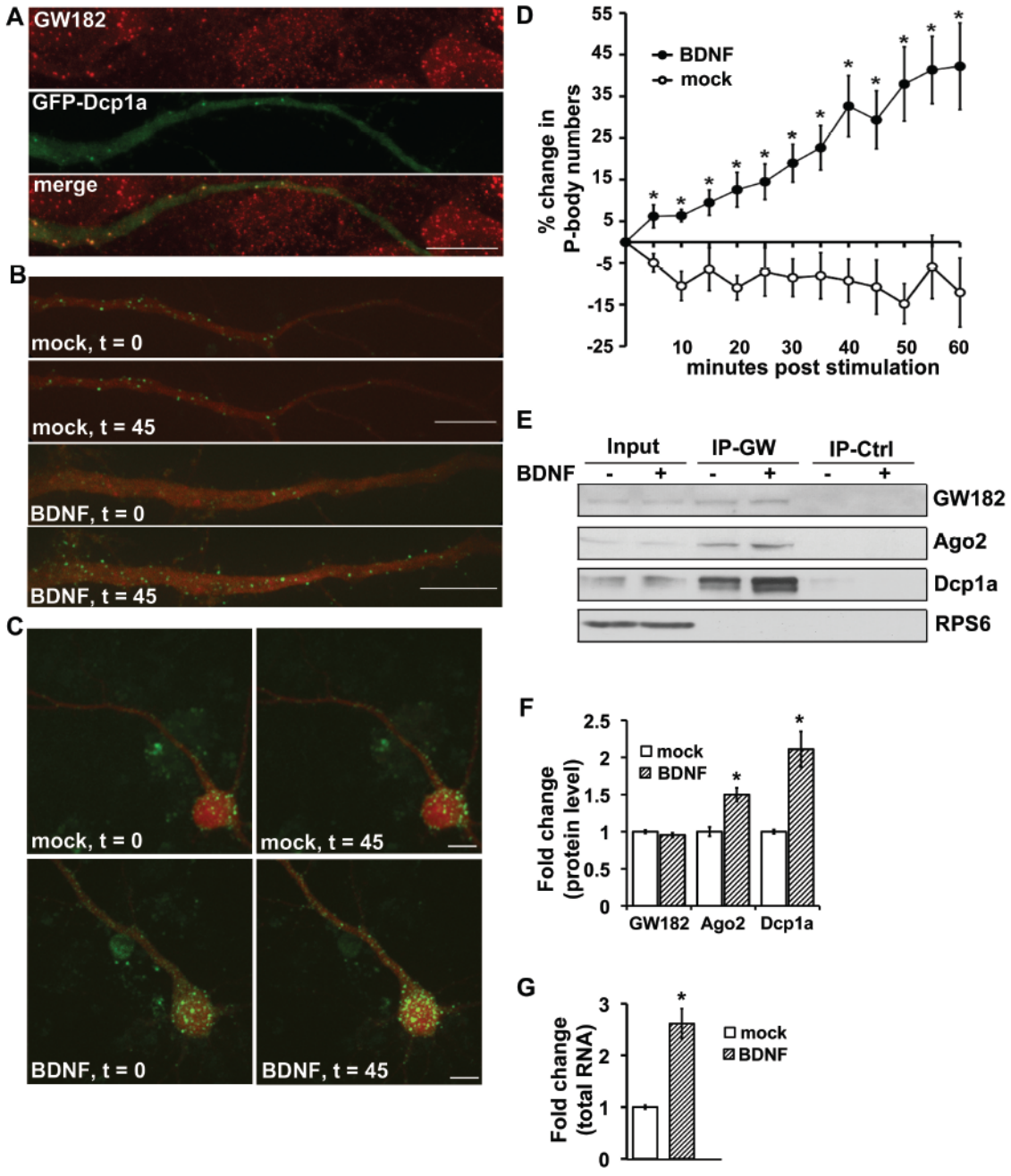
A
GW182
GFP-Dcp1a
merge
B
mock, t = 0
mock, t = 45
BDNF, t = 0
BDNF, t = 45
C
mock, t = 0
mock, t = 45
BDNF, t = 0
BDNF, t = 45
D
BDNF
mock
% change in P-body numbers
minutes post stimulation
E
Input
IP-GW
IP-Ctrl
BDNF
GW182
Ago2
Dcp1a
RPS6
F
mock
BDNF
Fold change (protein level)
GW182
Ago2
Dcp1a
G
mock
BDNF
Fold change (total RNA)

Figure 2.2 Composition of neuronal P-bodies.

Endogenous Dcp1a (top panel, red) colocalizes with GFP-Dcp1a (middle panel, green) in a confocal projection of hippocampal pyramidal neuron dendrites. Bottom panel, overlaid image. (B) mCherry-tagged Dcp1a (top panel, red) colocalizes with GFP-tagged Ago2 (middle panel, green) in a confocal projection. Bottom panel, overlaid image. (C) Endogenous Rck/p54 (top panel, red) colocalizes with endogenous GW182 (middle panel, green) in a confocal projection. Bottom panel, overlaid image. (D) Consistent with the lack of translation in P-bodies, endogenous ribosomal RNA, stained with Y10b (top panel, red) does not colocalize with GFP-tagged Dcp1a (middle panel, green) in dendrites of hippocampal pyramidal neurons. Bottom panel, overlaid image. Images shown are a single confocal slice to better appreciate co-localization given the relatively larger volume of Y10b staining. Inset: enlarged view of imaged region in dashed box, showing Y10b puncta closely opposed to but not colocalizing with GFP-Dcp1a puncta. (E) mCherry-tagged Dcp1a (top panel, red) does not colocalize with GFP-tagged Staufen (middle panel, green) in confocal projections from dendrites of hippocampal pyramidal neurons. Bottom panel, overlaid image. Inset: enlarged view of imaged region in dashed box, showing GFP-Staufen surrounding but not colocalizing with a GFP-Dcp1a puncta. (F) EBFP2-tagged Dcp1a (BFP-Dcp1a; top panel, blue) colocalizes with YFP-tagged Pat1b (YFP-Pat1b; middle panel, green). Scale bar represents 10 μm in all images. Images are confocal z-stack projections unless otherwise indicated. (G) Immunostaining of endogenous P-bodies with anti-GW182 antibody shows a high variability in basal dendritic P-body number that is collectively and on average shifted to greater numbers of P-bodies in BDNF-stimulated neurons. Scatter plot of endogenous P-body numbers in

individual neuronal dendrites from distinct pyramidal neurons quantified from GW182 immunostaining 75 min after mock- (open circles) or BDNF-stimulation (filled circle). Bar represents mean. Mean values ± SEM are 11.36 ± 1.21 (mock), 15.48 ± 1.26 (BDNF), $p < 0.05$ by Student's t-test. (H) Left: Immunoblot showing GFP-Dcp1a and endogenous Dcp1a and GW182 protein levels following 45 minutes mock (-) or BDNF (+) stimulation. Right: Relative quantification of protein levels normalized to β-tubulin III. (I) BDNF rapidly enhances the colocalization of P-body components by increasing their recruitment to P-bodies, rather than by altering their synthesis. Top panel: The fraction of total fluorescence of two co-expressed P-body markers, YFP-Pat1b and BFP-Dcp1a, that co-localized was quantified from hippocampal dendrites imaged before and after BDNF stimulation using the spots function and co-localize spots tool in Imaris software (Bitplane). The fraction of colocalized fluorescence within a dendritic segment was calculated for each P-body component by first summing the aggregate fluorescence values that co-localized with the other P-body marker, then dividing this quantity by the value of the total fluorescence intensity within the dendrite for that channel, and multiplying by 100. The percent of the total fluorescence that colocalized was significantly increased for both YFP-Pat1b and BFP-Dcp1a by BDNF (hatched bars) but not mock (checkered bars) stimulation. Middle panel: The degree of colocalization within a given P-body is not changed by BDNF stimulation. While the total amount of fluorescence found in P-bodies was increased by BDNF for both YFP-Pat1b and BFP-Dcp1a, P-bodies always demonstrated a high degree of co-localization for the two P-body markers that was not significantly altered by BDNF. Percent colocalization within P-bodies was calculated by measuring the amount of fluorescence of YFP-Pat1b or BFP

Dcp1a that co-localized within defined P-body punctae, dividing this by the aggregate fluorescence value within all defined P-body punctae, and multiplying by 100. Bottom panel: Total fluorescence of YFP-Pat1b or BFP-Dcp1a within dendritic segments did not significantly change during mock (checkered bars) or BDNF (hatched bars) stimulation. Error bars represent SEM. * = $p < 0.05$ by unpaired Student's t-test.

The experiments performed in A-C and E of this figure were done by Elizabeth Eyler and also published in her thesis.

Figure 2.2

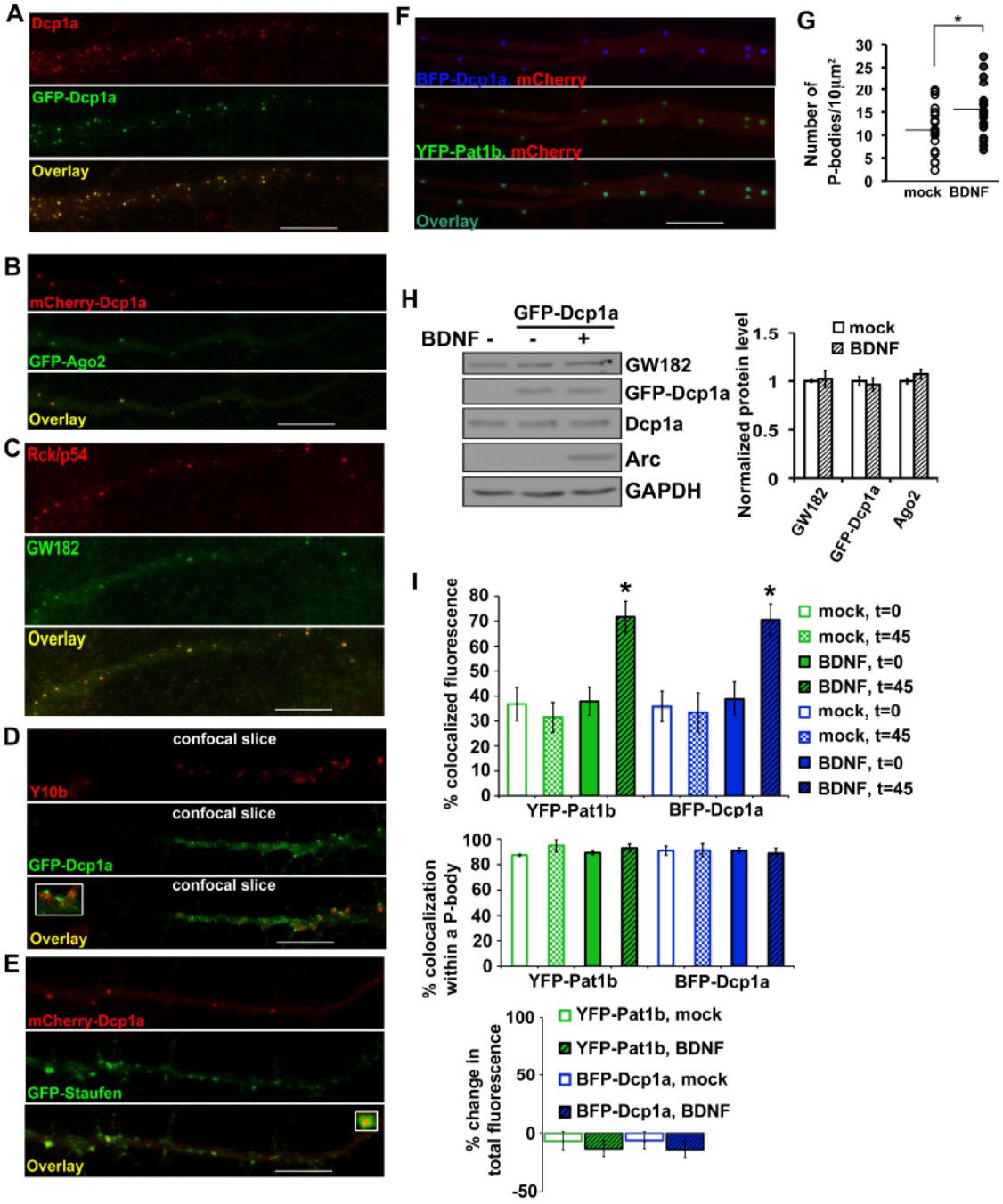
A
Dcp1a
GFP-Dcp1a
Overlay
B
mCherry-Dcp1a
GFP-Ago2
Overlay
C
Rck/p54
GW182
Overlay
D
confocal slice
Y10b
confocal slice
GFP-Dcp1a
confocal slice
Overlay
E
mCherry-Dcp1a
GFP-Staufen
Overlay
F
BFP-Dcp1a, mCherry
YFP-Pat1b, mCherry
Overlay
G
Number of P-bodies/10μm²
mock BDNF
H
GFP-Dcp1a
BDNF - - +
GW182
GFP-Dcp1a
Dcp1a
Arc
GAPDH
Normalized protein level
mock
BDNF
GW182
GFP-Dcp1a
Ago2
I
% colocalized fluorescence
YFP-Pat1b
BFP-Dcp1a
mock, t=0
mock, t=45
BDNF, t=0
BDNF, t=45
% colocalization within a P-body
% change in total fluorescence
YFP-Pat1b, mock
YFP-Pat1b, BDNF
BFP-Dcp1a, mock
BFP-Dcp1a, BDNF

Figure 2.3 miRNA-mediated repression is enhanced by BDNF and associated with BDNF target specificity.

(A) Loss of GW182 function by shRNA targeting GW182 (GW182KD) or GFP-DNGW182 expression does not alter BDNF-enhancement of aggregate protein synthesis relative to control (uninfected) cells, or cells expressing scrambled GW182 shRNA or GFP alone. Total protein synthesis was monitored under mock (open bars) or BDNF (hatched bars, 100 ng/ml, 2 hr) stimulated conditions, and plotted relative to the control mock condition set as 1.0 (first open bar). A translation inhibitor (rapamycin, 20 μg/ml) demonstrates that observed changes are due to translation. (B) Left: Immunoblotting for BDNF target proteins in neurons either uninfected or infected with lentivirus expressing GW182 shRNA (GW182KD) or a mismatched control shRNA (sh-Control-1). mCherry is co-expressed from the virus. Right: Protein levels, normalized to b-tubulin, of representative BDNF-upregulated targets under mock- (open bars) or BDNF- (hatched bars, 100 ng/ml, 2 hr) stimulation in the presence or absence of GW182KD (control mock, white bars, set as 1.0); n = 6 independent experiments. (C) Left: Immunoblotting for BDNF target proteins in neurons either uninfected or infected with lentivirus expressing GFP-DNGW182 or GFP. Right: Protein levels, normalized to b-tubulin, of representative BDNF up- or down-regulated targets under mock (open bars) and BDNF (hatched bars) stimulated conditions in cells expressing GFP-DNGW182, GFP, or control uninfected cells (control mock, white bars, set as 1.0); n = 6 independent experiments. (D) miRNA function is inhibited by GW182KD and GFP-DNGW182 but not by knockdown of LSm5 (LSm5KD). Left: luciferase activities of siRNA- or miRNA-reporter constructs in cells expressing reporter alone (- sh-CXCR4), or co-expressing

reporter and CXCR4 shRNA (+ sh-CXCR4), with or without GW182KD, GFP-DNGW182, or LSm5KD. Normalized luciferase values are shown relative to levels without sh-CXCR4 (set as 1.0). Right: Diagram of reporter constructs. (E) LSm5 knockdown did not alter protein synthesis of representative BDNF targets. Left: Immunoblotting for BDNF targets in neurons expressing control shRNA (sh-Control-2) or shRNA against LSm5 (LSm5KD) following mock (-) or BDNF (+) stimulation (100 ng/ml, 2 hr). Right: Densitometric quantification of 3 independent immunoblots, normalized to GAPDH and plotted relative to mock-stimulated controls (sh-Control-2 - mock). (F) BDNF enhances repression of a miRNA-reporter by a small RNA hairpin (sh-CXCR4). Normalized luciferase values are shown for mock (open bars) or BDNF-stimulated (hatched bars) neurons co-expressing the miRNA reporter and either sh-Control-2 or a dose-titration of sh-CXCR4. Low-dose sh-CXCR4 repressed the miRNA-reporter in BDNF- but not mock-stimulated conditions. All experiments done in the presence of Actinomycin-D. Error bars represent SEM. * = $p<0.05$ in comparison to reporter alone condition (- sh-CXCR4, D and F) or mock (open bars) by unpaired Student's t-test.

The experiments performed in this figure were conducted by Alvin Huang and also published in his thesis.

Figure 2.3

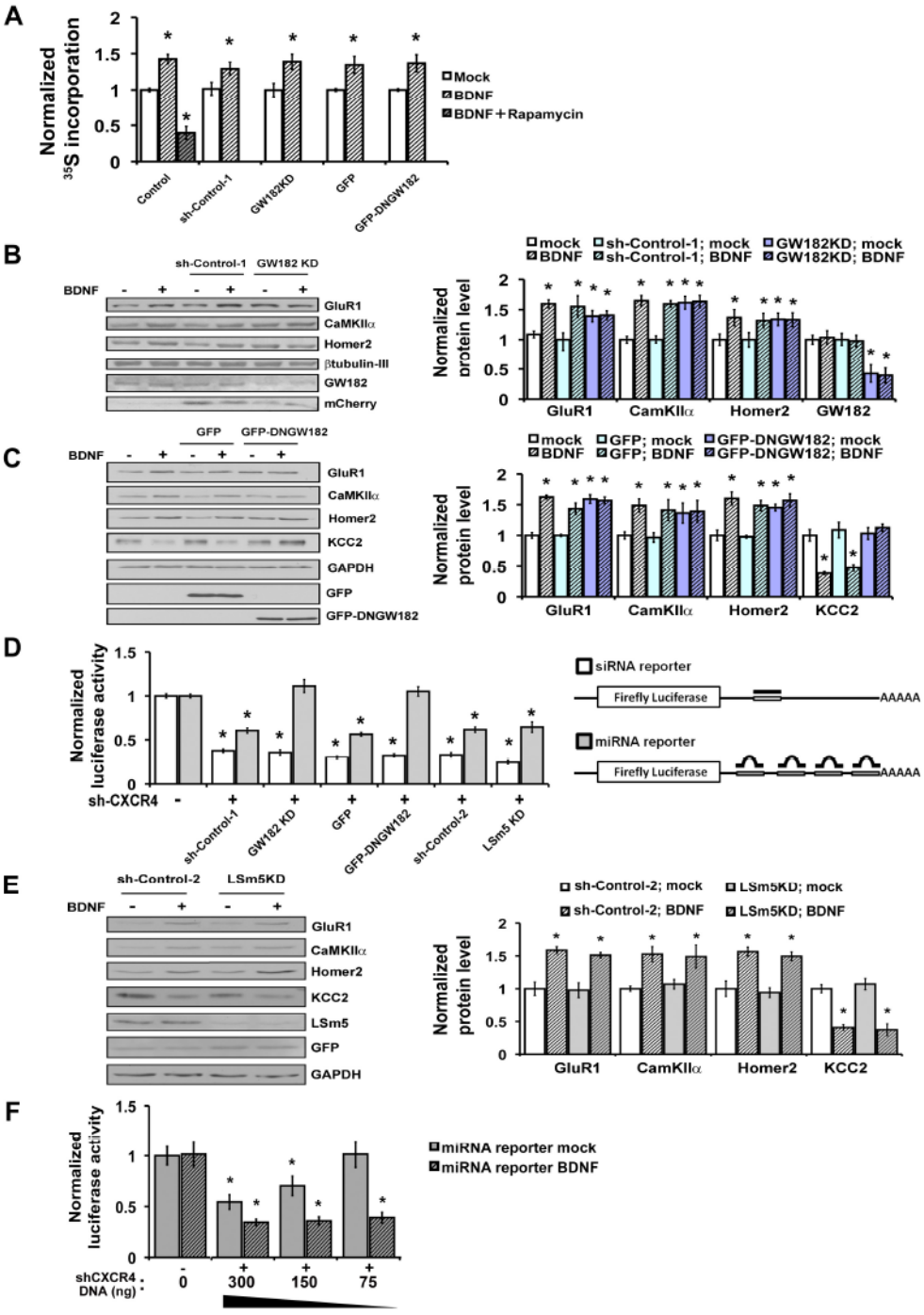
A
Normalized ^{35}S incorporation
Mock
BDNF
BDNF + Rapamycin
Control
sh-Control-1
GW182KD
GFP
GFP-DNGW182
B
sh-Control-1
GW182 KD
BDNF
GluR1
CaMKIIα
Homer2
βtubulin-III
GW182
mCherry
mock
sh-Control-1; mock
GW182KD; mock
BDNF
sh-Control-1; BDNF
GW182KD; BDNF
Normalized protein level
GluR1
CamKIIα
Homer2
GW182
C
GFP
GFP-DNGW182
BDNF
GluR1
CaMKIIα
Homer2
KCC2
GAPDH
GFP
GFP-DNGW182
mock
GFP; mock
GFP-DNGW182; mock
BDNF
GFP; BDNF
GFP-DNGW182; BDNF
Normalized protein level
GluR1
CamKIIα
Homer2
KCC2
D
Normalized luciferase activity
sh-CXCR4
sh-Control-1
GW182 KD
GFP
GFP-DNGW182
sh-Control-2
LSm5 KD
siRNA reporter
Firefly Luciferase
AAAAA
miRNA reporter
Firefly Luciferase
AAAAA
E
sh-Control-2
LSm5KD
BDNF
GluR1
CaMKIIα
Homer2
KCC2
LSm5
GFP
GAPDH
sh-Control-2; mock
LSm5KD; mock
sh-Control-2; BDNF
LSm5KD; BDNF
Normalized protein level
GluR1
CamKIIα
Homer2
KCC2
F
Normalized luciferase activity
shCXCR4 DNA (ng)
0
300
150
75
miRNA reporter mock
miRNA reporter BDNF

Figure 2.4 Loss of P-bodies in neurons lacking either GW182 or LSm5 leaves other cellular responses to BDNF intact.

GW182 was chosen as an initial target for P-body disruption since it may perform a scaffolding role in P-bodies and does not possess a known enzymatic activity that could be required for general cellular function. (A) Cultured hippocampal neurons (DIV 14) were infected with replication-incompetent lentivirus expressing mCherry and shRNA targeting GW182, or a control non-target shRNA and mCherry. Immunohistochemistry for endogenous GW182 indicated effective loss of P-bodies in cells expressing GW182 shRNA (GW182KD), but not in control shRNA infected cells. (B) Immunoblot demonstrating effective knockdown of GW182 using a rabbit polyclonal antibody raised against GW182 (16 amino acid peptide of TNRC6a absent from other TNRC6 isoforms, Abcam ab84403) with no cross-reaction to isoforms TNRC6B and TNRC6C, or Ge-1, another P-body component. Neurons expressing either shRNA against GW182 (GW182KD) or scrambled shRNA (sh-control-1) received mock or BDNF stimulation in the presence of Actinomycin-D as previously described (Figure 2). Quantification relative to the control mock condition (set as 100 %) of protein levels normalized to β-tubulin is indicated under GW182 bands. (C) Immunohistochemistry for endogenous Dcp1a showed loss of P bodies in neurons expressing GFP-DNGW182. (D) BDNF-induced activation of the cAMP response element-binding protein (CREB) transcription factor remains intact in neurons expressing GFP-DNGW182. A luciferase reporter harboring cAMP response-elements (CRE) to monitor CREB activation was expressed in neurons with or without DNGW182. Mock (open bars) and BDNF (hatched bars, 100 ng / ml 3.5 hours) stimulation were performed in the absence of a transcription blocker.

Luciferase activity was normalized to coexpressed constitutive β-galactosidase activity and plotted relative to the mock condition. * = $p < 0.05$ by unpaired Student's t-test. (E) mRNA abundance in neurons as measured by RT-qPCR with all conditions normalized to mock stimulation (open bars; set as 1.0). mRNA levels of BDNF-upregulated targets were unaltered from basal values (mock) by BDNF stimulation (BDNF), or by GW182 knockdown (GW182KD, left panel) or GFP-DNGW182 expression (right panel). The BDNF-induced downregulation of KCC2 transcripts was abolished by loss of GW182 function (right panel). All RT-qPCR reactions were normalized to β-tubulin III (neuron-specific isoform) values, which are unchanged by BDNF, within individual cDNA samples to control for consistency between amplification assays. Expression of control shRNA (sh-control-1, left panel) or GFP (right panel) serve as controls for GW182KD or GFP-DNGW182, respectively. (All experiments done in the presence of Actinomycin-D to isolate changes due only to translation. (F) Immunohistochemical staining for endogenous P-body component LSm5 (middle, green) showed extensive colocalization with another endogenous P-body component, GW182 (top panel, red; overlay, bottom panel) (G) Immunohistochemistry for endogenous Dcp1a showed loss of P bodies in neurons expressing shRNA against LSm5 (LSm5KD) but not in control-shRNA-expressing neurons (sh-Control-2). GFP expression served to visualize neuron morphology. Scale bars represent 10 μm in all images. (H) Increased total protein synthesis in response to BDNF is unaltered after P-body disruption by loss of LSm5. Total protein synthesis was assayed by measuring ^{35}S incorporation in sh-Control-2 and LSm5KD neurons, undergoing mock (- BDNF) or BDNF (+ BDNF) stimulation 100

ng/ml for 2 hours, in the presence of Actinomycin-D (0.5 μg/ml, pre-incubated 10 min before stimulation). * = $p < 0.05$ by unpaired Student's t-test.

The experiments performed in this figure were conducted by Alvin Huang and also published in his thesis.

Figure 2.4

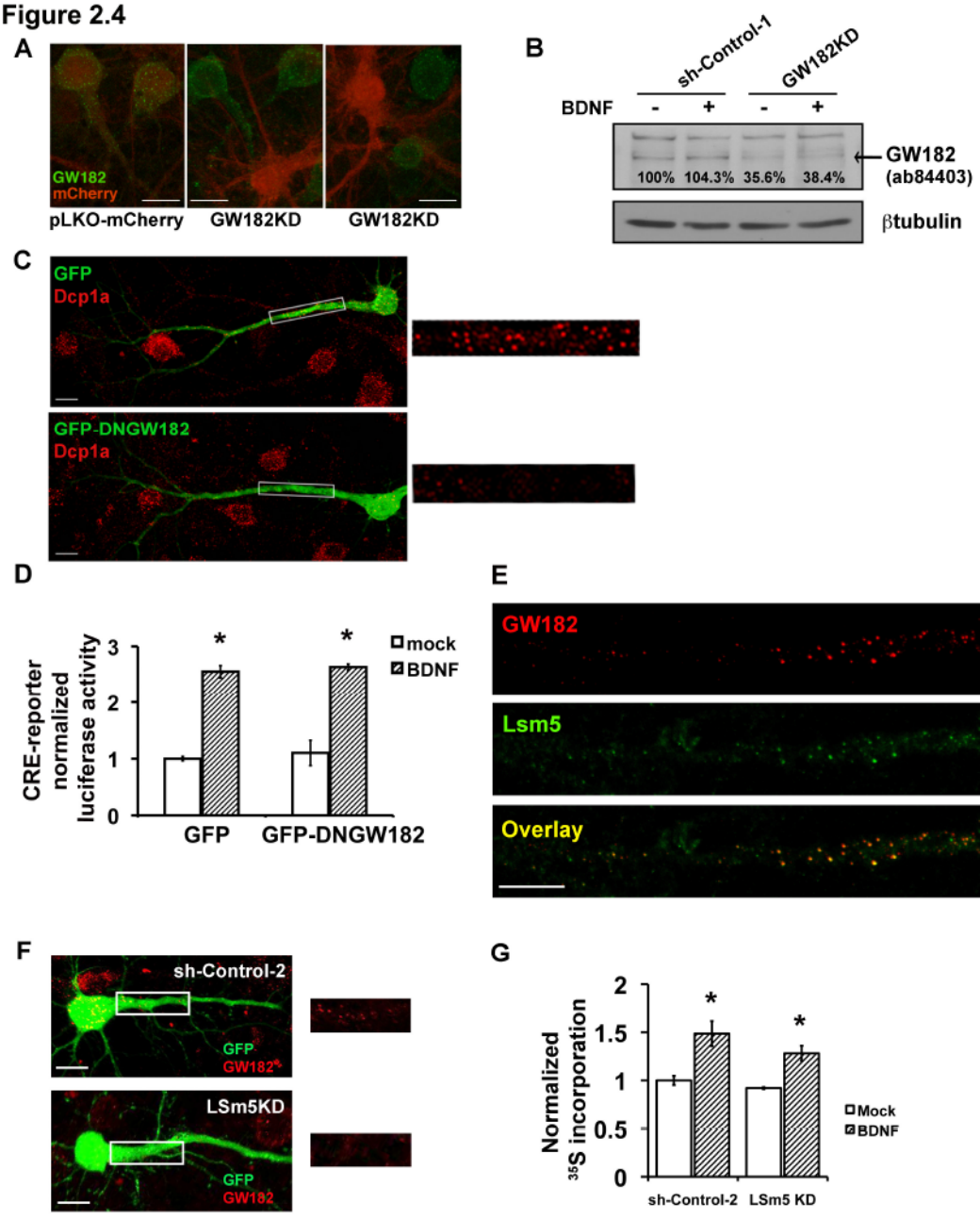
A
GW182
mCherry
pLKO-mCherry
GW182KD
GW182KD
B
sh-Control-1
GW182KD
BDNF
- + - +
GW182
(ab84403)
100% 104.3% 35.6% 38.4%
βtubulin
C
GFP
Dcp1a
GFP-DNGW182
Dcp1a
D
CRE-reporter normalized luciferase activity
mock
BDNF
GFP
GFP-DNGW182
E
GW182
Lsm5
Overlay
F
sh-Control-2
GFP
GW182
LSm5KD
GFP
GW182
G
Normalized 35S incorporation
Mock
BDNF
sh-Control-2
LSm5 KD

Figure 2.5 The transcription inhibitor Actinomycin-D does not alter BDNF-induced protein synthesis under the assayed conditions.

(A) Immunoblotting for BDNF targets in cultured neurons treated mock (-) or BDNF (+ ; 100 ng/ml for 2 hours) stimulation in the absence (- Act-D) or presence of Actinomycin-D (+ Act-D; 0.5 μg/ml added 10 min before stimulation). Arc demonstrates strong transcription-dependent upregulation by BDNF and serves as an indicator for Actinomycin-D efficacy. (B) Protein levels of BDNF targets relative to the mock-stimulated condition (open bars, set as 1.0). Quantification is by densitometry with internal normalization to β-tubulin. Error bars represent SEM. * = $p < 0.05$ by unpaired Student's t-test.

The experiments performed in this figure were conducted by Alvin Huang and also published in his thesis.

Figure 2.5

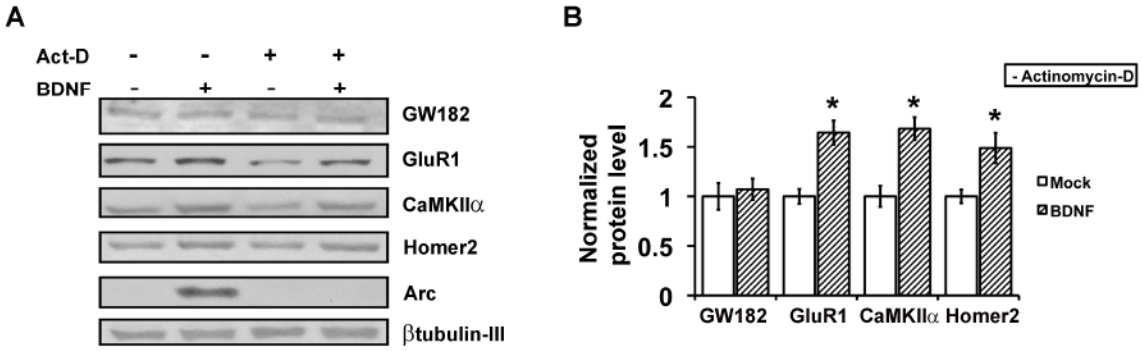

Figure 2.6 Control experiments supporting involvement of the miRNA pathway in BDNF-regulation of protein synthesis.

(A) Activity of a luciferase reporter lacking binding sites is not affected by expression of shRNA targeting CXCR4. Luciferase reporter assay was carried out in neurons expressing a control luciferase reporter free of any binding site for shRNA against CXCR4 (sh-CXCR4) and treated with mock (- BDNF) or BDNF (+ BDNF) stimulation at 100 ng/ml for 2 hours in the presence of Actinomycin-D (0.5 μg/ml, added 20 min before stimulation). (B) Global activation of miRNA biogenesis by Dicer stabilization with enoxacin does not significantly alter the quantity of total cellular protein synthesis. Total protein synthesis was assayed by measuring ^{35}S incorporation in neurons, undergoing mock or BDNF stimulation (100 ng/ml for 2 hours), with or without enoxacin, in the presence of Actinomycin-D (0.5 μg/ml, added 20 min before stimulation). Oxalinic acid, a structurally similar control for enoxacin, also does not alter total cellular protein synthesis. Error bars represent SEM. * = $p < 0.05$ by unpaired Student's t-test.

The experiments performed in this figure were conducted by Alvin Huang and also published in his thesis.

Figure 2.6

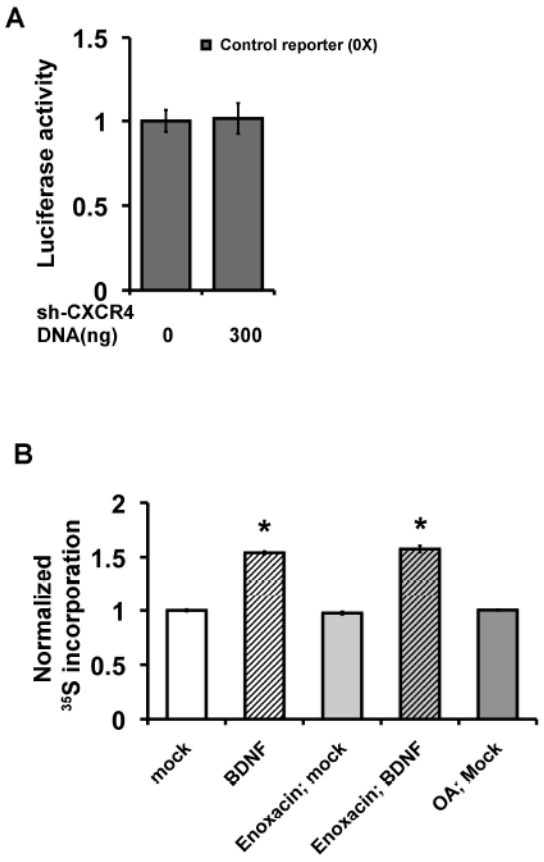

Figure 2.7 BDNF increases Dicer levels and the biogenesis of mature miRNAs.

(A) Left: percentage of miRNAs from TaqMan miRNA array with levels decreased over 50% (open bar) or increased over 2-fold (black bar) by BDNF (30 min., plus Actinomycin-D) Right: scatter plot of relative quantities (RQ) of individual miRNA species (solid circles) following BDNF relative to mock-stimulation. Red line = 1.0 or no change; each dot above the line represents a miRNA species increased by BDNF, each dot below the line represents a miRNA species decreased by BDNF. Normalization is to averaged reference RNAs U6snRNA, and snoRNA202, which are unchanged by BDNF; n = 3 separate miRNA array pairs for mock and BDNF conditions. (B) Immunoblot of cultured hippocampal neurons stimulated with BDNF for indicated min in the presence of

Actinomycin-D. Dicer peaks near 20 and declines by 60 min. (C) Top panel, BDNF enhances TRBP and ERK phosphorylation as shown by immunoblot for TRBP and phospho-Erk. Cultured hippocampal neurons were stimulated with BDNF for indicated min in the presence of Actinomycin-D. Bottom panel, lysates incubated with λ-phosphatase (λ-phos) as indicated demonstrate loss of phosphorylated TRBP (upper band). (D) P-body appearance in dendrites of hippocampal pyramidal neurons expressing control (sh-control-2, top panels) or Dicer-targeting shRNA (DicerKD, bottom panels) following BDNF, t = min post-stimulation. (E) Quantification and time course of P-body numbers in Dicer-deficient (DicerKD, boxes) or control (sh-control-2, circles) expressing hippocampal neurons following mock- (open shapes) or BDNF-stimulation (closed shapes). (F) Quantification and time course of P-body numbers in hippocampal pyramidal neurons treated with enoxacin (15 μM, closed circles) or oxolinic acid (15 μM, open circles). (G) The effect of Dicer loss on BDNF-regulated protein synthesis. Top panel, immunoblotting for BDNF target proteins in Dicer-wildtype ($Dicer^{flox/flox}$) or Dicer-deficient ($Dicer^{-/-}$) neurons. Cre^{ERT2}-expressing cells were treated with 4-hydroxy tamoxifen (800 nM) to induce recombination for 2.5 days before BDNF stimulation. Asterisk indicates non-specific band. Bottom panel, densitometric quantification of immunoblots. All error bars represent SEM. * = $p<0.05$ by unpaired Student's t-test.

The experiments in A of this figure were performed by Elizabeth Huang and also published in her thesis; experiments in G was performed by Alvin Huang and also published in his thesis.

Figure 2.7

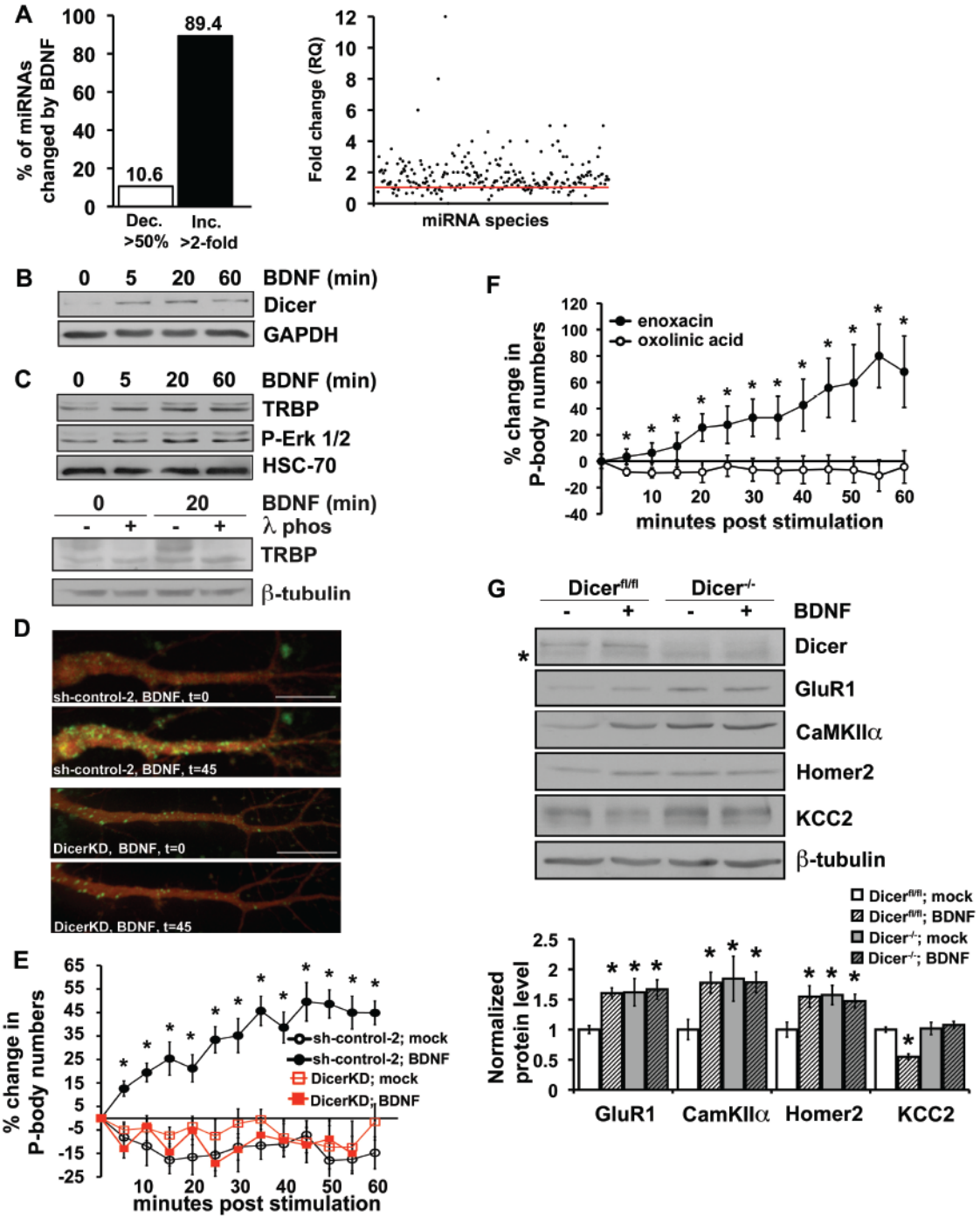
A
% of miRNAs changed by BDNF
89.4
10.6
Dec. >50%
Inc. >2-fold
Fold change (RQ)
miRNA species
B
BDNF (min)
Dicer
GAPDH
C
TRBP
P-Erk 1/2
HSC-70
λ phos
β-tubulin
D
sh-control-2, BDNF, t=0
sh-control-2, BDNF, t=45
DicerKD, BDNF, t=0
DicerKD, BDNF, t=45
E
% change in P-body numbers
sh-control-2; mock
sh-control-2; BDNF
DicerKD; mock
DicerKD; BDNF
minutes post stimulation
F
enoxacin
oxolinic acid
% change in P-body numbers
minutes post stimulation
G
Dicer^fl/fl
Dicer^-/-
BDNF
Dicer
GluR1
CaMKIIα
Homer2
KCC2
β-tubulin
Dicer^fl/fl; mock
Dicer^fl/fl; BDNF
Dicer^-/-; mock
Dicer^-/-; BDNF
Normalized protein level
GluR1
CamKIIα
Homer2
KCC2

Figure 2.8 BDNF induces Lin28, selectively diminishes Lin28-regulated miRNAs, and specifically upregulates a heterologous reporter containing Let-7 binding sites. (A) Lin28a (top panel) and Lin28b (lower panel) immunoblots of lysates from cultured hippocampal neurons stimulated with BDNF for indicated min. (B) Timecourse of BDNF-induced reductions in Lin28-regulated miRNA levels by individual TaqMan RT-qPCR reactions in mock- (BDNF 0') or BDNF-stimulated neurons. miRNA levels were normalized to 18s rRNA and plotted relative to each mock-stimulated condition (set as 1.0). All samples underwent equal duration Actinomycin-D incubation prior to harvest. (C) Northern blot (left) and quantitation (right) of pre- and mature miRNA levels of a Lin28-target (Let-7a) or control miRNA (miR-17) in mock or BDNF-treated (30 min) neurons. (D) A binding site for Let-7 miRNAs in the 3'UTR of an mRNA confers upregulation of protein synthesis in response to BDNF. Neurons expressing Let-7 reporters containing two functional (Let-7 WT) or mutated (Let-7 Mut) Let-7 miRNA binding sites in the 3'UTR of firefly luciferase, or a reporter lacking miRNA binding sites were mock- or BDNF-stimulated (4 hr). Luciferase activities are normalized to co-expressed constitutive β-galactosidase activity and plotted relative to mock-stimulation for each reporter. All error bars represent SEM. * = $p < 0.05$ by unpaired Student's t-test. (E) Predicted binding sites for Lin28-targeted miRNA. The presence of a Lin28-targeted miRNA binding site in the 3'UTR of transcripts for which translation is BDNF-upregulated (green), BDNF-downregulated (red), and BDNF-nonregulated (black) as predicted by TargetScan, PITA, Pictar, MiRanda, and miRwalk. Pink boxes denote the presence of a miRNA binding site in which the miRNA seed sequence (nucleotides 2 – 7)

paired as a perfect or G-U wobble-containing match. Gray boxes denote the absence of a miRNA binding site. See also Figure 2.11.

Experiments in B and D of this figure were performed by Alvin Huang and also published in his thesis.

Figure 2.8

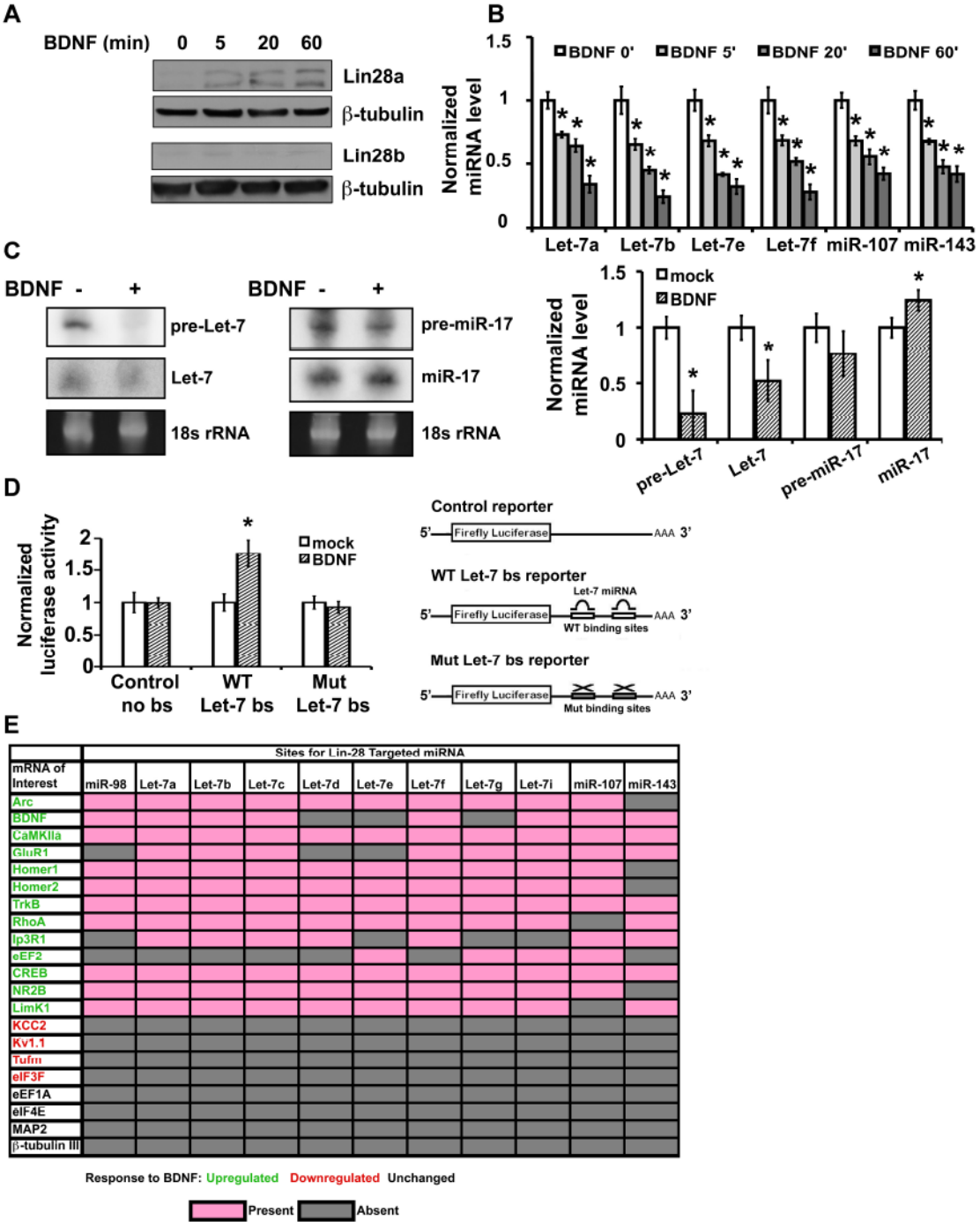
A
BDNF (min) 0 5 20 60
Lin28a
β-tubulin
Lin28b
β-tubulin
B
BDNF 0'
BDNF 5'
BDNF 20'
BDNF 60'
Normalized miRNA level
Let-7a
Let-7b
Let-7e
Let-7f
miR-107
miR-143
C
BDNF - +
BDNF - +
pre-Let-7
Let-7
18s rRNA
pre-miR-17
miR-17
18s rRNA
mock
BDNF
Normalized miRNA level
pre-Let-7
Let-7
pre-miR-17
miR-17
D
Normalized luciferase activity
mock
BDNF
Control no bs
WT Let-7 bs
Mut Let-7 bs
Control reporter
5'
Firefly Luciferase
AAA 3'
WT Let-7 bs reporter
Let-7 miRNA
WT binding sites
Mut Let-7 bs reporter
Mut binding sites
E
Sites for Lin-28 Targeted miRNA
mRNA of Interest
miR-98
Let-7a
Let-7b
Let-7c
Let-7d
Let-7e
Let-7f
Let-7g
Let-7i
miR-107
miR-143
Arc
BDNF
CaMKIIa
GluR1
Homer1
Homer2
TrkB
RhoA
Ip3R1
eEF2
CREB
NR2B
LimK1
KCC2
Kv1.1
Tufm
eIF3F
eEF1A
eIF4E
MAP2
β-tubulin III
Response to BDNF: Upregulated Downregulated Unchanged
Present
Absent

Figure 2.9 Lin28 is required for relief of miRNA-mediated repression and selective induction of BDNF-upregulated mRNA targets.

(A) Loss of Lin28 prevents BDNF-induced decreases in mature Let-7a levels. Mature Let-7a levels were assessed by RT-qPCR from neurons infected with lentivirus expressing either control shRNA (sh-control-2) or shRNA targeting Lin28a (Lin28aKD) and mock- or BDNF-stimulated for 20 min (no Actinomycin-D); normalization was to control mock values (open bar, set as 1.0, n = 3). (B) Effect of Lin28a loss on BDNF-regulated protein synthesis. Immunoblotting of BDNF targets in control or Lin28a-deficient cells, mock- or BDNF-stimulated (left panel). Densitometric quantification of protein levels (right, top panel, n = 6 each condition). Total mRNA levels for both BDNF-upregulated or downregulated targets (right, bottom panel). (C) Effect of Lin28a KD on BDNF-induced association of protein and RNA P-body components. Lysates were immunoprecipitated with anti-GW182 antibody in control (sh-Control-2) or Lin28a-deficient cells, mock- or BDNF-stimulated. Immunoblotting for co-IP'd Ago2 and Dcp1a (left panel) and densitometric quantification (right, top panel, n = 3). Total RNA from GW182 IP of equal lysate inputs from Lin28a knockdown (Lin28aKD) or control (sh-Control-2) neurons; mock (open bars) set as 1.0. BDNF-induced increase in GW182-associated total RNA remains intact after Lin28a knockdown (right, bottom panel). (D) Abundance of BDNF mRNA targets associated with GW182 in control (sh-Control-2) or Lin28a-deficient cells. In Lin28a-deficient neurons, mRNAs for BDNF-upregulated targets remain associated with GW182 in the presence of BDNF while the response of mRNAs for BDNF-downregulated targets is unchanged. 18s rRNA is nondetectable, ND. Error bars represent SEM. * = $p<0.05$ Student's t-test.

Experiments in this figure were performed by Alvin Huang and also published in his thesis.

Figure 2.9

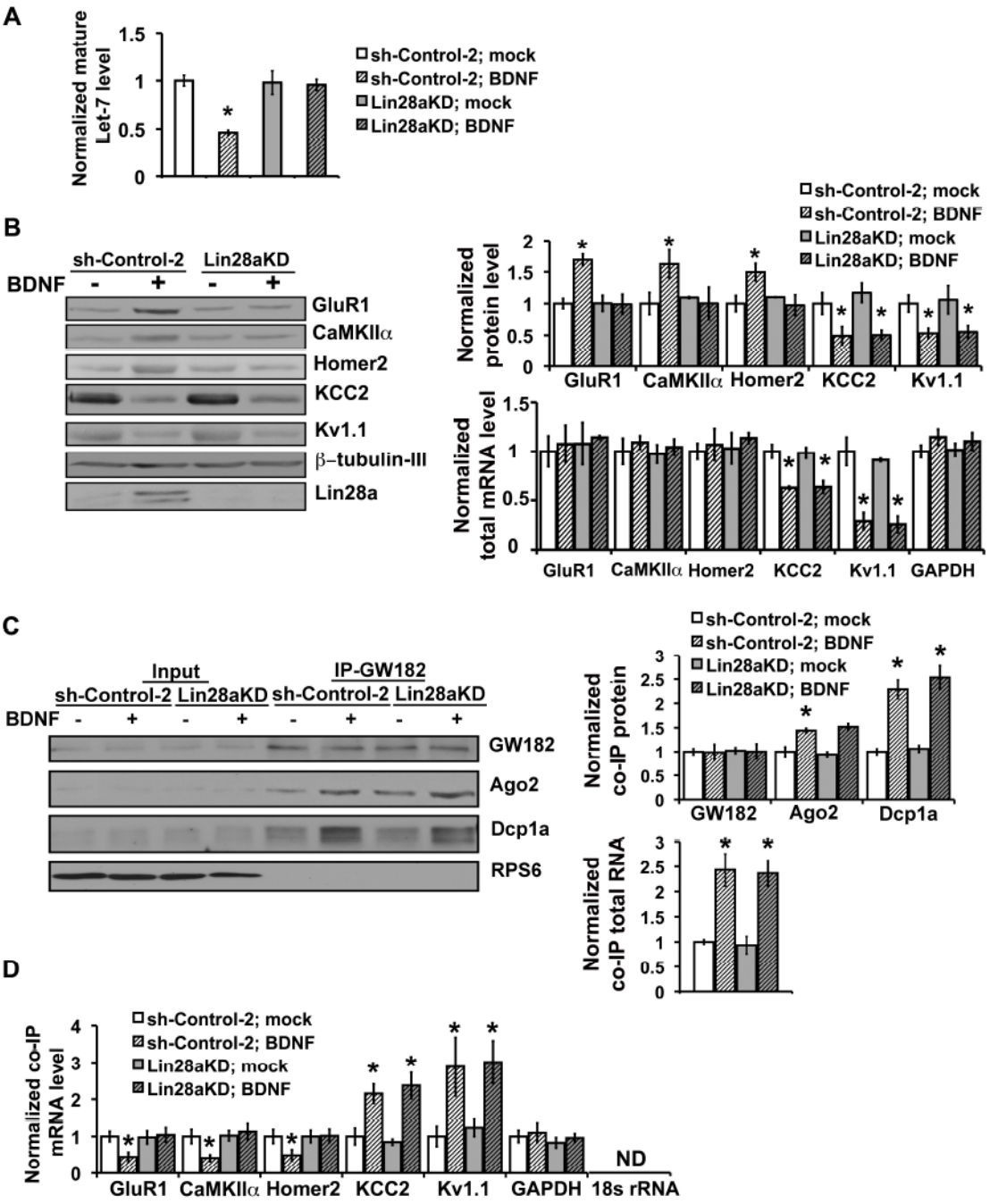

Figure 2.10 Lin28-mediated degradation of Let-7 precursors is required for induction of BDNF-upregulated targets and neuronal outgrowth.

(A) Lentiviral-mediated expression of wild-type (Let-7^{WT}) or Lin28-resistant (Let-7^{LR}) Let-7 pre-miRNAs in neurons produced dose-dependent enhancement of mature Let-7a miRNA levels assessed by RT-qPCR and shown as fold change relative to infection with virus expressing GFP alone (gray bar, set as 1.0); 1x or 2x refers to viral dose (B) Expression of Let-7^{LR}, but not Let-7^{WT}, blocks specificity of BDNF for upregulated targets. Reporter assays in mock- (open bars or BDNF-stimulated (hatched bars) neurons with luciferase constructs fused to the 3'UTR from BDNF-upregulated targets (GluA1 or CaMKIIα) or a downregulated target (KCC2). (C) BDNF-induced dendrite outgrowth requires Lin28-mediated degradation of miRNA precursors. Dendrite complexity is quantitated for neurons expressing Let-7^{WT} (black circles) or Let-7^{LR} (red triangles) following mock- (open shapes) or BDNF- (25 ng / ml, closed shapes) treatment. * = $p < 0.05$ by unpaired Student's t-test or unpaired one-way ANOVA between Let-7^{WT} and Let-7^{LR} in mock and BDNF conditions. (D) Soma size (left panel) and total dendritic length (right panel) did not significantly differ between Let-7^{WT} and Let-7^{LR} in mock or BDNF treatment. Error bars represent SEM. All experiments were done in the presence of Actinomycin D.

Experiments in A-B of this figure were performed by Alvin Huang and also published in his thesis.

Figure 2.10

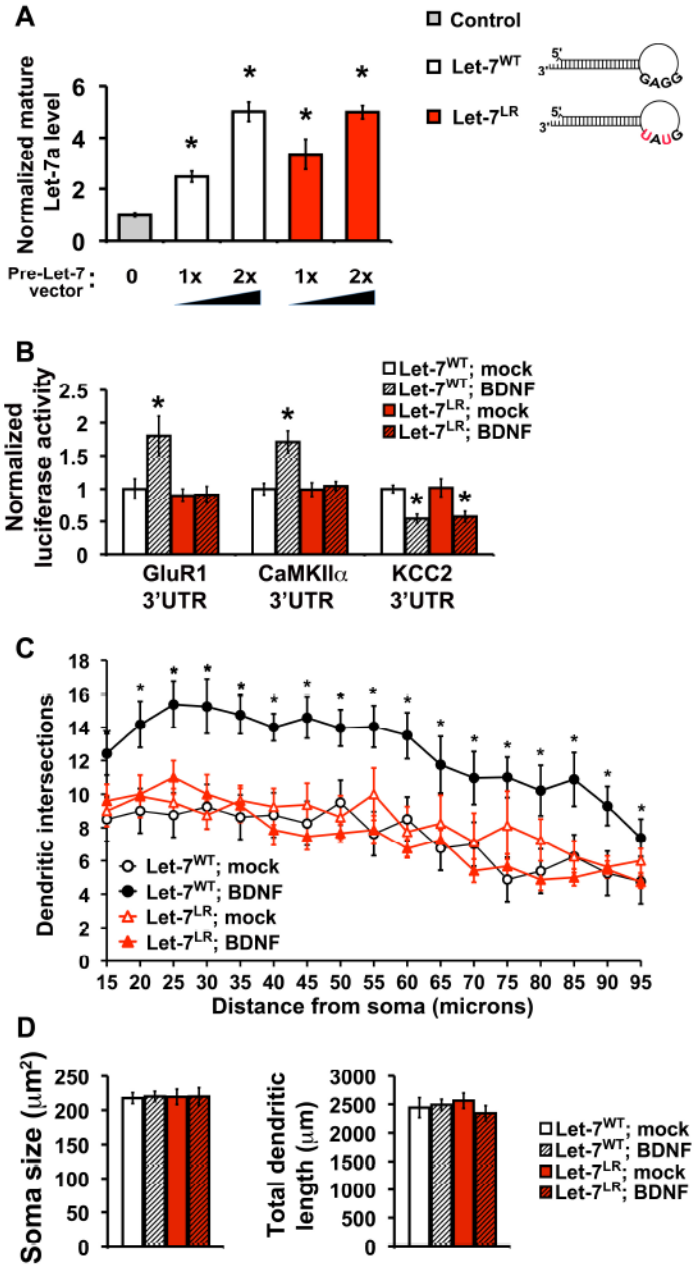
A
Control
Let-7WT
Let-7LR
5'
3'
GAGG
UAUG
Normalized mature Let-7a level
0
2
4
6
*
Pre-Let-7 vector:
0
1x
2x
1x
2x
B
Let-7WT; mock
Let-7WT; BDNF
Let-7LR; mock
Let-7LR; BDNF
Normalized luciferase activity
0
0.5
1
1.5
2
2.5
GluR1 3'UTR
CaMKIIα 3'UTR
KCC2 3'UTR
C
Dendritic intersections
0
2
4
6
8
10
12
14
16
18
15 20 25 30 35 40 45 50 55 60 65 70 75 80 85 90 95
Distance from soma (microns)
Let-7WT; mock
Let-7WT; BDNF
Let-7LR; mock
Let-7LR; BDNF
D
Soma size (μm2)
0
50
100
150
200
250
Total dendritic length (μm)
0
500
1000
1500
2000
2500
3000
Let-7WT; mock
Let-7WT; BDNF
Let-7LR; mock
Let-7LR; BDNF

Figure 2.11 Binding sites for Lin28-regulated miRNAs (let-7, miR-143, and miR-107) in the 3'UTRs of example BDNF-upregulated targets, CaMKIIα and GluA1. The binding region for the miRNA seed sequence (nucleotides 2-7 of the miRNA) is underlined and in red. Complementary base pairing is denoted by uppercase letters, noncomplementary base pairing are in lowercase letters, and G:U wobbles are in blue font. Base pair position indicates the base in the 3'UTR of the mRNA where the miRNA 5' end binds. microRNA seeds having an average phylogenetic conservation score higher than 0.8 are denoted by the pound (#) sign. The conservation score is based on alignment of the longest 3'UTR for 17 vertebrates, including mammalian, amphibian, bird and fish species. Conservation scores range from 0 to 1, with 1 being perfectly conserved and scores over 0.8 predictive of functional relevance (PITA) (Kertesz et al., 2007).

Figure 2.11

A

CaMKIIα 3'UTR

	Base Pair	5'	3'	miRNA
	520	ccAGuGagCcaGgaAcUGCUGCu		miR-107
	617	gugccccacuCacuCUgCCUCu		miR-98
	617	gugccccacuCacuCUgCCUCu		let-7a, let-7f
#	617	gugCcCcacuCacuCUgCCUCu		let-7b
	617	gugccCcacuCacuCUgCCUCu		let-7c
	617	gugccccacuCacuCUgCCUCu		let-7d
	617	ugCcccacuCacuCUgCCUCu		let-7e
	617	gugccccacucacuCUgCCUCu		let-7g
	617	gugccCcacucacuCUgCCUCu		let-7i
	1130	uuaucuagacuuggCAUCUCu		miR-143
	1159	gAgAcUuCAcuaccCUACuUCc		miR-98
	1159	gAgacuuCAcuaccCUACuUCc		let-7a
#	1159	gAgacCuCAcuaccCUACuUCc		let-7b
	1159	gAgaccuCAcuaccCUACuUCc		let-7c, let-7d
	1159	AgaccUCAcuacCCUACuUCc		let-7e
	1159	gAgaccuCAcUaccCUACuUCc		let-7f
	1159	gAgaccuCAcuaccCUACuUCc		let-7g
	1159	gAgacCuCAcuaccCUACuUCc		let-7i
	1193	ccCgAauCAuuGUgCUAuCUCu		miR-98
	1193	ccCGAauCAuugUgCUAuCUCu		let-7a
	1193	ccCgAauCAuugUgCUAuCUCu		let-7b, let-7c, let-7d
	1193	ccgaAUCAuugUgCUAuCUCu		let-7e
	1193	ccCgAauCAuUgUgCUAuCUCu		let-7f
	1193	ccCgaauCAuugUgCUAuCUCu		let-7g, let-7i
	1294	AgaAAcuuAuuUuCCUACuUCA		miR-98
	1294	AgaaAcuuAuuuUcCUACuUCA		let-7a
	1294	AgaaACuuAuuuUcCUACuUCA		let-7b
	1294	AgaaAcuuAuuuUcCUACuUCA		let-7c, let-7d
	1294	gAaacUuAuuuUCCUACuUCA		let-7e
	1294	AgaaAcuuAuUuUcCUACuUCA		let-7f
	1294	AgaaacuuAuuuUcCUACuUCA		let-7g
	1294	AgaAaCuuAuuuUcCUACuUCA		let-7i
	1340	ucuAuUgugcCcGcCUgCCUCc		miR-98
	1340	ucuauUgugcCCGcCUgCCUCc		let-7a
	1340	ucuauugugcCCGcCUgCCUCc		let-7b
	1340	ucuauUgugcCCGcCUgCCUCc		let-7c
	1340	ucuauUGugcCCGcCUgCCUCc		let-7d
	1340	cuaUugugcCCGCCUgCCUCc		let-7e
	1340	ucuauUgugccCGcCUgCCUCc		let-7f
	1340	ucuaUUgugccCGcCUgCCUCc		let-7g
	1340	ucuauugugccCGcCUgCCUCc		let-7i
	1554	UGgcucuugUaUggAAUGCUGta		miR-107
#	1751	aacUuGGACU-UACGUUGCUGCc		miR-107
#	1754	uuggAcuuAcgUUgCUgCCUCu		miR-98
#	1754	uuggAcuuAcguUgCUgCCUCu		let-7a
#	1754	uuggACuuAcguUgCUgCCUCu		let-7b
#	1754	uuggAcuuAcguUgCUgCCUCu		let-7c, let-7d, let-7f
#	1754	uggucUuAcguUgCUgCCUCu		let-7e
#	1754	uuggacuuAcguUgCUgCCUCu		let-7g
#	1754	uuggaCuuAcguUgCUgCCUCu		let-7i
#	1993	cGcUccaCuCUcUcaAAUcCUGc		miR-107
	2008	GCugccCAGgGaCaaGUACAGg		let-7g*

GluR1 3'UTR

	Base Pair	5'	3'	miRNA
#	252	aGAUGGUC-a-CUaacuCuAUGCUGCa		miR-107
	698	GuaacuguGaagagCAUCUCA		miR-143
	737	aaAGGGgGGaUGGgCagaGUACAGU		let-7g*
	1067	cUgGcauaaGaGgCAAUGuUGCc		miR-107
	1691	ucUGGCuUAuuCUcCUAcCCUCu		let-7i
	1824	cAGCGgacaacCacCAUCUCu		miR-143
#	2266	GaGAAaGaAGuUAccUUGUAUua		let-7b*, let-7f*
#	2267	aGAAAGAaGuUAccUUGUAUua		let-7a*
#	2267	agAAAGAaGuUAccUUGUAUua		let-7c-2

Capital letter = complementary
Lower case letter = noncomplentary
Seed sequence
G:U wobble
= >0.8 conservation score

Figure 2.12 Loss of P bodies in neurons expressing dominant-negative form of GW182 (DNGW182) inhibits BDNF-induced dendritic arborization.

(A) Representative images of neurons expressing untagged mCherry and either GFP (top panels) or GFP-DNGW182 (bottom panels) following 72 hrs of mock- or BDNF- (25 ng / ml) treatment. Images show red channel (mCherry) only. Scale bar represents 50 mm. (B) Sholl analysis representing dendritic complexity at increasing distances from the cell body for GFP- (circles) or GFP-DNGW182- (triangles) expressing neurons following mock- (open shapes) or BDNF- (25 ng / mL, closed shapes) treatment. * = $p < 0.05$ by unpaired one-way ANOVA; Mann-Whitney U test modified Bonferroni correction. (C) Total dendritic length (top panel) and soma size (bottom panel) are not significantly different between control and GFP-DNGW182-expressing neurons following mock or 25 ng / mL BDNF treatment. Error bars represent SEM. mock, n=30 cells; BDNF, n=27; GFP-DNGW182, mock, n=21; GFP-DNGW182, BDNF, n=27.

Experiments in this figure were performed by Elizabeth Eyler and also published in her thesis.

Figure 2.12

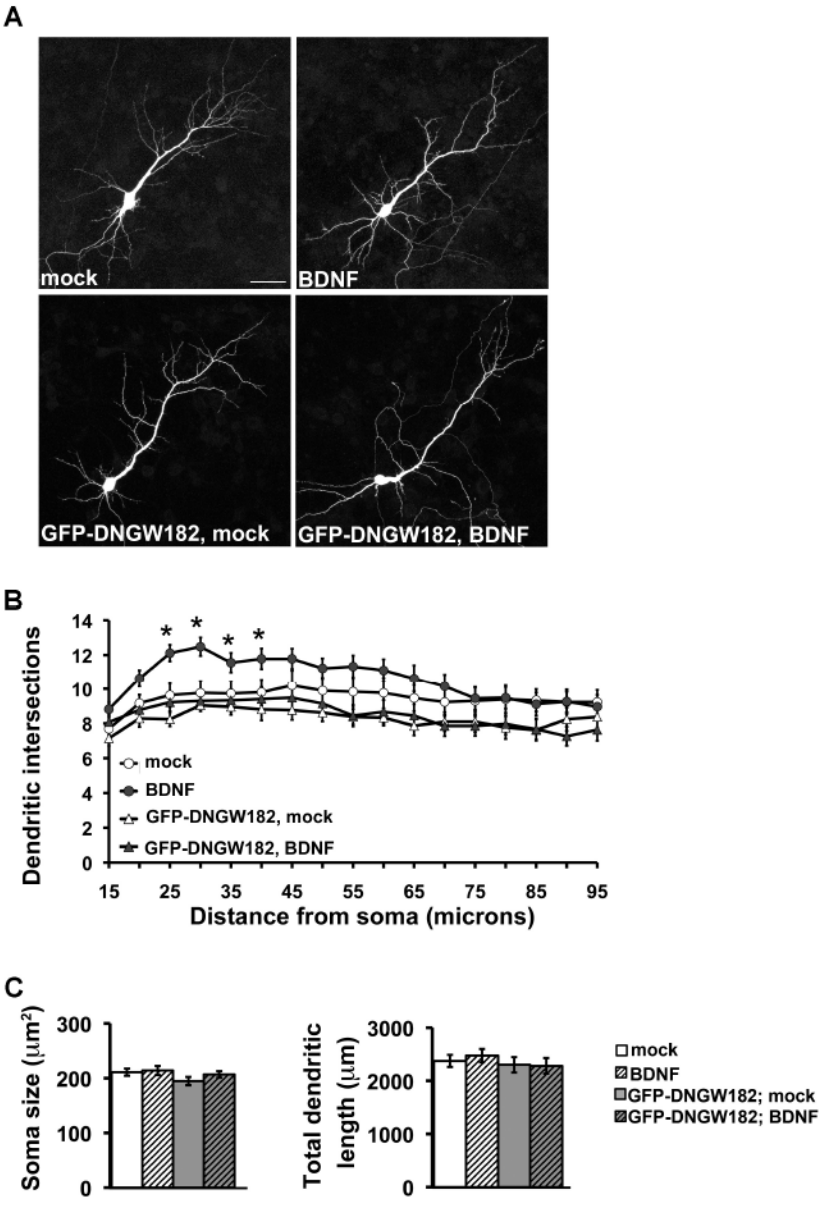
A
mock
BDNF
GFP-DNGW182, mock
GFP-DNGW182, BDNF
B
Dendritic intersections
Distance from soma (microns)
mock
BDNF
GFP-DNGW182, mock
GFP-DNGW182, BDNF
C
Soma size (μm²)
Total dendritic length (μm)
mock
BDNF
GFP-DNGW182; mock
GFP-DNGW182; BDNF

Figure 2.13 Proposed model for the determination of mRNA target specificity in BDNF-mediated translation.

Left panel: In the absence of BDNF stimulation, both Lin28-targeted precursor miRNAs (GGAG, red) and non-Lin28-targeted precursor miRNAs (blue) are processed into mature miRNAs. mRNAs targeted for translational repression or degradation by these mature miRNAs accumulate in P-bodies. Right panel: BDNF induces both positive and negative regulation of miRNA biogenesis. In the presence of BDNF, TRBP phosphorylation and Dicer protein levels increase leading to a general enhancement of processing of precursor miRNAs (blue) into mature miRNAs. Increased abundance of mature miRNAs leads to an increase in targeting of mRNAs for repression and increases the number of P-bodies in cells. However, Lin28a protein levels also increase in response to BDNF (far right). Because Lin28a selectively *prevents* processing of its targeted precursor miRNAs (GGAG, red) into mature miRNAs, this population of miRNAs is diminished and mRNA targets of these miRNAs are no longer efficiently repressed and become more readily available for translation. The differential effects of BDNF on distinct miRNA populations can explain the selective increase in translation of only specific mRNAs in response to BDNF.

Figure 2.13

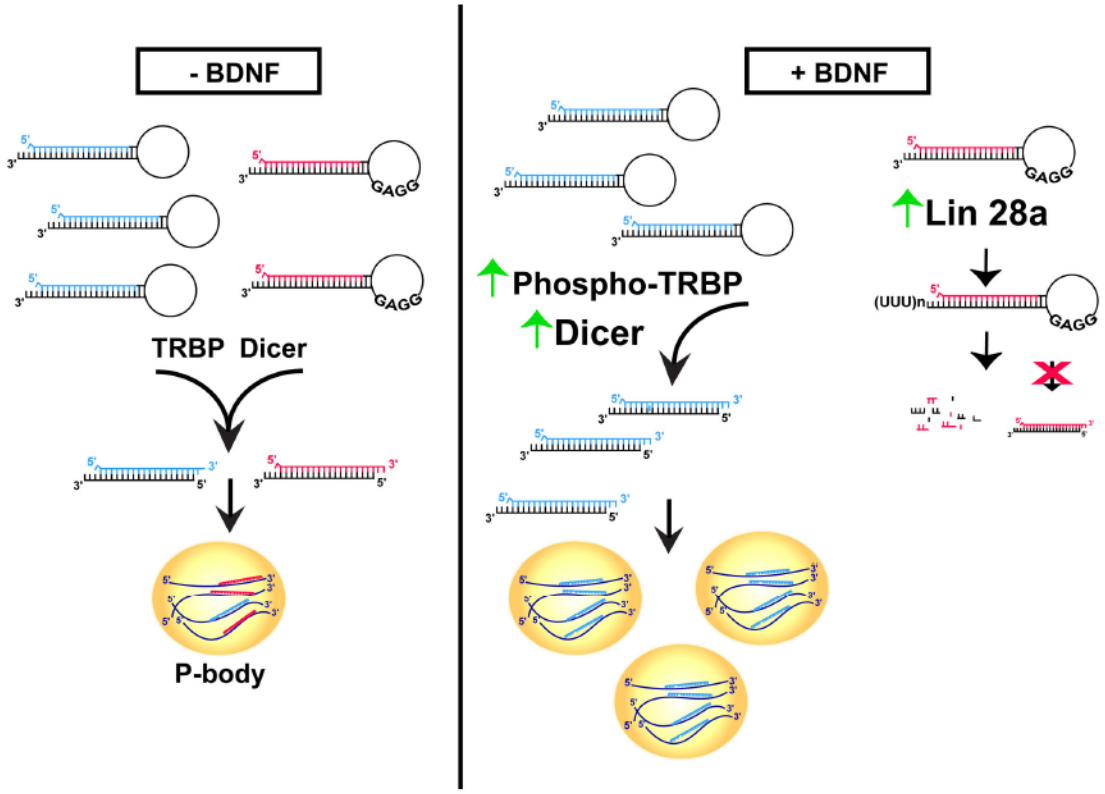
- BDNF
GAGG
GAGG
TRBP Dicer
P-body
+ BDNF
Phospho-TRBP
Dicer
GAGG
Lin 28a
(UUU)n
GAGG

Experimental Methods

Hippocampal cultures and stimulation

All animal procedures conformed to animal care guidelines approved by the Institutional Animal Care and Use Committee. Dissociated hippocampal cultures were prepared from postnatal day 0 (P0) mice as previously described (Meffert et al., 2003). Knockdown was by lentiviral-mediated delivery of shRNA to cultures at multiplicity of infection of 5 – 10, 48 hr before imaging or 4 – 5 days for GW182. Cultures were preincubated 10 – 20 min. and mock- or BDNF-stimulated (100 ng/ml BDNF) in the presence of Actinomycin-D (0.5 μg/ml), unless indicated otherwise.

RNA analysis

For RT-qPCR, TaqMan Gene Expression and MicroRNA Assays (Applied Biosystems) were performed with quantitation by the standard-curve method and no preamplification, RQ was calculated as $2^{-DCtBDNF} / 2^{-DCtmock}$ where DCt = (cycle threshold for miRNA of interest) – (cycle threshold for reference control).

Reporter Assays

The following CXCR4 siRNA/miRNA reporter assay constructs (Addgene) were used: siRNA reporter (PCD FL1P, Plasmid 12567), miRNA reporter (PCD FL4X, 12565), control luciferase reporter (PCD FL0X, 12563), and CXCR4 shRNA (pLKO.1 puro CXCR4 siRNA-2, 12272) (Wang et al., 2006). Let-7 luciferase reporters with wild-type or mutated Let-7 miRNA binding sites were gifts from G. Hannon (Liu et al., 2005b).

3'UTR reporters were constructed by inserting 3'UTRs from GluA1, CaMKIIα or KCC2 downstream of luciferase in pGL3-Control vector (Promega). A Lin28-resistant Let-7 pre-miRNA was generated by mutation of the conserved Lin28 "GGAG" recognition motif to "GtAt" in the terminal loop of pLV-hsa-let-7a-1 (Biosettia).

Imaging and quantification

For live cells: Confocal images of hippocampal pyramidal neurons (excitatory, determined by morphology) in 0.24 – 0.3 mm Z sections were acquired using a 40x, 1.3 NA, EC Plan Neofluoar (whole cells) or a 100x, 1.4 NA Plan Apochromat oil immersion objective (dendrites) on a Yokogawa spinning disk system (Cell Observer, Carl Zeiss) at 37°C in Tyrodes buffer (in mM: 119 NaCl, 5 KCl, 2 $CaCl_2$, 0.2 $MgCl_2$, 30 Glucose, 25 Hepes, .01 Glycine, pH 7.4). EBFP2 was excited at 405 nm and emissions collected at 425 - 475 nm. GFP was excited at 488 nm and emissions collected at 500 – 550 nm; mCherry was excited at 561 nm and emissions collected at 598 - 660 nm. Laser power and exposure time were adjusted to minimize phototoxicity and avoid saturation. All experiments were from a minimum of 3 independent cultures, and no more than 3 neurons per dish; the experimenter was blinded to conditions during analysis.

For fixed cells, confocal images were acquired in 0.3 mm (dendrites) or 1.7 mm (whole cells for arborization) Z sections on an LSM5 Pascal system (Carl Zeiss) using a 63x, 1.4 NA Plan Apochromat oil immersion objective and 2X optical zoom (dendrites) or using a 25x, 0.80 NA Plan-Neofluor multi-immersion objective and 0.7x – 1x optical zoom (for whole cells). GFP was excited at 488 nm and emissions collected at 505 - 530 nm; mCherry was excited at 543 nm and emissions collected above 560 nm. Laser power

and exposure time were adjusted to minimize photobleaching and avoid saturation. All experiments were from a minimum of 3 independent cultures and no more than 3 neurons per dish

Z-stacks containing the entire neuron or process of interest were analyzed using Imaris 7.0.0 (Bitplane) and ImageJ software. Automated analysis of P-body numbers was conducted using Spots detection in Imaris. A quality filter and intensity median filter for the red channel were used to restrict detection of puncta within dendrites only. Colocalization analysis was performed using the Colocalize Spots function. The percent colocalization of P-body components was calculated by subtracting the number of colocalized BFP-Dcp1a or YFP-Pat1b puncta from the total number of BFP-Dcp1a or YFP-Pat1b puncta and multiplied by 100. The percent of colocalized fluorescence was calculated for each P-body component by first summing the aggregate fluorescence values that co-localized with the other P-body marker in 'spots', then dividing this quantity by the value of the total fluorescence intensity within the dendrite for that channel, and multiplying by 100. The Surfaces tool in Imaris was used to create a representation of the dendrite in order to determine total fluorescence intensity corresponding to the dendrite region alone. The red channel (soluble mCherry expression) was used as the source channel to compute the Surfaces. Total fluorescence of a dendritic segment was calculated by summing the intensity fluorescence values of all of the Surfaces representing a single dendrite. Sholl analysis was performed using the Sholl analysis plugin in ImageJ (A. Ghosh lab) from Z-compressed projections traced semi-automatically in NeuronJ. For analysis, dendritic intersections were counted using a

circle of 15 μm diameter centered on the cell soma and subsequent circles of increasing 5 μm diameter increments.

Immunoblotting

Primary cultures of mouse hippocampal neurons (DIV 14~15) were incubated in serum-reduced medium (0.5% B27 supplement) for 2 hours, followed by 0.5 μg/ml Actinomycin-D for 10~30 min. Bath application of BDNF (100 ng/ml) was for designated periods (5 min ~ 2 hours). The cultures were washed 3 times and harvested on ice with lysis buffer (50 mM Hepes, 150 mM NaCl, 10% Glycerol, 1 mM EDTA, 1% Triton-X-100, 0.2% SDS) plus freshly added protease inhibitor cocktail (Roche) and PMSF. Protein concentration was determined by Bradford Assay. If required, lysates were treated with Lambda Protein Phosphatase according to manufacturer's instructions (New England Biolabs P0753S). Equal amounts of lysate protein were resolved on SDS-PAGE gels, and electrotransferred to PVDF membrane. Membrane was blocked with 5% milk in Tris-buffered saline tween 20 (TBST) and probed with primary antibodies in 5% milk or BSA in TBST: GluA1 (Millipore AB1504), CaMKIIα (Zymed 13-7300), Homer2 (gift of P.Worley), KCC2 (Upstate 07-432), Kv1.1 (NeuroMab 73-007), btubulin (U.Iowa DSHB, clone E-7), GAPDH (gift of S.Snyder), GW182 (18033 gift of M. Fritzler or Abcam ab84403), Dcp1a (gift of J. Lykke-Andersen or NeuroMab clone3G4), phospho-ERK ½ (Sigma M 7802), Dicer (NeuroMab clone N167/7), TRBP (Abcam ab72110), Lin28a (Cell Signaling A177), Lin28b (gift of E. Moss or Cell Signaling 5422), Arc (SantaCruz 17839), mCherry (Clontech 632496), GFP (NeuroMab N86/8).

^{35}S-labelling

Cultured neurons were pre-incubated in media containing reduced-serum and Actinomycin-D as previously described, followed by washing and incubation for 10 min with methionine- and cysteine-free DMEM (Mediatech, Inc.), and ^{35}S labeling in the same DMEM with the addition of ^{35}S-methionine/cysteine (^{35}S Met/Cys EasyTag Mix, Perkin Elmer) to a final concentration of 100 μCi/ml. Mock- or BDNF stimulation was for 2 hours. Cells were washed and lysed with lysis buffer (see immunoblotting). Lysates were centrifuged and collected supernatants subjected to Bradford assay. To asses newly synthesized proteins, 200-500 μg of lysates proteins were precipitated with 10% trichloroacetic acid (TCA) for 1 hour on ice in the presence of 0.5% deoxycholate (DOC) to remove interfering phenol red. After centrifugation, protein pellets were washed with ice-cold 95% ethanol, solubilized in denaturing buffer (50 mM Tris pH 8.3, 5 mM EDTA, 0.05% SDS, 6M urea), and subjected to liquid scintillation counting (Econofluor, New England Nuclear, Inc.). ^{35}S Disintegration per minute (DPM) was used to quantitate protein synthesis after subtraction of background readings

Immunopurification of GW182

Proteins and mRNAs associated with P-body component GW182 were isolated through immunoprecipitation of GW182 by modification of previously published protocols (Keene et al., 2006; Moser et al., 2009). Primary cultures of mouse hippocampal neurons (DIV 14-15) were incubated in serum-reduced medium (0.5% B27 supplement) for 2 hours, followed by 0.5 μg/ml Actinomycin-D for 10~30 min. and mock or BDNF-stimulation for 30~60 min. Cell lysates were harvested in polysomal lysis buffer (100

mM KCl, 5mM $MgCl_2$, 10 mM HEPES pH 7.0, 0.5% NP-40) with protease inhibitor cocktail and freshly added 20 mM EDTA, 1mM DTT, 100 U/ml RNase inhibitor (RNaseOut, Invitrogen) and 400 mM Vanadyl ribonucleoside complexes (SIGMA). Lysates were centrifuged and the supernatants pre-cleared by one-hour incubation with recombinant protein G beads pre-washed in NT2 buffer (50 mM Tris-HCl pH 7.4, 150 mM NaCl, 1 mM MgCl2, 0.05% NP-40). Antibody coating of protein G beads was carried out with antiserum against GW182 (18033, gift of M. Fritzler) or control isotype-specific serum in NT2 buffer plus protease inhibitor for 4 hours after blocking with NT2 buffer plus 5% BSA and 1mg/ml heparin for 1 hour. For immunoprecipitation (IP), equal amounts of lysate protein (2 - 5 mg) was incubated with antibody-coated beads and tumbled for 4 hours at 4°C, followed by washing. RNAs were recovered from GW182 immunoprecipitates by Tri-Reagent as described below.

Recovered RNAs were resuspended in nuclease-free water, measured for RNA concentration, and immediately reverse transcribed into cDNA using a combination of random decamers and oligo(dT) primers. RT-qPCR was carried out as described below. To examine proteins co-immunoprecipitated with GW182, the washed IP beads were incubated in sample buffer at 95°C for 5 minutes and subjected to SDS-PAGE electrophoresis and immunoblotting.

RNA extraction, quantitative PCR for individual mRNA and miRNA species

Total RNA from primary cultures of mouse hippocampal neurons was isolated by Tri-Reagent (Molecular Research Center, Inc.) according to the manufacturer's protocol. Cultures were either homogenized in Tri-Reagent directly, or were first lysed in lysis

buffer plus RNase inhibitor (if protein from the same sample was required) followed by Tri-Reagent addition to a portion of lysate. RNA pellets were air-dried and resuspended in nuclease-free water. RNA concentration and quality were assayed by spectrophotometric measurements at an optical density (OD) 260/280/230 nm.

For analysis of mRNA abundance: 1 μg of RNA was immediately reverse-transcribed into cDNA with a TaqMan reverse transcripton kit (Applied Biosystems) and a mixture of random decamer and oligo(dT) primers in a final volume of 30 μl and subjected to TaqMan Gene Expression Assays (Applied Biosystems) for GluA1 (assay ID: Mm00433753_m1), CaMKIIα (Mm00437967_m1), Homer2 (Mm01314936_m1), KCC2 (Mm00803929_m1), Kv1.1 (Mm00439977_s1),GW 182 (Mm00523487_m1), GAPDH (Mm99999915_g1), and b-tubulin-III (Mm00727586_s1). RT-qPCR was performed using a Stratagene Mx3000P machine and software in 20 μl reactions on a 96-well optical plate at 95°C for 5 min, followed by 40 cycles of 95°C for 30 sec, 55 °C for 1 min and 72 °C for 30 sec. The threshold and threshold cycle (Ct) values were determined using default settings. Standard curves were constructed and used for quantitation of target transcript abundance. In this method, 1:5 dilution series of an independent Standard sample are amplified to generate a curve that relates the initial quantity of the specific target in the Standard samples to the Ct. The standard curve is then used to derive by interpolation the initial sample template quantities based on their Ct values. All derived quantities were further normalized to neuron-specific β-tubulin III, whose translational status is unchanged by BDNF (Schratt et al., 2004). Data were plotted as fold change relative to mock control.

For individual microRNA abundance assays (Applied Biosystems), 100 ng of total isolated RNA was prepared for reverse transcription with stem-looped primers specific for individual mature miRNAs in a final volume of 15 µl according to manufacturer's protocol; 4°C for 5 min, 16°C for 30 min, 42°C for 30 min, 85°C for 5 min. and subjected to TaqMan MicroRNA Assays (Applied Biosystems) for Let-7a (assay ID: 000377), Let-7b (002619), Let-7e (002406), Let-7f1 (000382), miR-107 (000443) and miR-143 (0024). RT-QPCR was performed using a Stratagene Mx3000P machine and software with quantities derived by standard-curve quantitation method, as described. The abundance of non-coding 18s rRNA in each sample was used as an internal control to normalize all miRNA species.

miRNA profiling arrays and analysis

Murine hippocampal cultures were preincubated for 10-20 minutes with 0.5 µg / ml Actinomycin D and either mock- or BDNF- (100 ng / ml) stimulated for 30 minutes before harvesting.

For miRNA arrays, 1 µg of total RNA for each sample was reverse-transcribed with stem-looped Megaplex RT Primers (Applied Biosystems) in a final volume of 7.5 µL according to manufacturer's instructions: preincubation at 4°C for 5 min; 16 °C for 2 min, 42 °C for 1 min, 50 °C for 1 sec, 40 cycles; 85 °C for 5 min. The entire cDNA RT product (7.5 µl) was subjected to RT-qPCR on an Applied Biosystems 7900HT Fast Real-Time PCR system using Taqman Rodent MicroRNA Array A. Data were compiled in SDS RQ Manager 1.2.1 (Applied Biosystems) and analyzed in Data Assist 2.0 (Applied Biosystems). Thresholds and cycle threshold (Ct) values were determined using

default settings and the maximum allowable Ct value was set at 35.0 inclusive. Data were normalized by arithmetic mean using MammU6 (4395470) and snoRNA202 (4380914) reference RNAs as controls. miRNA array data reposited with the NCBI Gene Expression Omnibus (GEO). Initial experiments using an alternative miRNA array platform (Geniom microfluidic miRNA profiling, Febit Inc.) similarly indicated a BDNF-mediated increase in the majority of detectable mature miRNA species.

Lentivirus preparation

Lentiviral stocks were prepared as previously described (Lois et al., 2002). HEK-293T cells were trypsinized and seeded onto 15 cm plates, then grown at 37°C in 1X DMEM supplemented with 10% fetal bovine serum, penicillin/streptomycin, and glutamine to a confluency of ~65-85% before transfection by calcium phosphate. For each transfection reaction, 7.5 μg of the viral construct plus 7.5 μg each of the pMDLg/pRRE, RSV-Rev, and VSV-G viral packaging plasmids were mixed with 248 μL 2M $CaCl_2$ and dH_2O to a final volume of 2 mL. 2 mL of 2X HBSS (50 mM Hepes, 280 mM NaCl, 1.5 mM Na_2HPO_4 pH 7.06-7.1) was then added to each reaction and bubbled vigorously by pipetting up and down ~15-20 times. The mixture was then dripped onto cells and the dish rocked back and forth to evenly distribute the transfection complexes before returning the cells to incubate at 37°C. ~8 hours after transfection, media was aspirated and replaced with 15 mL fresh media per dish. Cells were allowed to expand and produce virus for ~40-48 hours and the supernatant collected. Recovered supernatant was centrifuged for 5 minutes at 900 rpm (150 g) to pellet cell debris and filtered with a 0.45 μm filter before concentration by ultracentrifugation (25900 rpm in a Beckman-Coulter

swinging bucket SW32Ti rotor for 90 minutes at 4°C). Supernatant was discarded and viral pellets were resuspended in 100 μL cold PBS (plus 1 mM $CaCl_2$ and 0.5 mM $MgCl_2$). Virus was aliquoted and frozen at 80°C or used immediately.

Luciferase Reporter Assays

The siRNA- or miRNA-reporter constructs harbor one perfectly matched or four bulged CXCR4 siRNA target sites, respectively, in the 3'UTR of firefly luciferase mRNA. In the presence of CXCR4 shRNA, perfectly matched sequences are cleaved by siRISC and bulge-containing sequences are targets for translation suppression by miRISC. miRNA and siRNA pathway function were assayed in cells transiently transfected and expressing either the miRNA or siRNA reporters alone (no sh-CXCR4), or co-expressing either of the reporters and CXCR4 shRNA with or without P-body disruption (sh-Control-1 or GW182 KD, GFP or GFP-DNGW182, sh-Control-2 or LSm5 KD).

Let-7 luciferase reporters (gift of G. Hannon) harbor a wildtype or a mutant Let-7 miRNA binding site. The Let-7 miRNA binding sites are derived from a short 3'UTR segment of C. elegans Lin41 mRNA containing two adjacent proven Let-7 miRNA biding sites and are cloned into 3'UTR of firefly luciferase in a pcDNA backbone. Mutations in seed regions of both Let-7 binding sites were made for a negative control reporter, which was documented not regulated by endogenous Let-7 miRNAs.

Co-transfection of the pCSK-lacZ vector, which constitutively expresses b-galactosidase and is not regulated by shRNA, served to normalize transfection efficiency and extract recovery for each sample in all reporter assays. The DNA amounts used for each well (24 well plate) were 15 ng of any luciferase reporter, 85 ng of β-gal (CSK-

LacZ), and/or 75 - 300 ng of CXCR4 shRNA. Each reporter experiment included extracts from cells transfected with pcDNA3.1 alone as a reference control.

44 hours post-transfection, hippocampal cultures were treated with serum-reduced media (0.5% B27) and Actinomycin-D (0.5 μg/ml) as previously described, followed by BDNF stimulation 100 ng/ml for 4 hours. Cell lysates were collected in 1X lysis buffer (reporter lysis buffer, Promega), and luciferase (Promega) and chemiluminescent β-gal (Roche) reporter assays carried out according to manufacturer instructions using a plate-reading luminometer (Perkin Elmer). Samples were compared by subtracting the background activity of the reference control, and then normalizing the luciferase activity of each sample to its β-gal activity. When required, fold change was calculated by dividing normalized stimulated samples by normalized unstimulated samples.

Plasmids and fluorescently tagged constructs:

GFP-Dcp1a was a generous gift from J. Lykke-Andersen (UCSD). GFP-Staufen was a generous gift from L. DesGroseillers (U. Montreal). YFP-Pat1b was a generous gift from G. Stoecklin (U. Heidelberg). BFP-Dcp1a was generated by subcloning with EBFP2. GFP-hAgo2 (11590) and GFP-GW182Δ1 (DNGW182, 11592) were purchased from Addgene.

Cloning of let-7a-1 GGAG mutant

A let-7a-1 precursor miRNA with the conserved Lin28 "GGAG" recognition motif mutated to "GtAt" was generated by two-step PCR site-directed mutagenesis from the pLV-hsa-let-7a-1 vector (Biosettia, mir-p001) using the following primers:

TATAGGATCCTCACACAGGAAACCA (forward, outside; P1)

TATAGCTAGCGCTGCACTACATCTC (reverse, outside; P2)

CCCACCACTGGTATATAACTATACAATCTACTG (forward, inside; P3)

TGTATAGTTATATACCAGTGGTGGGTGTGA (reverse, inside; P4)

The P1 and P4 primers and the P2 and P3 primers were paired for the first round of PCR reactions. The products of these PCR reactions were then included with the P1 and P2 primers for the second round of PCR reactions to generate the final "GtAt" mutant let-7a-1 fragment. This fragment was then subcloned into the BamHI and NheI sites of the parent plv-hsa-let-7a-1 parent vector.

Statistical and bioinformatics analysis

Student's t-tests were performed in Excel. Nonparametric unpaired one-way ANOVA with post hoc Bonferroni analysis, and Mann-Whitney U tests were performed in OpenStat 11.9.08 (Softonic) or STATA 10.0 (StataCorp.).

Chapter III: TRBP mediates differential induction of Lin28 paralogs by neurotrophin signaling

Background

Appropriate regulation of neuronal and synaptic protein composition in response to BDNF is critical for normal brain function. Our lab has found that specificity in BDNF-induced translation is achieved through regulation of the miRNA biogenesis pathway (Huang et al., 2012). Negative regulation of miRNA biogenesis occurs through BDNF-induced upregulation of Lin28 that blocks the processing a subset of precursor miRNAs (e.g. Let-7 family miRNAs). This allows for mRNA targets of these miRNAs to undergo a relief of translational repression and enhanced translation in response to BDNF. We found that regulation of the miRNA biogenesis pathway through induction of Lin28a is essential for BDNF to correctly specify the protein synthesis of its upregulated targets. Positive regulation of miRNA biogenesis, and enhanced abundance of non-Let-7 family miRNAs, also occurs as a result of BDNF-induced increase in Dicer protein levels; this can explain how the majority of mRNAs are excluded from translation in response to BDNF. Lin28 has previously been considered to be absent from differentiated cells making our finding that Lin28 function is critical for the effects of BDNF on plasticity-related processes including translation regulation and dendrite morphogenesis exciting and unexpected.

This chapter of my thesis describes my work to uncover the mechanism of neurotrophin-induced upregulation of Lin28 in mature neurons, and is part of ongoing work in the lab which will be submitted for publication in the next few months. The goal of this portion of my thesis and ongoing work, has been to elucidate the signaling

mechanisms responsible for the rapid and transcription-independent induction of Lin28a by BDNF. By focusing on the critical initiating events in this pathway, we hope to reveal vital regulatory points that may be essential to the physiological impact of BDNF on brain function. Uncovering this mechanism may have important implications in the field of stem cell, cancer, and developmental biology, given the critical role Lin28a plays in these cellular contexts.

Lin28 paralogs: Lin28a and Lin28b

Unlike in *C. elegans* where a single Lin28 gene is found, vertebrates have a Lin28a paralog, Lin28b, which shares ~77% identity with Lin28a at the protein level and also functions to block Let-7 miRNA biogenesis. In humans the Lin28a gene encodes a 209 amino acid (aa) protein while the Lin28b protein is 250 aa. Despite a high degree of homology in structure, Lin28a and Lin28b exert their effects on let-7 miRNAs through distinct mechanisms primarily due to their differential subcellular localizations. Lin28a is primarily cytoplasmic whereas Lin28b is predominantly localized to the nucleus due to its nuclear localization signals found in the extended C terminus region of Lin28b (Piskounova et al., 2011). While Lin28a blocks the processing of pre-Let-7 family precursors into mature Let-7 miRNAs, Lin28b acts upstream to block processing of pri-Let-7 family miRNAs to pre-Let-7 by the DGCR8 and Drosha. Like Lin28a, Lin28b also functions as an oncogene and is associated with advanced human malignancies. Interestingly, a number of primary human cancers overexpress *either* Lin28a or Lin28b. As well as elucidating the mechanism of rapid BDNF-mediated Lin28a induction, an additional goal of this project is to provide insight into the distinct biological roles of

these paralogs, which may help us understand how their re-activation in different cancer types is uniquely regulated.

Results

BDNF induces rapid posttranscriptional upregulation of Lin28a protein but has no effect on its paralog Lin28b

To initiate our investigations into the regulation of Lin28a by BDNF we first addressed the question of whether transcription is necessary for BDNF-induced upregulation of Lin28a in hippocampal neurons. We treated hippocampal neurons with Actinomycin-D to inhibit new transcription and either mock-stimulated or BDNF-stimulated for 5, 20, or 60 minutes. Lin28a protein level was significantly elevated in response to 5, 20, and 60 minute-stimulation with BDNF in both the presence and absence of Actinomycin-D (Figure 3.1). There was no statistically significant difference between Lin28a induction in the presence of Actinomycin-D compared to vehicle control condition. This result indicates that transcription is not required for the full effect of BDNF on the rapid induction of Lin28a protein levels during this timecourse of BDNF stimulation. To further test the role of transcription in rapid BDNF-mediated Lin28a induction, we used qRT-PCR assays (TaqMan, Applied Biosystems) to evaluate Lin28a mRNA levels in BDNF-stimulated hippocampal neurons. We found that BDNF has no significant effect on Lin28a mRNA levels at 5-,20-, and 120-minute time points (Figure 3.1.B). These findings collectively indicate that BDNF acts post-transcriptionally to induce Lin28a protein levels and prompted us to investigate whether BDNF might regulate Lin28a mRNA translation or Lin28a protein stability. We tested whether BDNF

could elevate Lin28a protein levels from an exogenous FLAG-tagged construct containing the Lin28a protein-coding sequence (FL-Lin28a), but lacking the regulatory Lin28a untranslated regions (5' and 3' UTRs). The response of this protein-coding region only construct was compared to endogenous Lin28a to independently assess BDNF effects at the level of protein or translation. We found that BDNF rapidly elevates the levels of FL-Lin28a at 5-, 20-, and 60-minute time points in a manner that is indistinguishable from endogenous Lin28a (Figure 3.1.C) This finding demonstrates that the initial induction by BDNF requires only the protein-coding region of Lin28a.

We previously reported that endogenous Lin28b protein level is not affected by BDNF stimulation (Huang et al. 2012). Given the current evidence that Lin28b has a differential subcellular localization than Lin28a, we wanted to test whether BDNF treatment would alter the levels of a Lin28b nuclear localization signal (NLS) mutant that localizes to the cytoplasm. To answer this question we expressed either wildtype FLAG-tagged Lin28b (Fl-Lin28b) or a FLAG-tagged Lin28bΔNLS and compared this to endogenous Lin28b levels in response to 5, 20, or 60 minute BDNF stimulation in the presence of Actinomycin-D. Our results show that BDNF had no effect on endogenous Lin28b, Fl-Lin28b, or Fl-Lin28bΔNLS protein level (Figure 3.1.D). This result demonstrates that Lin28a and Lin28b are subject to differential posttranscriptional regulation by BDNF, and prompted us to further investigate whether BDNF might act at the protein level to selectively induce Lin28a. Ongoing experiments are addressing the protein half-lives of Lin28a and Lin28b and how these are altered by BDNF.

BDNF modulates TRBP phosphorylation to stabilize Lin28a

Upon binding to its TrkB receptor BDNF activates multiple signaling pathways, including the MAPK/Erk pathway. Work from our lab shows that BDNF enhances both Erk and TRBP phosphorylation (Huang et al., 2012), consistent with a recent publication finding Erk-dependent phosphorylation of TRBP in a cell line (Paroo et al., 2009). In experiments aimed at defining the critical signaling intermediates mediating Lin28 induction downstream of BDNF, we observed that blocking Erk signaling, using an Erk1/2 inhibitor (U0126) prevents BDNF-induced upregulation of Lin28a in hippocampal neurons (Figure 3.2.A). Interestingly, a previous report showed that expression of a phosphomimetic-TRBP mutant (TRBP SΔD) not only enhanced Dicer stabilization and increased levels of many miRNAs, but also selectively decreased levels of Let-7 family miRNAs by an unexplored mechanism. An intriguing hypothesis, consistent with our own findings, would be that TRBP stabilizes not only Dicer but also Lin28a protein; thereby explaining the observed reduced Let-7 levels. To determine whether TRBP is necessary for BDNF-induced regulation of Lin28a we used lentiviral-mediated shRNA knockdown of TRBP in hippocampal neurons and evaluated protein levels of Lin28a. We found that loss of TRBP results in a significant downregulation of Lin28a protein under basal conditions, and prevents BDNF-induced upregulation of Lin28a in hippocampal neurons (Figure 3.2.B). In contrast, loss of Dicer has no effect on basal Lin28a levels (Fig 3.2.C). These results indicate that TRBP is required for Lin28a induction and heightened our interest in further investigating the role of TRBP in BDNF-induced regulation of Lin28a.

Phosphorylation of TRBP is critical for the stabilization of Dicer protein (Paroo et al. 2009). We hypothesized that BDNF-mediated phosphorylation of TRBP and increase in total TRBP levels (Huang et al., 2012) might simultaneously mediate the stabilization and induction of both Lin28 and Dicer. To evaluate the role of TRBP phosphorylation in the rapid BDNF-mediated induction of Lin28a, we used a lentivirus vector under a neuron-specific promoter (synapsin) to express wildtype (WT) TRBP, phospho-mutant (SΔA) TRBP, or phosphomimetic (SΔD) TRBP in hippocampal neurons and examined the effect on Lin28a protein level. We found that expression of TRBP SΔD significantly elevated Lin28a protein and occluded induction by BDNF. Compared to expression of TRBP WT, Lin28a levels were lower in neurons expressing TRBP SΔA (Figure 3.2.D). However, BDNF still modestly induced Lin28a in neurons expressing SΔA TRBP, possibly due to the presence of endogenous TRBP. To circumvent this issue we knocked-down endogenous TRBP and replaced it with SΔA TRBP; BDNF was no longer able to induce Lin28a in neurons that lacked endogenous TRBP and only expressed SΔA TRBP (Figure 3.2.E). These exciting results suggest that TRBP phosphorylation is necessary and sufficient for BDNF-mediated post-transcriptional induction of Lin28a. Furthermore, we found that expression of WT TRBP, TRBP SΔA, and TRBP SΔD elevates Lin28a from baseline compared to a condition where TRBP is not exogenously expressed (Figure 3.3.A). This data indicates that the presence of TRBP itself is sufficient to elevate Lin28a protein but that TRBP phosphorylation enhances this effect. Interestingly, Lin28b ΔNLS levels were not altered by the expression of WT TRBP, TRBP SΔA, and TRBP SΔD (Figure 3.3.A), which highlights a critical point of differential regulation of these two paralogs. To further investigate the importance of TRBP phosphorylation on Lin28a

induction we expressed FL-Lin28a and FL-WT TRBP, -TRBP -SΔA, and -TRBP SΔD and normalized FL-Lin28a and FL-TRBP protein to GAPDH. Then we plotted the amount of FL-Lin28a protein per amount of FL-TRBP protein (Figure 3.3.B). We found that expression of all FL-TRBP constructs elevated FL-Lin28a protein, but that the extent of this elevation was the greatest when TRBP SΔD was expressed. Next, we hypothesized that since TRBP SΔD is sufficient to induce Lin28a levels then we might expect that TRBP SΔD is also sufficient to cause a reduction in Let-7 miRNA levels. To test this prediction we expressed either control virus or FSW-FL-TRBP SΔD in hippocampal neurons under mock or BDNF stimulation conditions and examined levels of Let-7a and Let-7c using TaqMan qRT-PCR. Results showed that expression of TRBP SΔD was sufficient to significantly reduce Let-7 levels in a manner that mimicked and occluded the effects of BDNF (Figure 3.3.C). This exciting finding suggests that TRBP mediates the BDNF-induced increase in Lin28a and resulting decrease in Let-7 levels.

Lin28a, but not Lin28b, exists in a protein complex with TRBP and Dicer

We hypothesized that BDNF might elevate Lin28a protein levels by inducing a stabilizing change in the protein-binding partners associated with Lin28a; in particular with a protein complex including TRBP and Dicer. Co-immunoprecipitation (Co-IP) experiments revealed the exciting finding that endogenous Dicer and Lin28a associate with IP'd FL-TRBP, and not with control rabbit IgG (Figure 3.4.A). In the reciprocal IP, we found that endogenous TRBP and Dicer co-associated with IP'd FL-Lin28a, and not with control mouse IgG (Figure 3.4.B). These results suggest a possible mechanism for Lin28a stabilization similar to TRBP-mediated stabilization of Dicer protein. FL-TRBP

does not co-IP Lin28b protein, even when Lin28b is localized to the cytoplasm (Figure 3.4.C), revealing specificity in the regulation of these paralogs. To test whether Lin28a, TRBP, and Dicer may be components of a single multi-protein complex, we expressed Myc-TRBP and FL-Lin28a in HEK 293T cells and conducted sequential IPs. First, using a Myc antibody we pulled down Myc-TRBP and detected co-association of endogenous Dicer protein and FL-Lin28a. Next, we IP'd the eluent with anti-FL antibody and pulled down FL-Lin28a. We detected the presence of both Dicer and Myc-TRBP indicating that Lin28a, TRBP, and Dicer can exist in a single complex (Figure 3.4.D).

Lin28a and TRBP are regulated by ubiquitin modifications

Since basal levels of Lin28a are low in mature neurons, we hypothesized that Lin28a protein may have a relatively short half-life, generating low basal levels that are rapidly elevated by Lin28a binding to TRBP. We next sought to determine whether Lin28a levels in mature hippocampal neurons are controlled at the level of protein degradation. We examined the effect of inhibition of 26S-proteasomal degradation on Lin28a protein level by immunoblotting for Lin28a in lysates from cultured hippocampal neurons (DIV14) undergoing mock or BDNF stimulation (for 20 min.), in the absence or presence of MG132 (proteasomal inhibitor). Inhibition of proteasomal degradation significantly elevates Lin28a levels in a rapid manner that mimics and occludes further induction by BDNF (Figure 3.5.A). In contrast, Lin28b levels, which are unaffected by BDNF, are also unaffected by 60 minute MG132 (Figure 3.5.B), further highlighting differential cellular regulatory mechanisms for these Lin28 paralogs. We also examined the effects of MG132 on TRBP and noted a significant elevation of TRBP protein in

neurons treated with MG132 for 20 minutes (Figure 3.5.C). Constitutive proteasomal degradation implies that Lin28a, or a protein required to stabilize Lin28a (such as TRBP), is undergoing constitutive ubiquitination and proteasomal degradation. To determine whether Lin28a, itself, might be ubiquitinated we first expressed FL-Lin28a and HA-Ubiquitin Wildtype (HA-Ub WT) in HEK293T cells and in hippocampal neurons and carried out a stringent IP for Lin28a with anti-Flag antibody followed by immunoblotting for HA. We found that in the presence of MG132 (26S proteasome inhibitor) and PR619 (deubiquitinase inhibitor), HA-Ubiquitin co-precipitated with FL-Lin28a in heterologous cells and in hippocampal neurons but not in the control condition (lysates from cells expressing HA-Ub WT but not FL-Lin28a) (Figure 3.5.D). Lysates were treated with denaturing conditions (high salt, high detergent) to determine if HA-Ub WT is directly conjugated to Lin28a and rule out the possibility that HA-Ub WT is indirectly associated by a protein complex with Lin28a. Disruption of non-covalent interactions by stringent IP conditions is confirmed by the absence of TRBP co-IP under these conditions (Figure 3.5.D). This data indicates that Lin28a can be post-translationally modified by ubiquitin and suggests that BDNF signaling could alter the degradation of Lin28a through the 26S proteasomal pathway to increase Lin28a protein stability.

Although ubiquitin, a 76 aa protein, is best known for targeting proteins to the 26S proteasome for degradation, nonproteolytic signaling functions of ubiquitin modification are also well known. Substrate proteins are linked to ubiquitin using distinct ubiquitin lysine (K) residues (K6, K11, K27, K29, K33, K48, and K63). Each lysine residue can be further conjugated by another ubiquitin to create polyubiquitin chains. Nonproteolytic functions of ubiquitin include regulation of protein localization and

activity, membrane trafficking, DNA repair, and chromatin dynamics. Unlike K48-linked ubiquitination, K63-linked ubiquitination does not trigger protein degradation but instead plays an important role in regulating protein/protein interactions and kinase signaling activation (Chen & Sun 2009, Wang et al. 2010). To investigate which type(s) of ubiquitin modification Lin28a undergoes, we obtained several HA-tagged ubiquitin constructs including a HA-Ubiquitin K63 (HA-Ub K63) and HA-Ubiquitin K48 (HA-Ub K48) (laboratory of Ted Dawson; (Lim et al. 2005)). The HA-Ub K63 construct contains arginine substitutions on all lysine residues except the lysine at position 63 and is therefore expected to only allow the proteasome-independent K63 ubiquitin linkage. The HA-Ub K48 construct contains arginine substitutions on all lysine residues except the lysine at position 48 and is expected to promote proteasome-dependent K48-linked ubiquitin chains. In heterologous cells we expressed FL-Lin28a and either HA-Ub, HA-Ub K63, or HA-Ub K48. Control conditions expressed HA-Ub, HA-Ub K63, or HA-Ub K48 alone. We used stringent IP conditions (high salt, high detergent) to disrupt non-covalent interactions and IP'd lysates with Fl-coated beads. Upon immunoblotting for HA we noted a ladder of anti-HA immuoreactivity present in each FL IP condition consistent with polyubiquitination of WT Ub, K63 Ub, and K48 Ub but not in the control conditions (Figure 3.5.E). Interestingly, in the HA-Ub K63 condition we detected a prominent and distinct band above the 37 kD molecular weight marker which we predict represents a K63-ubiquitinated form of Lin28a. These results indicate the Lin28a is subject to both proteasomal and proteasomal-independent ubiquitination via K48 and K63 linkages, respectively. Ongoing experiments are directed at evaluating whether Lin28 ubiquitination can be altered by BDNF.

Since we also observed that MG132 treatment elevates TRBP protein levels, we next set out to determine if TRBP itself is also subject to ubiquitin modification. We hypothesized that since TRBP phosphorylation serves to stabilize TRBP protein itself, we might observe decreased ubiquitination of TRBP SΔD compared to cells expressing TRBP SΔA. To test this hypothesis, we expressed HA- K48 Ub and either FL-WT TRBP, -TRBP SΔD, or -TRBP SΔA in HEK 293T cells. In control conditions we expressed HA-K48 Ub alone. As described above, we used a stringent IP protocol to pull-down FL-TRBP (WT, SΔD, and SΔA) and immunoblotted for HA to determine whether HA-K48 Ub conjugates to FL-TRBP. Our results show higher HA immunoreactivity in TRBP SΔA expressing cells compared to TRBP SΔD and WT TRBP conditions (Figure 3.5.F). We do not detect any HA bands in control conditions. These results demonstrate that TRBP undergoes K48-linked ubiquitin modification and that the phosphorylation status of TRBP determines the extent of this ubiquitination. This data raises the exciting possibility that BDNF-induced TRBP phosphorylation might lead to decreased proteasome-mediated degradation of TRBP protein allowing increased levels of TRBP that can bind to and stabilize Lin28a protein. Ongoing work is seeking to determine whether BDNF stimulation leads to decreased TRBP ubiquitination, and to assess the importance of phospho-TRBP in BDNF-mediated neuronal growth responses.

Discussion

Our work has uncovered a novel signaling mechanism responsible for the rapid post-transcriptional upregulation of Lin28a by BDNF. The results from this thesis chapter demonstrate that Lin28a can associate with a miRNA machinery component, TRBP

protein. We also provide the first evidence that TRBP phosphorylation is critical for the stabilization of Lin28a. Our studies also show that Lin28a is post-translationally modified by ubiquitin and that TRBP undergoes K48-linked poly-ubiquitination. Interestingly, we observed that the phosphorylation status of TRBP might determine the degree of this post-translational modification. Furthermore, we reveal that BDNF has a distinct impact on Lin28a and its paralog Lin28b. Both Lin28a and Lin28b are crucial regulators of cell growth, developmental timing, and pluripotency and exert their effects by controlling the abundance of Let-7 family miRNAs. However, we find that in the context of neurotrophin signaling Lin28a and Lin28b are subject to differential post-transcriptional regulation. Given the high degree of homology between the two paralogs, future studies will be directed at identifying distinct residues that might confer regulation to Lin28a but not Lin28b in BDNF signaling. An additional topic of interest is investigating the effect of TRBP phosphorylation on a physiological effect of BDNF such as dendritic spine density. BDNF-induced spine density depends upon its ability to regulate new protein synthesis and therefore we suspect that TRBP phosphorylation and subsequent induction of Lin28a might be sufficient to mediate a physiological effect of BDNF. We expect that knowledge from our studies will have far-reaching implications for further establishing the critical role of miRNA biogenesis and its regulation in shaping changes in pro-growth programs of gene expression in the central nervous system important for learning and memory.

Figures and Legends

Figure 3.1 Lin28a, but not its paralog Lin28b, is regulated by BDNF in a rapid, transcription-independent manner.

(A) (Left) Protein levels, normalized to GAPDH, of Lin28a under mock (0 min) or BDNF stimulation (5 min, 20 min, 60 min; 100 ng/ml) in the presence (gray bars) or absence (white bars) of Actinomycin-D (0.5 μg/ml). (Right) Immunoblotting for Lin28a protein in neurons undergoing mock or BDNF stimulation for indicated minutes (min) in the presence (+) or absence (-) of Actinomycin-D. (B) Quantification of Lin28a mRNA level by individual TaqMan qRT-PCR reaction in hippocampal neurons undergoing mock or BDNF stimulation (20 min, 60 min,120 min). (C) (Left) Densitometric quantification of protein levels of endogenous Lin28a (white bars) or Flag-Lin28a (gray bars) in mock (0 min) or BDNF stimulated conditions (5 min, 20 min, 60 min). (Right) Immunoblotting of endogenous Lin28a or FLAG-Lin28a in hippocampal neurons infected with lentivirus expressing FLAG-Lin28a undergoing mock (0 min) or BDNF stimulation (5 min, 20 min, 60 min). (D) Normalized protein level of endogenous Lin28b (white bars), FLAG-Lin28b (gray bars) in neurons infected with lentivirus expressing FLAG-Lin28b , or FLAG-Lin28bΔNLS (dark gray bars) in neurons infected with lentivirus expressing FLAG-Lin28bΔNLS. Neurons were stimulated with BDNF for 0, 5, 20, or 60 min. (Right) Immunoblotting of endogenous Lin28b, FLAG-Lin28b, or FLAG-Lin28bΔNLS in hippocampal neurons. All error bars represent SEM. *$p < 0.05$ by unpaired Student's t test.

Experiments in panel D of this figure were performed by Alexandra Amen and will also be published in her thesis.

Figure 3.1

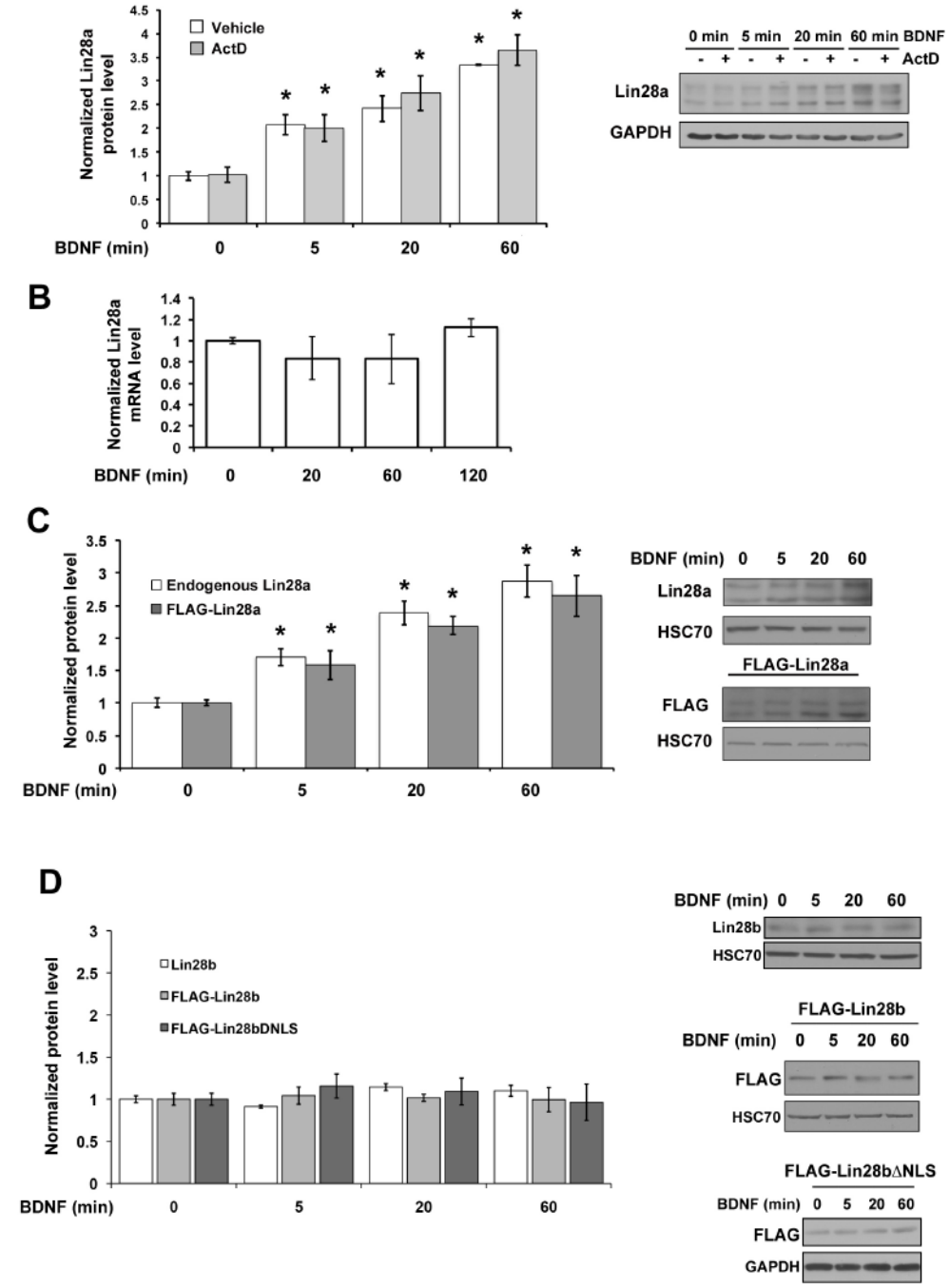
A
Normalized Lin28a protein level
Vehicle
ActD
BDNF (min) 0 5 20 60
0 min 5 min 20 min 60 min BDNF
- + - + - + - + ActD
Lin28a
GAPDH
B
Normalized Lin28a mRNA level
BDNF (min) 0 20 60 120
C
Normalized protein level
Endogenous Lin28a
FLAG-Lin28a
BDNF (min) 0 5 20 60
BDNF (min) 0 5 20 60
Lin28a
HSC70
FLAG-Lin28a
FLAG
HSC70
D
Normalized protein level
Lin28b
FLAG-Lin28b
FLAG-Lin28bDNLS
BDNF (min) 0 5 20 60
BDNF (min) 0 5 20 60
Lin28b
HSC70
FLAG-Lin28b
BDNF (min) 0 5 20 60
FLAG
HSC70
FLAG-Lin28bΔNLS
BDNF (min) 0 5 20 60
FLAG
GAPDH

Figure 3.2 BDNF modulates TRBP phosphorylation to induce Lin28a.

(A) (Left) Densitometric quantification of Lin28a protein level in hippocampal neurons treated with vehicle (DMSO) or Erk 1/2 inhibitor U0126 for 30 minutes prior to mock (open bars) or BDNF stimulation for 60 minutes (hatched bars). (Right) Immunoblot of Lin28a in vehicle or U0126 conditions in the presence or absence of BDNF. (B) Effect of TRBP loss on Lin28a protein level and BDNF-regulated Lin28a induction. Lin28a protein levels were assessed from neurons infected with lentivirus expressing either control shRNA (NTshRNA) or shRNA targeting TRBP (TRBPshRNA) (Left) Densitometric quantification of protein levels. (Right) Immunoblotting of Lin28a and TRBP in control or TRBP-deficient neurons under mock or BDNF stimulated conditions. (C) Loss of Dicer has no effect on Lin28a protein level. (Left) Quantification of Dicer and Lin28a protein levels in hippocampal neurons expressing control shRNA (NTshRNA) or Dicer-targeting shRNA (Dicer shRNA). (Right) Immunoblotting of Lin28a and Dicer in control or Dicer-deficient neurons. (D) (Left) Quantification of FL-Lin28a protein level in hippocampal neurons infected with lentivirus expressing either WT TRBP, SΔD TRBP, SΔA TRBP in the presence or absence of 60 minute BDNF treatment. (Right) Immunoblotting of FL-TRBP and FL-Lin28a in neurons expressing SΔA TRBP, SΔD TRBP, or WT TRBP. (E) (Left) Quantification of Lin28a, TRBP, and Flag-TRBP SΔA in hippocampal neurons infected with lentivirus expressing either control (NTsh; blue bars) or shRNA targeting TRBP (TRBPsh; purple bars) in mock or BDNF-stimulated conditions. (Right) Immunoblotting for FL-TRBP, FL-Lin28a, and endogenous TRBP.

Figure 3.2

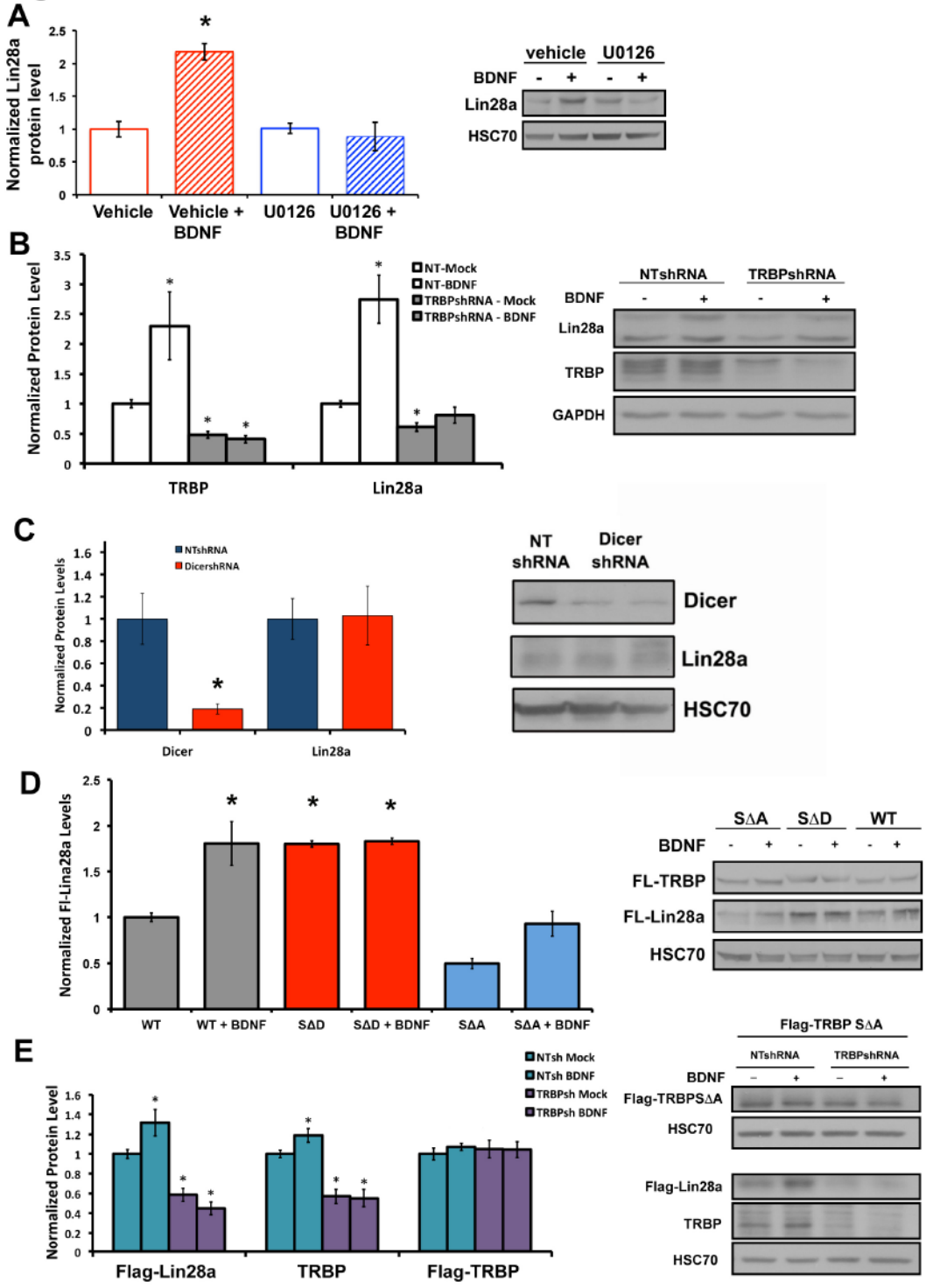
A
Normalized Lin28a protein level
Vehicle
Vehicle + BDNF
U0126
U0126 + BDNF
vehicle
U0126
BDNF
Lin28a
HSC70
B
Normalized Protein Level
NT-Mock
NT-BDNF
TRBPshRNA - Mock
TRBPshRNA - BDNF
TRBP
Lin28a
NTshRNA
TRBPshRNA
GAPDH
C
NTshRNA
DicershRNA
Normalized Protein Levels
Dicer
Lin28a
NT shRNA
Dicer shRNA
HSC70
D
Normalized Fl-Lina28a Levels
WT
WT + BDNF
SΔD
SΔD + BDNF
SΔA
SΔA + BDNF
SΔA
SΔD
WT
FL-TRBP
FL-Lin28a
E
NTsh Mock
NTsh BDNF
TRBPsh Mock
TRBPsh BDNF
Normalized Protein Level
Flag-Lin28a
TRBP
Flag-TRBP
Flag-TRBP SΔA
Flag-TRBPSΔA
Flag-Lin28a

Figure 3.3 TRBP is sufficient to induce Lin28a protein and reduce Let-7 miRNAs.

(A) (Top Left) Immunoblotting of FL-TRBP and FL-Lin28bΔNLS in HEK 293T cells expressing control empty vector (PCDNA), WT TRBP, SΔA TRBP, or SΔD TRBP. (Bottom Left) Immunoblotting of FL-TRBP and FL-Lin28a in HEK 293T cells expressing WT TRBP, SΔA TRBP, or SΔD TRBP. (Right) Quantification of FLAG-Lin28a and FLAG- Lin28bΔNLS. (B) HEK 293T cells were transfected with FL-Lin28a and WT TRBP, SΔA TRBP, or SΔD TRBP. Scatter plot shows FL-Lin28a protein concentration per amount of FL-TRBP protein. Expression of WT TRBP, SΔA TRBP, and SΔD TRBP elevated FL-Lin28a protein level. Induction of FL-Lin28a by SΔD TRBP was greater compared to WT TRBP and SΔA TRBP conditions. The positive slope was greatest in SΔD TRBP-expressing cells and the slope was the lowest for SΔA TRBP-expressing cells (C) Quantification of Let-7 miRNA levels by individual TaqMan qRT-PCR reactions in neurons expressing control virus (green bars) or SΔD TRBP (orange bars) undergoing mock or BDNF treatment (60 minutes). miRNA levels were normalized to U6 snRNA and plotted relative to each mock-stimulated control virus condition (set as 1.0). *$p < 0.05$ and **$p < 0.01$ by unpaired Student's t test. Experiments in panel A and B were conducted by Alexandra Amen and will also be published in her thesis.

Figure 3.3

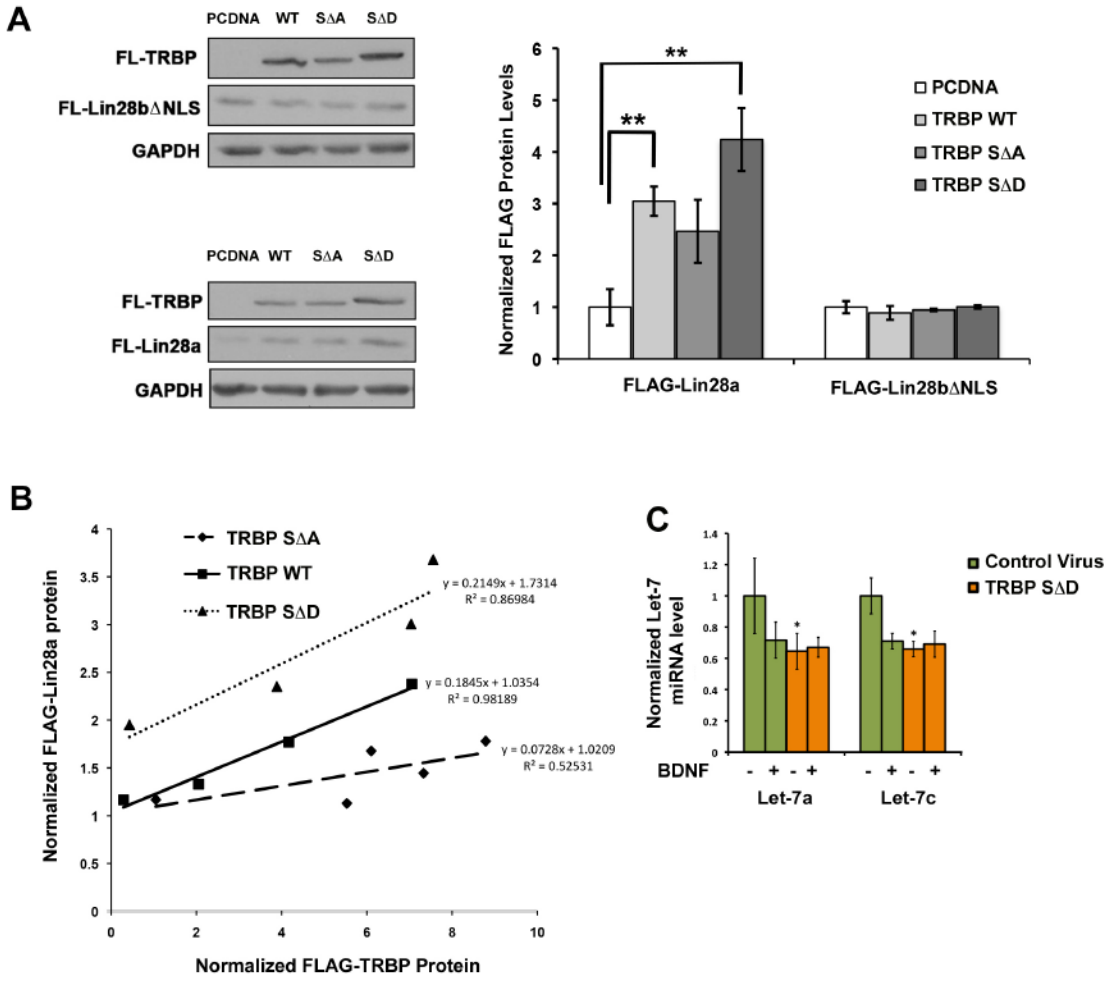
A
PCDNA WT SΔA SΔD
FL-TRBP
FL-Lin28bΔNLS
GAPDH
PCDNA WT SΔA SΔD
FL-TRBP
FL-Lin28a
GAPDH
Normalized FLAG Protein Levels
**
**
PCDNA
TRBP WT
TRBP SΔA
TRBP SΔD
FLAG-Lin28a
FLAG-Lin28bΔNLS
B
TRBP SΔA
TRBP WT
TRBP SΔD
y = 0.2149x + 1.7314
R² = 0.86984
y = 0.1845x + 1.0354
R² = 0.98189
y = 0.0728x + 1.0209
R² = 0.52531
Normalized FLAG-Lin28a protein
Normalized FLAG-TRBP Protein
C
Normalized Let-7 miRNA level
Control Virus
TRBP SΔD
BDNF
- + - +
- + - +
Let-7a
Let-7c

Figure 3.4 Dicer and TRBP can co-associate in a protein complex with Lin28a but not Lin28b.

(A) Lin28a is a novel TRBP binding partner. HEK 293T cell lysates were IP'd with control rabbit IgG (rIgG) or anti-FLAG antibody to pull down FL-TRBP. Immunoblotting for Dicer and Lin28a show co-association with FL-TRBP but not with control IgG. (B) HEK 293T cell lysates were IP'd with control mouse IgG (mIgG) or anti-FLAG antibody to pull down FL-Lin28a. Immunoblotting for Dicer and TRBP demonstrate co-association in the FL pull down condition but in control IgG condition. (C) HEK 293T cells expressing FL-Lin28bΔNLS were IP'd with anti-FLAG antibody. Dicer and TRBP are only present in the input condition but not in the IP'd Flag condition. (D) HEK 293T cells expressing Myc-TRBP and FL-Lin28a were first IP'd using an anti-Myc antibody and co-association of endogenous Dicer protein and FL-Lin28a was detected. For the sequential IP the eluent was IP'd with anti-FLAG antibody and both Dicer and Myc-TRBP co-associated.

Experiments in this figure were performed by Alexandra Amen and will also be published in her thesis.

Figure 3.4

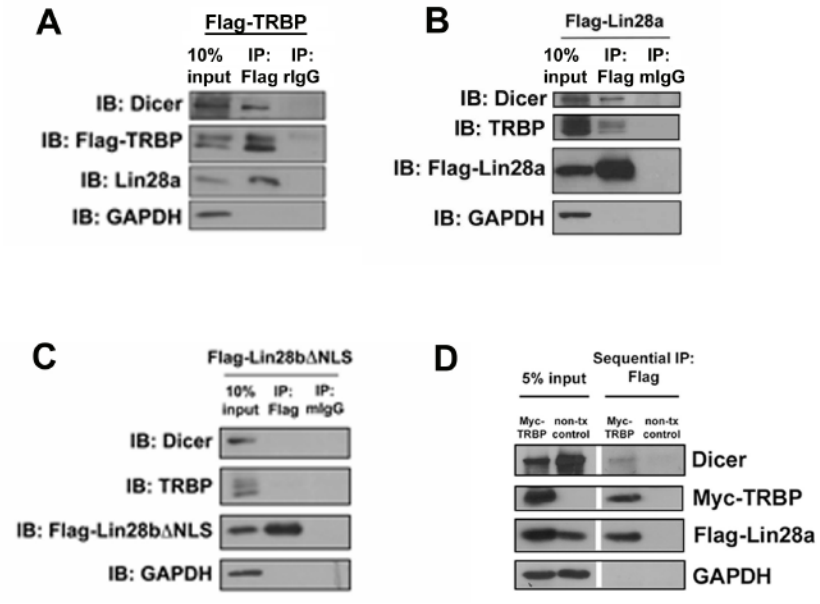

Figure 3.5 Lin28a and TRBP are rapidly turned over and subject to modification by ubiquitin.

(A) (Top) Densitometric quantification of Lin28a protein level. Hippocampal neurons were treated with vehicle (DMSO; gray bars) or 10 μM MG132 (20 min; red bar) and either mock or BDNF stimulated (20 min). (Bottom) Immunoblotting for Lin28a protein in control or MG132 treated neurons, mock and BDNF-stimulated. (B) (Top) Hippocampal neurons were treated with vehicle (DMSO; gray bars) or 10 μM MG132 (60 min; red bar) and either mock or BDNF stimulated (60 min). (Bottom) Immunoblotting for Lin28b protein in control or MG132 treated neurons, mock and BDNF-stimulated. (C) Quantification of TRBP protein in hippocampal neurons treated with vehicle (DMSO; gray bar) or 10 μM MG132 (20 min; red bar). (D) (Left) Hippocampal neurons were infected with lentivirus expressing FL-Lin28a and HA-Ub. In

the IP control (Ctrl) condition neurons expressed only HA-Ub. In both conditions anti-FLAG antibody was used to IP FL-Lin28a under stringent (high salt, high detergent) conditions. HA immunoreactivity was detected in only the FL IP condition. (Right) HEK 293T cells were transfected with FL-Lin28a and HA-Ub and stringent IP was conducted to IP FL-Lin28a. (E) HEK 293T cells were transfected with FL-Lin28a and either HA-UB WT (WT), HA- K63 UB (K63), HA-K48 Ub (K48). Control (Ctrl) conditions expressed only HA WT, K63, or K48. Stringent IP was conducted using anti-FLAG antibody. Distinct HA immunoreactivity is detected in each FL IP condition but not in the control condition. (F) HEK293T cells were transfected with FL-WT TRBP, -SΔA TRBP, or -SΔD TRBP and HA-K48 Ub. Control condition was transfected with HA-K48 Ub alone. FLAG-coated beads were used to IP FL-TRBP constructs under stringent conditions. HA banding was more prominent in SΔA TRBP condition. No HA immunoreactivity was detected in control condition.

Figure 3.5

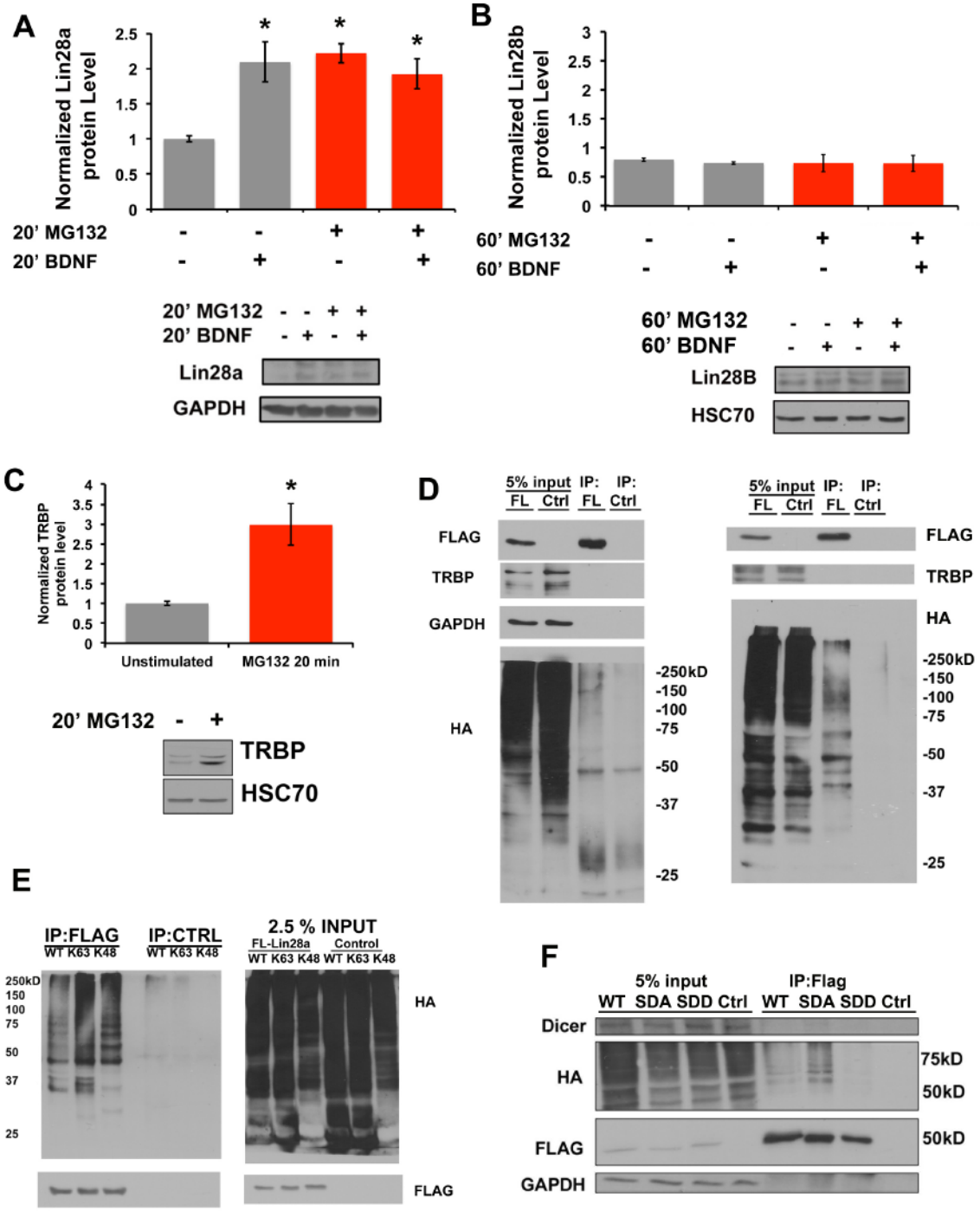
A
Normalized Lin28a protein Level
2.5
2
1.5
1
0.5
0
*
*
*
20' MG132 - - + +
20' BDNF - + - +
20' MG132 - - + +
20' BDNF - + - +
Lin28a
GAPDH
B
Normalized Lin28b protein Level
3
2.5
2
1.5
1
0.5
0
60' MG132 - - + +
60' BDNF - + - +
60' MG132 - - + +
60' BDNF - + - +
Lin28B
HSC70
C
Normalized TRBP protein level
4
3.5
3
2.5
2
1.5
1
0.5
0
*
Unstimulated
MG132 20 min
20' MG132 - +
TRBP
HSC70
D
5% input FL
IP: FL
IP: Ctrl
FLAG
TRBP
GAPDH
HA
-250kD
-150
-100
-75
-50
-37
-25
5% input FL
IP: FL
IP: Ctrl
FLAG
TRBP
HA
-250kD
-150
-100
-75
-50
-37
-25
E
IP:FLAG
WT K63 K48
IP:CTRL
WT K63 K48
2.5 % INPUT
FL-Lin28a
WT K63 K48
Control
WT K63 K48
250kD
150
100
75
50
37
25
HA
FLAG
F
5% input
WT SDA SDD Ctrl
IP:Flag
WT SDA SDD Ctrl
Dicer
HA
75kD
50kD
FLAG
50kD
GAPDH

Experimental Methods

Immunoblotting

Primary cultures of mouse hippocampal neurons (DIV 14~15) were incubated in serum-reduced medium (0.5% B27 supplement) for 2 hours, followed by preincubation with Actinomycin-D (0.5 μg/ml) for 10~30 min. Bath application of BDNF (100 ng/ml) was for designated periods (5 min - 2 hours). The cultures were washed 3 times and harvested on ice with lysis buffer (50 mM Hepes, 150 mM NaCl, 10% Glycerol, 1 mM EDTA, 1% Triton-X-100, 0.2% SDS) plus freshly added protease inhibitor cocktail (Roche) and phosphatase inhibitor (sodium orthovanadate 0.2mM, sodium pyrophosphate 1mM) and NEM (50 mM). Protein concentration was determined by Bradford Assay or Bicinchoninic (BCA) assay. Equal amounts of lysate protein were resolved on SDS-PAGE gels, and electrotransferred to PVDF membrane. Membrane was blocked with 5% BSA in Tris-buffered saline tween 20 (TBST 0.1%) for 2-4 hours and probed with primary antibodies in 5% BSA in TBST: Lin28a (Cell Signaling D9F5), FLAG M2 (Sigma F3165), HA (Invitrogen 71-5500), GAPDH (Millipore 6C5), TRBP (Abcam ab72110), Lin28b (Cell Signaling 5422), Myc peptide (Sigma M2435). For IP experiments we used the following reagents: 3X Flag peptide (Sigma F4799-4MG), 1X Flag peptide: (Sigma F3290-4MG), Control Mouse IgG (Santa Cruz sc-2025), Control Rabbit IgG (Santa Cruz sc-2027), Dicer (Sigma SAB4200087).

Immunoprecipitation

Stringent IP Protocol for Ubiquitination Assessment

Stringent Polysomal Lysis Buffer: 100mM KCl, 10 mM HEPES, 4 mM MgCl2, 50 μM ZnCl2, 1% Triton-X, 0.25% SDS, 50 mM NEM, 1 mM DTT, PR619 5 μM, pH=7.3

Stringent Wash buffer: 1M NaCl, 50 μM ZnCl2, 1 mM MgCl2, 50 mM HEPES, 20% Glycerol, 50 mM NEM, 1% NP40, 0.1% SDS, pH=7.8

Procedure:

1. Block protein G sepharose beads in 1mL Stringent Wash buffer + 5% BSA for 1 hour.
2. Centrifuge beads at 2000xg for 25 sec at 4°C, suction off supernatant, and resuspend in Stringent Wash buffer +protease inhibitor+phosphatase inhibitor+NEM (to 50% slurry).
3. Coat beads with FLAG or MYC antibody (2-4 μg/IP) or control isotype-specific serum (IgG) rotating at 4° C overnight.
4. Prepare beads:
    - **a.** Wash beads
        - **i.** Antibody coated beads from previous day + beads for preclearing (overestimate 25μl/sample x 2). Wash with 500 μl chilled Stringent Wash buffer (invert, spin 2000g for 25 sec at 4°C, suction off buffer with needle and repeat).
    - **b.** Resuspend beads in 2x excess of Stringent Wash buffer plus protease/phosphatase inhibitor. Keep on ice until ready to use.
5. Lysis:
    a. Wash cells 2x with ice-cold PBS + 0.9mM MgCl2
    b. Harvest lysate in Stringent Polysomal Lysis Buffer (900-1000 μl for 10 cm dishes or 70 μl for 24 well plates) with protease inhibitor cocktail,

phosphatase inhibitors, and freshly added 1mM DTT. Let cells sit in lysis buffer on ice 10 min, scrape, and rotate at 4 °C 10 minutes.

c. Centrifuge lysate at 13.2 x g, 4 °C for 15 minutes. Remove supernatant.

6. Protein assay (Bradford or BCA) to determine concentration
7. Lysate pre-clearing:
    a. Pre-clear lysate with protein G sepharose beads pre-washed in Stringent Wash buffer Add 37.5 µl 3x bead dilution to lysates.
    b. Incubate 30-45 min rotating at 4 °C, then spin 2000g for 1 minute at 4°C and remove cleared lysate to new tube.
8. Remove 2.5% lysate protein sample for input, add SDS, boil, and freeze to run on gel later
9. Add 45 µl antibody-bound beads to protein lysate (1000-2600 µg) and incubate rotating 4 hours at 4 °C
10. Washes
    a. Wash 3x with 1 mL cold Stringent Wash buffer plus proteasome and phosphatase inhibitors rotating 10 min at 4°C. Centrifuge at 2000g, 4°C for 25sec. Use vacuum line with needle to suction off supernatant (careful not to remove the beads!)
    b. Wash 1x with 1mL cold Stringent Wash buffer WITHOUT protease/phosphatase inhibitors and rotate for 5 min at 4°C. Spin for 1 minute at 2000g 4°C, and remove buffer entirely with vacuum suction.
11. Boil Elution

a. Add 30 µl of Stringent Wash buffer without protease/phosphatase inhibitor and 6 µl of 6x SDS PAGE loading buffer.
b. Boil at 85-90 °C for 10-15 minutes
c. Spin for 1 minute at 13,000g at room temperature and transfer supernatant to a new eppendorf tube to run on SDS PAGE gel

TRBP/Lin28a coIP Protocol (maximized RNA stability)

Polysomal lysis buffer (PLB): 100mM KCl, 4mM MgCl2, 10mM HEPES (pH 7.3), 50µM ZnCl, 0.5% NP-40 (add to 10mL: protease inhibitors, phosphatase inhibitors, 20mM NEM)

NT2 Buffer: 50mM HEPES (pH=7.8), 150mM NaCl, 1mM MgCl2, 50µM ZnCl, 0.05% NP-40 (add to 10mL: protease inhibitors, phosphatase inhibitors, 20mM NEM)

***For PLB and NT2 buffers use DEPC H20

Day 0:

1) Block protein G sepharose beads in 1.5mL NT2 buffer + 5% BSA for 1 hour.
    i. use 30µl 50% bead slurry per sample

2) Centrifuge beads at 2000xg for 25 sec at 4°C, suction off supernatant, and resuspend in NT2+protease inhibitor+phosphatase inhibitor+NEM (to 50% slurry).

3) Coat beads with Flag antibody or control isotype-specific serum (IgG) rotating at 4° C overnight.

   a. Use about 1μg antibody per 200μg protein sample

Day1:

1) Prepare beads:

   a. Wash beads

      i. Wash antibody coated beads from day 0 and beads for preclearing (30μL 50% slurry per sample) with 1.5mL chilled NT2 (invert, spin 2000g for 25 sec at 4°C, suction off buffer with needle).

      ii. Repeat wash

   b. Resuspend beads in 2x excess of NT2+protease/phosphatase inhibitor (45μL per IP final volume).

Neurons (DIV14)

2) BDNF stimulation:

   -Incubate primary mouse hippocampal cultures, DIV14, in serum-reduced media (1/4 B27) for 2 hrs

   -Dilute stock Actinomycin-D 1:1250 in NBA and add 100μl to each well. Incubate 5 min prior to BDNF/mock stimulation.

   -Add 40μl of 1ng/μl BDNF (diluted in NBA) to a final concentration of 100ng/mL. Incubate 60 minutes.

3) Lysis:

   -Wash cells 2x with ice-cold PBS + 0.9mM MgCl2

-Harvest lysate in polysomal lysis buffer + protease inhibitor cocktail, phosphatase inhibitors, 20mM NEM, and freshly added 1mM DTT. Let cells sit in lysis buffer on ice 10 min prior to scraping.

-Add 70µL to first well, and 40µL to subsequent wells. Transfer lysate from previous to next well before scraping.

-Rotate harvested lysate for 10min at 4°C.

-Centrifuge lysate at 13.2 x g, 4°C for 15 minutes. Remove supernatant.

HEK293T cells

2) Ensure 100% confluency of 10cm dishes. No stimulation required.

3) Lysis:

-Wash cells 2x with ice-cold PBS + 0.9mM MgCl2

-Harvest lysate in 1mL polysomal lysis buffer + protease inhibitor cocktail, phosphatase inhibitors, 20mM NEM, and freshly added 1mM DTT per dish. Let cells sit in lysis buffer on ice 10 min prior to scraping.

-Rotate harvested lysate for 10min at 4°C.

-Centrifuge lysate at 13.2 x g, 4°C for 15 minutes. Remove supernatant.

All cell types

4) Protein assay (Bradford) to determine concentration.

5) Lysate pre-clearing:

-Pre-clear lysate with protein G sepharose beads pre-washed in NT2 buffer (from step 1). Add 45µL 3x bead dilution to lysate sample.

-Incubate 30 min rotating at 4°C, then spin 2000g for 1 minute at 4°C and remove cleared lysate to new tube.

6) Remove a 2.5-10% lysate protein sample (depending on amount to IP), add SDS, boil, and freeze to run on gel later.

7) Add 45µL antibody bound beads (now 15µl beads in 33% suspension) to protein lysate.

-Use p200 tips with ends cut off

-Incubate rotating 3-4 hours at 4°C

8) Washes

-Wash 3x with 1.5µl cold NT2 + protease and phosphatase inhibitors+NEM by filling tube, resuspending, and then briefly centrifuging the breads in an eppendorf tube. Centrifuge at 2000g, 4°C for 25sec. Use vacuum line to suction off supernatant; crush pipette tip with tweezers to decrease tip diameter (careful not to remove the beads!).

***For third wash, let rotate at 4°C for 5 minutes before suctioning off supernatant.

-Wash 1x with 1mL cold NT2 WITHOUT protease/phosphatase inhibitors, and spin for 1 minute at 2000g 4°C. Remove buffer entirely with vacuum suction.

10) Elution with flag (or myc) peptide

-Add 30µl of peptide, diluted in NT2 to 100µg/mL (flag peptide - 1:40 from stock; myc peptide – 1:500 from stock)

-Rotate 30 min-1 hr at ROOM TEMP

-Spin 10sec at 12000rpm at ROOM TEMP

-Collect 30µl of eluent 1

-Repeat steps and collect eluent 2

-Repeat steps and collect eluent 3

-Combine eluents (about 90µl) and spin for 10sec at 12000rpm

-Pipet off 30-45µl of eluent

-Boil samples with loading dye for SDS-PAGE analysis

TRBP/Lin28a/Dicer sequential IP Protocol

Polysomal lysis buffer (PLB): 100mM KCl, 4mM MgCl2, 10mM HEPES (pH 7.3), 50uM ZnCl, 0.5% NP-40 (add to 10mL: protease inhibitors, phosphatase inhibitors, 20mM NEM)

NT2 Buffer: 50mM HEPES (pH=7.8), 150mM NaCl, 1mM MgCl2, 50uM ZnCl, 0.05% NP-40 (add to 10mL: protease inhibitors, phosphatase inhibitors, 20mM NEM)

***For PLB and NT2 buffers use DEPC H20

Day 1:

1) Transfect 1 10cm dish with 0.25μg/mL flag-Lin28a and 0.5μg/mL myc-TRBP-WT
2) Transfect 1 10cm dish with 0.25 μg/mL flag-Lin28a only
    a. Bring up to 30μg total with PCDNA3.1 empty vector
    b. Add 124μL CaCl2 per dish
    c. Bring total volume up to 1mL with ddH2O
    d. Add 1mL 2XHBSS to 1mL DNA/CaCl2 solution. Bubble and add drop-wise to plate.
    e. Allow transfection to incubate for 8-12hours, then replace media.

Day 2:

5) Block protein G sepharose beads in 1.5mL NT2 buffer + 5% BSA for 1 hour.

    i. use 30μl 50% bead slurry per sample, overestimate by 1 sample = 30μl X 3 = 90μL

6) Centrifuge beads at 2000xg for 25 sec at 4°C, suction off supernatant, and resuspend in NT2+protease inhibitor+phosphatase inhibitor+NEM (to 50% slurry).

7) Coat half (45μL) of the beads with mouse anti-flag antibody, and the other half (45μL) of the beads with rabbit anti-myc antibody.

a. Use about 1ug antibody per 200µg protein sample

Day3:

4) Prepare beads:

a. Wash beads

i. Wash antibody coated beads from day 0 and beads for preclearing (30µL 50% slurry per sample) with 1.5mL chilled NT2 (invert, spin 2000g for 25 sec at 4°C, suction off buffer with needle).

ii. Repeat wash

b. Resuspend beads in 2x excess of NT2+protease/phosphatase inhibitor.

2) Ensure 100% confluency of 10cm dishes. No stimulation required.

3) Lysis:

-Wash cells 2x with ice-cold PBS + 0.9mM MgCl2

-Harvest lysate in 1mL polysomal lysis buffer + protease inhibitor cocktail, phosphatase inhibitors, 20mM NEM, and freshly added 1mM DTT per dish. Let cells sit in lysis buffer on ice 10 min prior to scraping.

-Rotate harvested lysate for 10min at 4°C.

-Centrifuge lysate at 13.2 x g, 4°C for 15 minutes. Remove supernatant.

8) Protein assay (Bradford) to determine concentration.

5) Lysate pre-clearing:

-Pre-clear lysate with protein G sepharose beads pre-washed in NT2 buffer (from step 1). Add 45µL 3x bead dilution to lysate sample.

-Incubate 30 min rotating at 4°C, then spin 2000g for 1 minute at 4°C and remove cleared lysate to new tube.

6) Remove a 2.5-10% lysate protein sample (depending on amount to IP), add SDS, boil, and freeze to run on gel later.

7) IP #1: Add 45µL myc-antibody bound beads (now 15µl beads in 33% suspension) to protein lysate.

-Use p200 tips with ends cut off

-Incubate rotating 3 hours at 4°C

8) Washes

-Wash 3x with 1.5mL cold NT2 + protease and phosphatase inhibitors+NEM by filling tube, resuspending, and then briefly centrifuging the breads in an eppendorf tube. Centrifuge at 2000g, 4°C for 25sec. Use vacuum line to suction off supernatant; crush pipette tip with tweezers to decrease tip diameter (careful not to remove the beads!).

***For third wash, let rotate at 4°C for 5 minutes before suctioning off supernatant.

-Wash 1x with 1mL cold NT2 WITHOUT protease/phosphatase inhibitors, and spin for 1 minute at 2000g 4°C. Remove buffer entirely with vacuum suction.

10) Elution with myc peptide

-Add 30µl of peptide, diluted in NT2 1:500 from stock

-Rotate 30 min at 4°C

-Spin 10sec at 12000rpm at 4°C

-Collect 30µl of eluent 1

-Repeat steps and collect eluent 2

-Repeat steps and collect eluent 3

-Combine eluents (about 90µl) and spin for 10sec at 12000rpm at 4°C

-Remove a 10% elution sample (about 9µL, to ensure that 1st IP worked) and bring up to 30µL with NT2. Boil samples with loading dye for SDS-PAGE analysis

11) IP #2: Add 45µL flag-antibody bound beads (now 15µl beads in 33% suspension) to protein lysate.

-Use p200 tips with ends cut off

-Incubate rotating 3 hours at 4°C

12) Washes

-Wash 3x with 1.5ul cold NT2 + protease and phohsphatase inhibitors+NEM by filling tube, resuspending, and then briefly centrifuging the breads in an eppendorf tube. Centrifuge at 2000g, 4°C for 25sec. Use vacuum line to suction off supernatant;

crush pipette tip with tweezers to decrease tip diameter (careful not to remove the beads!).

***For third wash, let rotate at 4°C for 5 minutes before suctioning off supernatant.

-Wash 1x with 1mL cold NT2 WITHOUT protease/phosphatase inhibitors, and spin for 1 minute at 2000g 4°C. Remove buffer entirely with vacuum suction.

13) Elution – boil off

-Add 30μL NT2 without inhibitors plus 6μL 6XSDS loading buffer to beads from each IP.

-Boil 10min

- Spin 10sec at 12000rpm at ROOM TEMP

-Remove liquid sample from the top of beads (around 35-40μL). Proceed directly to western blotting, or freeze overnight.

Plasmids

Wildtype (WT) TRBP, phospho-mutant (SΔA) TRBP, and phosphomimetic (SΔD) TRBP were generous gifts from Dr. Zain Paroo. Flag-Lin28a was a generous gift from Dr. Yinqun Huang. HA-Ubiquitin WT, K63, K48 constructs were generous gifts from Dr. Ted Dawson. The Richard Gregory laboratory kindly provided Lin28bΔNLS mutant. Myc-Lin28a and Myc-TRBP were subcloned using Myc-pcDNA 3.1 .

Reagents

MG132 (Sigma C2211), PR619 (LifeSensors SI9619), U0126 (Cell Signaling 9903S), NEM (Sigma 04260)

Lentivirus and Gene Knockdown using shRNA

TRBP shRNA Infection:

Reduce culture media to ~300µl and infect for *4 days* with:

- 50µl TRBP shRNA virus
- 20µl Non-Target shRNA (NT shRNA) virus
- Add media after *8 hours*
- Change media every 24 hours

Dicer shRNA Infection:

- Reduce culture media to ~300ul
- Infect for *4 days* with:
- 30µl Dicer shRNA virus
- 10µl Non-Target shRNA (NT shRNA) virus
- Add media after *8 hours*
- Change media every 24 hours

Quickchange Mutation Protocol to Generate shRNA-resistant TRBP SΔA Construct

Primer Design:

- Design two complementary primers:

- Contain mutation
- Mutation flanked by ~15 unmodified nucleotides (25 to 45 total nt)
- Minimum %GC > 40%
- Terminate in one or more G/C
- T_m > 78°C **

- Sequence for FSW-TRBPSΔA:

  GGCAATGAGGTGGAGCCCGATGATGACCACTTC

PCR Information:

- Size of Vector ~ 9500bp
- Primer Mix: 196µl + 2µl Forward Primer + 2µl Reverse Primer
- DNA Mix: 10ng DNA = 0.01µg DNA in 0.5µl → [DNA] = 0.02 µg/ul
- [FSW-TRBPΔA] = 0.9927µg/µl
- 0.9927/0.02 = 49.5 → 1:49.5 dilution

PCR Reaction Master Mixes:

-Mg^{2+}

Master Mix: -Mg^{2+} (Typically works better)			
Reagent	**Volume (1 RXN) (µl)**	**Number of Reactions**	**Volume (µl)**
dH_2O	17	5 (4+1)	85
Mg^{2+}	0	5	0
Primer Mix	2.5	5	12.5
dNTPs	2.0	5	10.0
Phusion Buffer	2.5	5	12.5
Phusion Polymerase	0.5	5	2.5
DNA	0.5		
	25		125

+Mg^{2+}

Master Mix: +Mg^{2+}			
Reagent	**Volume (1 RXN) (µl)**	**Number of Reactions**	**Volume (µl)**
dH_2O	14.5	5 (4+1)	72.5
Mg^{2+}	2.5	5	12.5
Primer Mix	2.5	5	12.5
dNTPs	2.0	5	10.0
Phusion Buffer	2.5	5	12.5
Phusion Polymerase	0.5	5	2.5
DNA	0.5		
	25		125

-Phusion Polymerase

Master Mix: -Phusion			
Reagent	**Volume (1 RXN) (µl)**	**Number of Reactions**	**Volume (µl)**
dH_2O	15	5 (4+1)	75
Mg^{2+}	2.5	5	12.5
Primer Mix	2.5	5	12.5
dNTPs	2.0	5	10.0
Phusion Buffer	2.5	5	12.5
Phusion Polymerase	0	5	0
DNA	0.5		
	25		125

PCR Program:

PCR Program			
Step	**Cycles**	**Temp (°C)**	**Time**
1	1	95	5:00
2	15	95	1:00
		69 (T_m = +3)	1:00
		72	10:00 (1min/kb)
3	1	72	10:00
4	Infinity	4	Infinity

Template Digest:

DPN1 Digest			
Reagent	**Volume (1 RXN) (µl)**	**Number of Reactions**	**Volume (µl)**
PCR Product (2x tubes)	40	2 tubes per reaction per condition	
NEB4 (10x)	5	6.5 (6+0.5)	32.5
DPN1	2	6.5	13
dH_2O	3	6.5	19.5
	50		

- Heat Inactivate 20 min @ 80°C
- Transform: 3µl DNA digest
- Plate:
    - 5µl + 75µl LB^+
    - Remaining

** Use:

- For *Primer Design*: $T_m = 81.5 + 0.41(\%GC) - 675/N - \%mismatch$, GC = percent GC, N = primer length (nt)
- For *Oligo melting temperature analysis:*

  http://www.idtdna.com/analyzer/applications/oligoanalyzer/

Chapter IV: Conclusions and Perspectives

BDNF-induced regulation of protein synthesis is crucial for its role in shaping synaptic structure, function, and plasticity. Dysregulation of BDNF signaling is implicated in a variety of neurological and neuropsychiatric disorders highlighting the necessity to better understand the mechanisms of BDNF action. A remarkable aspect of the post-transcriptional regulation of gene expression by BDNF is the high degree of transcript specificity. BDNF modulates protein synthesis in an extraordinarily specific manner with both selective enhancement and reduction in the levels of specific target genes. This tight control of protein synthesis enables BDNF to modulate synaptic function in a pro-growth manner. To unravel the molecular mechanisms that govern BDNF-dependent protein synthesis, my thesis work first addressed the following question: How does BDNF achieve post-transcriptional gene target specificity? We discovered that BDNF regulates miRNA biogenesis to generate translation specificity in hippocampal neurons and that BDNF-mediated post-transcriptional induction of Lin28a is essential for the enhanced translation of a specific set of pro-growth and plasticity-related genes. We also found that Lin28a function is critical for BDNF-mediated dendritic outgrowth. In particular, we showed that Lin28a-mediated downregulation of the Let-7 family of miRNAs was necessary for BDNF-enhanced dendrite growth and for relieving translational repression of BDNF target genes important for pro-growth effects of BDNF. These results heightened our interest in investigating the mechanism underlying BDNF-induced regulation of Lin28a.

The exciting and intriguing results obtained during the first portion of my thesis research emphasized the important role of the Lin28a/Let-7 axis in BDNF signaling,

which was very unexpected in light of the fact that Lin28a was previously thought to be absent from differentiated cells. Our finding that Lin28a could be induced by a neurotrophin in mature neurons (the first differentiated tissue reported to express Lin28a) and that its function was crucial for BDNF-dependent translational control led us to pose the second major question of my thesis work: what are the molecular mechanisms responsible for the rapid and post-transcriptional regulation of Lin28a by BDNF? Answering this question was the goal of the second portion, and chapter 3, of my doctoral work. We revealed that BDNF-induced phosphorylation of TRBP is necessary and sufficient for rapid (significant by 5 minutes) induction of Lin28a protein levels. We found that Lin28a protein can physically associate with TRBP in hippocampal neurons and that this interaction is enhanced when TRBP is phosphorylated in response to BDNF. In the absence of TRBP, BDNF is unable to mediate rapid induction of Lin28a protein levels. We also demonstrated that both Lin28a and TRBP undergo post-translational ubiquitin modifications. Ongoing work is aimed at determining the protein half-life of Lin28a, which we hypothesize will be short under basal conditions, and whether BDNF and TRBP phosphorylation might prolong Lin28a half-life by promoting Lin28a protein stabilty. We are also in the process of determining whether BDNF signaling can modulate the ubiquitination status of Lin28a and/or TRBP as a means of regulating protein turn over.

Another exciting area of our ongoing and future research is investigating the differential regulation of the Lin28 paralogs by BDNF. Mammals have evolved two forms of Lin28, Lin28a and Lin28b, that share ~77% identity at the protein level. Although both paralogs function to block biogenesis of Let-7 miRNAs, they do so

through distinct mechanisms. Lin28a exists primarily in the cytoplasm where it inhibits pre- to mature Let-7 miRNA processing, while Lin28b exists primarily in the nucleus where it inhibits pri- to pre-Let-7 processing. Our data showed that Lin28a, but not Lin28b, is subject to rapid and posttranscriptional regulation by BDNF in hippocampal neurons. Interestingly, TRBP phosphorylation had absolutely no effect on cellular Lin28b levels, whereas Lin28a protein level was dramatically enhanced by the phosphorylation of TRBP. Furthermore, unlike Lin28a, Lin28b does not bind to TRBP. These results demonstrate a critical difference in the regulation of these paralogs, which were at one point thought to be functionally redundant. Our work now emphasizes the unique biological role of these paralogs and suggests that at the protein level they may undergo different post-translational modifications and participate in distinct signaling pathways. Given the critical role that Lin28a and Lin28b play in development and growth as well as their role in tumorigenesis, we expect that elucidating the diverse molecular mechanisms regulating their function will have a broad impact on the fields of neuronal plasticity, as well as stem cell and tumor biology.

BDNF-dependent protein synthesis plays a crucial role in hippocampal-based learning and memory processing. For example, both novel object recognition and spatial learning are impaired in animals with a hippocampal-specific deletion of BDNF (Heldt et al., 2007). An exciting future direction will be to evaluate the effects of Lin28a loss in hippocampal-based learning. To accomplish this goal we have obtained a conditional Lin28a mouse line in which exons encoding the gene for Lin28a are flanked by loxP sites (*Lin28a*$^{fl/fl}$) from the laboratory of George Daley. By crossing the *Lin28a*$^{fl/fl}$ with a R26R/CAMKIIα-CreER^{T2} mouse line we plan to conditionally knockout Lin28a in

forebrain neurons. Investigations using this mouse line will allow the findings in this thesis to be extended and directly assess the importance of Lin28a in cognitive performance. Results from these experiments will be a significant step forward as they will be the first to test the role in adult brain of an evolutionarily conserved axis (Lin28/Let-7) known to control growth and developmental timing during embryogenesis. Multiple behavioral tests are known to be hippocampal-dependent and are impaired in mice that lack BDNF signaling. We expect that loss of Lin28a *in vivo* will impair memory formation and negatively affect the performance of animals on learning and memory tasks.

Dysregulated translation is associated with a range of cognitive disorders including Fragile X Syndrome (FXS), a neurodevelopmental disorder and autism spectrum disease associated with cognitive impairment, behavioral disturbance, and disrupted neuronal network function. Aberrant BDNF signaling has also been linked to autism spectrum disorders. Our discovery that Lin28a plays a crucial role in regulating the rapid effects of BDNF-induced protein synthesis, leads us to suspect that Lin28a might play a role in the pathophysiology of autism spectrum disorders. Future work in our lab will explore the involvement of BDNF and the Lin28/Let-7 axis in the pathogenesis of autism spectrum disorders and other instances of disordered synaptic and neuronal growth in the central nervous system. The coordination of a multitude of growth-related genes by the Lin28/Let-7 axis leads us to suspect that its dysregulation would be very likely to produce cognitive impairment and defects in learning and memory.

Overall my thesis addressed the broader question of how stimulus-dependent gene expression is post-transcriptionally regulated in the central nervous system to allow the coordinated induction of ensembles of pro-growth proteins. Regulation of the neuronal proteome is required for shaping appropriate synaptic function and is critical for neural circuit formation. Our work was the first description of a paradigm for the generation of translational specificity in BDNF-induced neuronal protein synthesis. We also established a novel role for Lin28a in mature neurons by demonstrating that Lin28a confers specificity to BDNF-regulation of translation by functioning as a critical selector molecule that blocks Let-7 miRNAs from being processed and allowing gene targets of Let-7 to undergo enhanced translation. Without Lin28a, BDNF is unable to upregulate the synthesis of growth-promoting targets that are important for neuronal plasticity and cognition. Ongoing work is focused on understanding how BDNF signaling controls Lin28a protein levels and future work will elucidate the role of Lin28a *in vivo*. Another topic of future interest will be to determine whether other activity-dependent stimuli may exert their effects on gene expression through a similar paradigm in which a unique selector molecule coordinates the expression of an entire suite of proteins. Since a single miRNA can regulate the expression of hundreds of transcripts, this makes miRNAs and miRNA regulators, such as RNA binding proteins, attractive candidates for coordinating complex biological responses. The insights provided in this thesis reveal the critical role of miRNA biogenesis regulation in BDNF signaling and pave the way for future studies on miRNA regulation in learning and memory, development, and disease.

References

Aakalu, G., Smith, W.B., Nguyen, N., Jiang, C., and Schuman, E.M. (2001). Dynamic visualization of local protein synthesis in hippocampal neurons. Neuron *30*, 489-502.

Abrahante, J.E., Daul, A.L., Li, M., Volk, M.L., Tennessen, J.M., Miller, E.A., and Rougvie, A.E. (2003). The Caenorhabditis elegans hunchback-like gene lin-57/hbl-1 controls developmental time and is regulated by microRNAs. Developmental cell *4*, 625-637.

Alder, J., Thakker-Varia, S., Crozier, R.A., Shaheen, A., Plummer, M.R., and Black, I.B. (2005). Early presynaptic and late postsynaptic components contribute independently to brain-derived neurotrophic factor-induced synaptic plasticity. J Neurosci *25*, 3080-3085.

Ambros, V., and Horvitz, H.R. (1984). Heterochronic mutants of the nematode Caenorhabditis elegans. Science *226*, 409-416.

Anderson, P., and Kedersha, N. (2006). RNA granules. J Cell Biol *172*, 803-808.

Andl, T., Murchison, E.P., Liu, F., Zhang, Y., Yunta-Gonzalez, M., Tobias, J.W., Andl, C.D., Seykora, J.T., Hannon, G.J., and Millar, S.E. (2006). The miRNA-processing enzyme dicer is essential for the morphogenesis and maintenance of hair follicles. Curr Biol *16*, 1041-1049.

Aoto, J., Nam, C.I., Poon, M.M., Ting, P., and Chen, L. (2008). Synaptic signaling by all-trans retinoic acid in homeostatic synaptic plasticity. Neuron *60*, 308-320.

Ashraf, S.I., McLoon, A.L., Sclarsic, S.M., and Kunes, S. (2006). Synaptic protein synthesis associated with memory is regulated by the RISC pathway in Drosophila. Cell *124*, 191-205.

Banerjee, S., Neveu, P., and Kosik, K.S. (2009). A coordinated local translational control point at the synapse involving relief from silencing and MOV10 degradation. Neuron *64*, 871-884.

Bartel, D.P. (2009). MicroRNAs: target recognition and regulatory functions. Cell *136*, 215-233.

Bassell, G.J., and Warren, S.T. (2008). Fragile X syndrome: loss of local mRNA regulation alters synaptic development and function. Neuron *60*, 201-214.

Bekinschtein, P., Cammarota, M., Igaz, L.M., Bevilaqua, L.R., Izquierdo, I., and Medina, J.H. (2007). Persistence of long-term memory storage requires a late protein synthesis- and BDNF- dependent phase in the hippocampus. Neuron *53*, 261-277.

Bonev, B., Pisco, A., and Papalopulu, N. (2011). MicroRNA-9 reveals regional diversity of neural progenitors along the anterior-posterior axis. Developmental cell *20*, 19-32.

Brengues, M., Teixeira, D., and Parker, R. (2005). Movement of eukaryotic mRNAs between polysomes and cytoplasmic processing bodies. Science *310*, 486-489.

Brown, V., Jin, P., Ceman, S., Darnell, J.C., O'Donnell, W.T., Tenenbaum, S.A., Jin, X., Feng, Y., Wilkinson, K.D., Keene, J.D., *et al.* (2001). Microarray identification of

FMRP-associated brain mRNAs and altered mRNA translational profiles in fragile X syndrome. Cell *107*, 477-487.

Caldeira, M.V., Melo, C.V., Pereira, D.B., Carvalho, R., Correia, S.S., Backos, D.S., Carvalho, A.L., Esteban, J.A., and Duarte, C.B. (2007a). Brain-derived neurotrophic factor regulates the expression and synaptic delivery of alpha-amino-3-hydroxy-5-methyl-4-isoxazole propionic acid receptor subunits in hippocampal neurons. The Journal of biological chemistry *282*, 12619-12628.

Caldeira, M.V., Melo, C.V., Pereira, D.B., Carvalho, R.F., Carvalho, A.L., and Duarte, C.B. (2007b). BDNF regulates the expression and traffic of NMDA receptors in cultured hippocampal neurons. Mol Cell Neurosci *35*, 208-219.

Calin, G.A., Sevignani, C., Dumitru, C.D., Hyslop, T., Noch, E., Yendamuri, S., Shimizu, M., Rattan, S., Bullrich, F., Negrini, M., *et al.* (2004). Human microRNA genes are frequently located at fragile sites and genomic regions involved in cancers. Proc Natl Acad Sci U S A *101*, 2999-3004.

Castren, M., Lampinen, K.E., Miettinen, R., Koponen, E., Sipola, I., Bakker, C.E., Oostra, B.A., and Castren, E. (2002). BDNF regulates the expression of fragile X mental retardation protein mRNA in the hippocampus. Neurobiology of disease *11*, 221-229.

Ceman, S., O'Donnell, W.T., Reed, M., Patton, S., Pohl, J., and Warren, S.T. (2003). Phosphorylation influences the translation state of FMRP-associated polyribosomes. Human molecular genetics *12*, 3295-3305.

Chang, H.M., Triboulet, R., Thornton, J.E., and Gregory, R.I. (2013). A role for the Perlman syndrome exonuclease Dis3l2 in the Lin28-let-7 pathway. Nature *497*, 244-248.

Chendrimada, T.P., Finn, K.J., Ji, X., Baillat, D., Gregory, R.I., Liebhaber, S.A., Pasquinelli, A.E., and Shiekhattar, R. (2007). MicroRNA silencing through RISC recruitment of eIF6. Nature *447*, 823-828.

Doench, J.G., Petersen, C.P., and Sharp, P.A. (2003). siRNAs can function as miRNAs. Genes Dev *17*, 438-442.

Du, L., and Richter, J.D. (2005). Activity-dependent polyadenylation in neurons. RNA *11*, 1340-1347.

Eulalio, A., Behm-Ansmant, I., Schweizer, D., and Izaurralde, E. (2007). P-body formation is a consequence, not the cause, of RNA-mediated gene silencing. Mol Cell Biol *27*, 3970-3981.

Gehrke, S., Imai, Y., Sokol, N., and Lu, B. (2010). Pathogenic LRRK2 negatively regulates microRNA-mediated translational repression. Nature *466*, 637-641.

Grimson, A., Farh, K.K., Johnston, W.K., Garrett-Engele, P., Lim, L.P., and Bartel, D.P. (2007). MicroRNA targeting specificity in mammals: determinants beyond seed pairing. Molecular cell *27*, 91-105.

Grosshans, H., Johnson, T., Reinert, K.L., Gerstein, M., and Slack, F.J. (2005). The temporal patterning microRNA let-7 regulates several transcription factors at the larval to adult transition in C. elegans. Developmental cell *8*, 321-330.

Guo, H., Ingolia, N.T., Weissman, J.S., and Bartel, D.P. (2010). Mammalian microRNAs predominantly act to decrease target mRNA levels. Nature *466*, 835-840.

Hagan, J.P., Piskounova, E., and Gregory, R.I. (2009). Lin28 recruits the TUTase Zcchc11 to inhibit let-7 maturation in mouse embryonic stem cells. Nat Struct Mol Biol *16*, 1021-1025.

He, C., Kraft, P., Chen, C., Buring, J.E., Pare, G., Hankinson, S.E., Chanock, S.J., Ridker, P.M., Hunter, D.J., and Chasman, D.I. (2009). Genome-wide association studies identify loci associated with age at menarche and age at natural menopause. Nature genetics *41*, 724-728.

Heldt, S.A., Stanek, L., Chhatwal, J.P., and Ressler, K.J. (2007). Hippocampus-specific deletion of BDNF in adult mice impairs spatial memory and extinction of aversive memories. Mol Psychiatry *12*, 656-670.

Hendrickson, D.G., Hogan, D.J., McCullough, H.L., Myers, J.W., Herschlag, D., Ferrell, J.E., and Brown, P.O. (2009). Concordant regulation of translation and mRNA abundance for hundreds of targets of a human microRNA. PLoS Biol *7*, e1000238.

Heo, I., Joo, C., Kim, Y.K., Ha, M., Yoon, M.J., Cho, J., Yeom, K.H., Han, J., and Kim, V.N. (2009). TUT4 in concert with Lin28 suppresses microRNA biogenesis through pre-microRNA uridylation. Cell *138*, 696-708.

Huang, E.J., and Reichardt, L.F. (2003). Trk receptors: roles in neuronal signal transduction. Annu Rev Biochem *72*, 609-642.

Huang, Y.S., Carson, J.H., Barbarese, E., and Richter, J.D. (2003). Facilitation of dendritic mRNA transport by CPEB. Genes & development *17*, 638-653.

Huang, Y.S., Jung, M.Y., Sarkissian, M., and Richter, J.D. (2002). N-methyl-D-aspartate receptor signaling results in Aurora kinase-catalyzed CPEB phosphorylation and alpha CaMKII mRNA polyadenylation at synapses. The EMBO journal *21*, 2139-2148.

Huang, Y.W., Ruiz, C.R., Eyler, E.C., Lin, K., and Meffert, M.K. (2012). Dual regulation of miRNA biogenesis generates target specificity in neurotrophin-induced protein synthesis. Cell *148*, 933-946.

Huber, K.M., Kayser, M.S., and Bear, M.F. (2000). Role for rapid dendritic protein synthesis in hippocampal mGluR-dependent long-term depression. Science *288*, 1254-1257.

Jakymiw, A., Lian, S., Eystathioy, T., Li, S., Satoh, M., Hamel, J.C., Fritzler, M.J., and Chan, E.K. (2005). Disruption of GW bodies impairs mammalian RNA interference. Nat Cell Biol *7*, 1267-1274.

Jaworski, J., Spangler, S., Seeburg, D.P., Hoogenraad, C.C., and Sheng, M. (2005). Control of dendritic arborization by the phosphoinositide-3'-kinase-Akt-mammalian target of rapamycin pathway. J Neurosci *25*, 11300-11312.

Johnson, C.D., Esquela-Kerscher, A., Stefani, G., Byrom, M., Kelnar, K., Ovcharenko, D., Wilson, M., Wang, X., Shelton, J., Shingara, J.*, et al.* (2007). The let-7 microRNA represses cell proliferation pathways in human cells. Cancer research *67*, 7713-7722.

Johnson, S.M., Grosshans, H., Shingara, J., Byrom, M., Jarvis, R., Cheng, A., Labourier, E., Reinert, K.L., Brown, D., and Slack, F.J. (2005). RAS is regulated by the let-7 microRNA family. Cell *120*, 635-647.

Jourdi, H., Hsu, Y.T., Zhou, M., Qin, Q., Bi, X., and Baudry, M. (2009). Positive AMPA receptor modulation rapidly stimulates BDNF release and increases dendritic mRNA translation. J Neurosci *29*, 8688-8697.

Juhila, J., Sipila, T., Icay, K., Nicorici, D., Ellonen, P., Kallio, A., Korpelainen, E., Greco, D., and Hovatta, I. (2011). MicroRNA expression profiling reveals miRNA families regulating specific biological pathways in mouse frontal cortex and hippocampus. PloS one *6*, e21495.

Kang, H., and Schuman, E.M. (1996). A requirement for local protein synthesis in neurotrophin-induced hippocampal synaptic plasticity. Science *273*, 1402-1406.

Kanhema, T., Dagestad, G., Panja, D., Tiron, A., Messaoudi, E., Havik, B., Ying, S.W., Nairn, A.C., Sonenberg, N., and Bramham, C.R. (2006). Dual regulation of translation initiation and peptide chain elongation during BDNF-induced LTP in vivo: evidence for compartment-specific translation control. Journal of neurochemistry *99*, 1328-1337.

Keene, J.D., Komisarow, J.M., and Friedersdorf, M.B. (2006). RIP-Chip: the isolation and identification of mRNAs, microRNAs and protein components of ribonucleoprotein complexes from cell extracts. Nat Protoc *1*, 302-307.

Kelleher, R.J., 3rd, Govindarajan, A., Jung, H.Y., Kang, H., and Tonegawa, S. (2004). Translational control by MAPK signaling in long-term synaptic plasticity and memory. Cell *116*, 467-479.

Kertesz, M., Iovino, N., Unnerstall, U., Gaul, U., and Segal, E. (2007). The role of site accessibility in microRNA target recognition. Nature genetics *39*, 1278-1284.

Korte, M., Carroll, P., Wolf, E., Brem, G., Thoenen, H., and Bonhoeffer, T. (1995). Hippocampal long-term potentiation is impaired in mice lacking brain- derived neurotrophic factor. Proc Natl Acad Sci U S A *92*, 8856-8860.

Krol, J., Busskamp, V., Markiewicz, I., Stadler, M.B., Ribi, S., Richter, J., Duebel, J., Bicker, S., Fehling, H.J., Schubeler, D., *et al.* (2010). Characterizing light-regulated retinal microRNAs reveals rapid turnover as a common property of neuronal microRNAs. Cell *141*, 618-631.

Kumar, M.S., Erkeland, S.J., Pester, R.E., Chen, C.Y., Ebert, M.S., Sharp, P.A., and Jacks, T. (2008). Suppression of non-small cell lung tumor development by the let-7 microRNA family. Proc Natl Acad Sci U S A *105*, 3903-3908.

Lee, R.C., Feinbaum, R.L., and Ambros, V. (1993). The C. elegans heterochronic gene lin-4 encodes small RNAs with antisense complementarity to lin-14. Cell *75*, 843-854.

Lettre, G., Jackson, A.U., Gieger, C., Schumacher, F.R., Berndt, S.I., Sanna, S., Eyheramendy, S., Voight, B.F., Butler, J.L., Guiducci, C., *et al.* (2008). Identification of ten loci associated with height highlights new biological pathways in human growth. Nature genetics *40*, 584-591.

Levine, E.S., Crozier, R.A., Black, I.B., and Plummer, M.R. (1998). Brain-derived neurotrophic factor modulates hippocampal synaptic transmission by increasing N-methyl-D-aspartic acid receptor activity. Proc Natl Acad Sci U S A *95*, 10235-10239.

Levine, E.S., and Kolb, J.E. (2000). Brain-derived neurotrophic factor increases activity of NR2B-containing N-methyl-D-aspartate receptors in excised patches from hippocampal neurons. Journal of neuroscience research *62*, 357-362.

Liao, L., Pilotte, J., Xu, T., Wong, C.C., Edelman, G.M., Vanderklish, P., and Yates, J.R., 3rd (2007). BDNF induces widespread changes in synaptic protein content and up-regulates components of the translation machinery: an analysis using high-throughput proteomics. J Proteome Res *6*, 1059-1071.

Lin, S.Y., Johnson, S.M., Abraham, M., Vella, M.C., Pasquinelli, A., Gamberi, C., Gottlieb, E., and Slack, F.J. (2003). The C elegans hunchback homolog, hbl-1, controls temporal patterning and is a probable microRNA target. Developmental cell *4*, 639-650.

Lin, S.Y., Wu, K., Levine, E.S., Mount, H.T., Suen, P.C., and Black, I.B. (1998). BDNF acutely increases tyrosine phosphorylation of the NMDA receptor subunit 2B in cortical and hippocampal postsynaptic densities. Brain research Molecular brain research *55*, 20-27.

Liu, J., Rivas, F.V., Wohlschlegel, J., Yates, J.R., 3rd, Parker, R., and Hannon, G.J. (2005a). A role for the P-body component GW182 in microRNA function. Nat Cell Biol *7*, 1261-1266.

Liu, J., Valencia-Sanchez, M.A., Hannon, G.J., and Parker, R. (2005b). MicroRNA-dependent localization of targeted mRNAs to mammalian P-bodies. Nat Cell Biol *7*, 719-723.

Lois, C., Hong, E.J., Pease, S., Brown, E.J., and Baltimore, D. (2002). Germline transmission and tissue-specific expression of transgenes delivered by lentiviral vectors. Science *295*, 868-872.

Lugli, G., Torvik, V.I., Larson, J., and Smalheiser, N.R. (2008). Expression of microRNAs and their precursors in synaptic fractions of adult mouse forebrain. J Neurochem *106*, 650-661.

Mathonnet, G., Fabian, M.R., Svitkin, Y.V., Parsyan, A., Huck, L., Murata, T., Biffo, S., Merrick, W.C., Darzynkiewicz, E., Pillai, R.S., *et al.* (2007). MicroRNA inhibition of translation initiation in vitro by targeting the cap-binding complex eIF4F. Science *317*, 1764-1767.

Meffert, M.K., Chang, J.M., Wiltgen, B.J., Fanselow, M.S., and Baltimore, D. (2003). NF-kappa B functions in synaptic signaling and behavior. Nat Neurosci *6*, 1072-1078.

Melo, S.A., Ropero, S., Moutinho, C., Aaltonen, L.A., Yamamoto, H., Calin, G.A., Rossi, S., Fernandez, A.F., Carneiro, F., Oliveira, C., *et al.* (2009). A TARBP2 mutation in human cancer impairs microRNA processing and DICER1 function. Nat Genet *41*, 365-370.

Meng, Y., Zhang, Y., Tregoubov, V., Janus, C., Cruz, L., Jackson, M., Lu, W.Y., MacDonald, J.F., Wang, J.Y., Falls, D.L., *et al.* (2002). Abnormal spine morphology and enhanced LTP in LIMK-1 knockout mice. Neuron *35*, 121-133.

Miyashiro, K.Y., Beckel-Mitchener, A., Purk, T.P., Becker, K.G., Barret, T., Liu, L., Carbonetto, S., Weiler, I.J., Greenough, W.T., and Eberwine, J. (2003). RNA cargoes associating with FMRP reveal deficits in cellular functioning in Fmr1 null mice. Neuron *37*, 417-431.

Moser, J.J., Chan, E.K., and Fritzler, M.J. (2009). Optimization of immunoprecipitation-western blot analysis in detecting GW182-associated components of GW/P bodies. Nat Protoc *4*, 674-685.

Moss, E.G., Lee, R.C., and Ambros, V. (1997). The cold shock domain protein LIN-28 controls developmental timing in C. elegans and is regulated by the lin-4 RNA. Cell *88*, 637-646.

Moss, E.G., and Tang, L. (2003). Conservation of the heterochronic regulator Lin-28, its developmental expression and microRNA complementary sites. Dev Biol *258*, 432-442.

Napoli, I., Mercaldo, V., Boyl, P.P., Eleuteri, B., Zalfa, F., De Rubeis, S., Di Marino, D., Mohr, E., Massimi, M., Falconi, M., *et al.* (2008). The fragile X syndrome protein represses activity-dependent translation through CYFIP1, a new 4E-BP. Cell *134*, 1042-1054.

Narayanan, U., Nalavadi, V., Nakamoto, M., Pallas, D.C., Ceman, S., Bassell, G.J., and Warren, S.T. (2007). FMRP phosphorylation reveals an immediate-early signaling pathway triggered by group I mGluR and mediated by PP2A. J Neurosci *27*, 14349-14357.

Narisawa-Saito, M., Carnahan, J., Araki, K., Yamaguchi, T., and Nawa, H. (1999). Brain-derived neurotrophic factor regulates the expression of AMPA receptor proteins in neocortical neurons. Neuroscience *88*, 1009-1014.

Newman, M.A., Thomson, J.M., and Hammond, S.M. (2008). Lin-28 interaction with the Let-7 precursor loop mediates regulated microRNA processing. Rna *14*, 1539-1549.

Nielsen, C.B., Shomron, N., Sandberg, R., Hornstein, E., Kitzman, J., and Burge, C.B. (2007). Determinants of targeting by endogenous and exogenous microRNAs and siRNAs. RNA *13*, 1894-1910.

Ong, K.K., Elks, C.E., Li, S., Zhao, J.H., Luan, J., Andersen, L.B., Bingham, S.A., Brage, S., Smith, G.D., Ekelund, U., *et al.* (2009). Genetic variation in LIN28B is associated with the timing of puberty. Nature genetics *41*, 729-733.

Pang, P.T., and Lu, B. (2004). Regulation of late-phase LTP and long-term memory in normal and aging hippocampus: role of secreted proteins tPA and BDNF. Ageing Res Rev *3*, 407-430.

Paroo, Z., Ye, X., Chen, S., and Liu, Q. (2009). Phosphorylation of the human microRNA-generating complex mediates MAPK/Erk signaling. Cell *139*, 112-122.

Patterson, S.L., Abel, T., Deuel, T.A., Martin, K.C., Rose, J.C., and Kandel, E.R. (1996). Recombinant BDNF rescues deficits in basal synaptic transmission and hippocampal LTP in BDNF knockout mice. Neuron *16*, 1137-1145.

Perry, J.R., Stolk, L., Franceschini, N., Lunetta, K.L., Zhai, G., McArdle, P.F., Smith, A.V., Aspelund, T., Bandinelli, S., Boerwinkle, E., *et al.* (2009). Meta-analysis of genome-wide association data identifies two loci influencing age at menarche. Nature genetics *41*, 648-650.

Petersen, C.P., Bordeleau, M.E., Pelletier, J., and Sharp, P.A. (2006). Short RNAs repress translation after initiation in mammalian cells. Mol Cell *21*, 533-542.

Piskounova, E., Polytarchou, C., Thornton, J.E., LaPierre, R.J., Pothoulakis, C., Hagan, J.P., Iliopoulos, D., and Gregory, R.I. (2011). Lin28A and Lin28B inhibit let-7 microRNA biogenesis by distinct mechanisms. Cell *147*, 1066-1079.

Poo, M.M. (2001). Neurotrophins as synaptic modulators. Nat Rev Neurosci *2*, 24-32.

Raab-Graham, K.F., Haddick, P.C., Jan, Y.N., and Jan, L.Y. (2006). Activity- and mTOR-dependent suppression of Kv1.1 channel mRNA translation in dendrites. Science *314*, 144-148.

Ramachandran, R., Fausett, B.V., and Goldman, D. (2010). Ascl1a regulates Muller glia dedifferentiation and retinal regeneration through a Lin-28-dependent, let-7 microRNA signalling pathway. Nature cell biology *12*, 1101-1107.

Rivera, C., Li, H., Thomas-Crusells, J., Lahtinen, H., Viitanen, T., Nanobashvili, A., Kokaia, Z., Airaksinen, M.S., Voipio, J., Kaila, K., *et al.* (2002). BDNF-induced TrkB activation down-regulates the K+-Cl- cotransporter KCC2 and impairs neuronal Cl- extrusion. The Journal of cell biology *159*, 747-752.

Sampson, V.B., Rong, N.H., Han, J., Yang, Q., Aris, V., Soteropoulos, P., Petrelli, N.J., Dunn, S.P., and Krueger, L.J. (2007). MicroRNA let-7a down-regulates MYC and reverts MYC-induced growth in Burkitt lymphoma cells. Cancer research *67*, 9762-9770.

Sarmiere, P.D., and Bamburg, J.R. (2002). Head, neck, and spines: a role for LIMK-1 in the hippocampus. Neuron *35*, 3-5.

Schratt, G.M., Nigh, E.A., Chen, W.G., Hu, L., and Greenberg, M.E. (2004). BDNF regulates the translation of a select group of mRNAs by a mammalian target of rapamycin-phosphatidylinositol 3-kinase-dependent pathway during neuronal development. J Neurosci *24*, 7366-7377.

Schratt, G.M., Tuebing, F., Nigh, E.A., Kane, C.G., Sabatini, M.E., Kiebler, M., and Greenberg, M.E. (2006). A brain-specific microRNA regulates dendritic spine development. Nature *439*, 283-289.

Sempere, L.F., Freemantle, S., Pitha-Rowe, I., Moss, E., Dmitrovsky, E., and Ambros, V. (2004). Expression profiling of mammalian microRNAs uncovers a subset of brain-expressed microRNAs with possible roles in murine and human neuronal differentiation. Genome Biol *5*, R13.

Sethi, P., and Lukiw, W.J. (2009). Micro-RNA abundance and stability in human brain: specific alterations in Alzheimer's disease temporal lobe neocortex. Neurosci Lett *459*, 100-104.

Shan, G., Li, Y., Zhang, J., Li, W., Szulwach, K.E., Duan, R., Faghihi, M.A., Khalil, A.M., Lu, L., Paroo, Z., *et al.* (2008). A small molecule enhances RNA interference and promotes microRNA processing. Nat Biotechnol *26*, 933-940.

Shell, S., Park, S.M., Radjabi, A.R., Schickel, R., Kistner, E.O., Jewell, D.A., Feig, C., Lengyel, E., and Peter, M.E. (2007). Let-7 expression defines two differentiation stages of cancer. Proc Natl Acad Sci U S A *104*, 11400-11405.

Shinohara, Y., Yahagi, K., Kawano, M., Nishiyori, H., Kawazu, C., Suzuki, N., Manabe, R., and Hirase, H. (2011). miRNA profiling of bilateral rat hippocampal CA3 by deep sequencing. Biochemical and biophysical research communications *409*, 293-298.

Sulem, P., Gudbjartsson, D.F., Rafnar, T., Holm, H., Olafsdottir, E.J., Olafsdottir, G.H., Jonsson, T., Alexandersen, P., Feenstra, B., Boyd, H.A., *et al.* (2009). Genome-wide association study identifies sequence variants on 6q21 associated with age at menarche. Nature genetics *41*, 734-738.

Takamizawa, J., Konishi, H., Yanagisawa, K., Tomida, S., Osada, H., Endoh, H., Harano, T., Yatabe, Y., Nagino, M., Nimura, Y., *et al.* (2004). Reduced expression of the let-7 microRNAs in human lung cancers in association with shortened postoperative survival. Cancer research *64*, 3753-3756.

Takei, N., Inamura, N., Kawamura, M., Namba, H., Hara, K., Yonezawa, K., and Nawa, H. (2004). Brain-derived neurotrophic factor induces mammalian target of rapamycin-dependent local activation of translation machinery and protein synthesis in neuronal dendrites. J Neurosci *24*, 9760-9769.

Takei, N., Kawamura, M., Ishizuka, Y., Kakiya, N., Inamura, N., Namba, H., and Nawa, H. (2009). Brain-derived neurotrophic factor enhances the basal rate of protein synthesis by increasing active eukaryotic elongation factor 2 levels and promoting translation elongation in cortical neurons. J Biol Chem *284*, 26340-26348.

Tanaka, J., Horiike, Y., Matsuzaki, M., Miyazaki, T., Ellis-Davies, G.C., and Kasai, H. (2008). Protein synthesis and neurotrophin-dependent structural plasticity of single dendritic spines. Science *319*, 1683-1687.

Teixeira, D., Sheth, U., Valencia-Sanchez, M.A., Brengues, M., and Parker, R. (2005). Processing bodies require RNA for assembly and contain nontranslating mRNAs. Rna *11*, 371-382.

Thomson, J.M., Parker, J., Perou, C.M., and Hammond, S.M. (2004). A custom microarray platform for analysis of microRNA gene expression. Nature methods *1*, 47-53.

Tyler, W.J., Alonso, M., Bramham, C.R., and Pozzo-Miller, L.D. (2002). From acquisition to consolidation: on the role of brain-derived neurotrophic factor signaling in hippocampal-dependent learning. Learn Mem *9*, 224-237.

Vanderklish, P.W., and Edelman, G.M. (2005). Differential translation and fragile X syndrome. Genes, brain, and behavior *4*, 360-384.

Viswanathan, S.R., Daley, G.Q., and Gregory, R.I. (2008). Selective blockade of microRNA processing by Lin28. Science *320*, 97-100.

Viswanathan, S.R., Powers, J.T., Einhorn, W., Hoshida, Y., Ng, T.L., Toffanin, S., O'Sullivan, M., Lu, J., Phillips, L.A., Lockhart, V.L., *et al.* (2009). Lin28 promotes transformation and is associated with advanced human malignancies. Nat Genet *41*, 843-848.

Wang, B., Love, T.M., Call, M.E., Doench, J.G., and Novina, C.D. (2006). Recapitulation of short RNA-directed translational gene silencing in vitro. Mol Cell *22*, 553-560.

Wang, D.O., Kim, S.M., Zhao, Y., Hwang, H., Miura, S.K., Sossin, W.S., and Martin, K.C. (2009). Synapse- and stimulus-specific local translation during long-term neuronal plasticity. Science *324*, 1536-1540.

Wang, W., Zhu, J.Z., Chang, K.T., and Min, K.T. (2012). DSCR1 interacts with FMRP and is required for spine morphogenesis and local protein synthesis. The EMBO journal *31*, 3655-3666.

Wardle, R.A., and Poo, M.M. (2003). Brain-derived neurotrophic factor modulation of GABAergic synapses by postsynaptic regulation of chloride transport. J Neurosci *23*, 8722-8732.

Wu, L., Wells, D., Tay, J., Mendis, D., Abbott, M.A., Barnitt, A., Quinlan, E., Heynen, A., Fallon, J.R., and Richter, J.D. (1998). CPEB-mediated cytoplasmic polyadenylation and the regulation of experience-dependent translation of alpha-CaMKII mRNA at synapses. Neuron *21*, 1129-1139.

Wulczyn, F.G., Smirnova, L., Rybak, A., Brandt, C., Kwidzinski, E., Ninnemann, O., Strehle, M., Seiler, A., Schumacher, S., and Nitsch, R. (2007). Post-transcriptional regulation of the let-7 microRNA during neural cell specification. FASEB journal : official publication of the Federation of American Societies for Experimental Biology *21*, 415-426.

Yin, Y., Edelman, G.M., and Vanderklish, P.W. (2002). The brain-derived neurotrophic factor enhances synthesis of Arc in synaptoneurosomes. Proc Natl Acad Sci U S A *99*, 2368-2373.

Ying, S.W., Futter, M., Rosenblum, K., Webber, M.J., Hunt, S.P., Bliss, T.V., and Bramham, C.R. (2002). Brain-derived neurotrophic factor induces long-term potentiation in intact adult hippocampus: requirement for ERK activation coupled to CREB and upregulation of Arc synthesis. J Neurosci *22*, 1532-1540.

Yu, F., Yao, H., Zhu, P., Zhang, X., Pan, Q., Gong, C., Huang, Y., Hu, X., Su, F., Lieberman, J., *et al.* (2007a). let-7 regulates self renewal and tumorigenicity of breast cancer cells. Cell *131*, 1109-1123.

Yu, J., Vodyanik, M.A., Smuga-Otto, K., Antosiewicz-Bourget, J., Frane, J.L., Tian, S., Nie, J., Jonsdottir, G.A., Ruotti, V., Stewart, R., *et al.* (2007b). Induced pluripotent stem cell lines derived from human somatic cells. Science *318*, 1917-1920.

Yu, J.Y., Chung, K.H., Deo, M., Thompson, R.C., and Turner, D.L. (2008). MicroRNA miR-124 regulates neurite outgrowth during neuronal differentiation. Experimental cell research *314*, 2618-2633.

Zalfa, F., Achsel, T., and Bagni, C. (2006). mRNPs, polysomes or granules: FMRP in neuronal protein synthesis. Current opinion in neurobiology *16*, 265-269.

Zhu, H., Shah, S., Shyh-Chang, N., Shinoda, G., Einhorn, W.S., Viswanathan, S.R., Takeuchi, A., Grasemann, C., Rinn, J.L., Lopez, M.F., *et al.* (2010). Lin28a transgenic mice manifest size and puberty phenotypes identified in human genetic association studies. Nature genetics *42*, 626-630.

Zhu, H., Shyh-Chang, N., Segre, A.V., Shinoda, G., Shah, S.P., Einhorn, W.S., Takeuchi, A., Engreitz, J.M., Hagan, J.P., Kharas, M.G., *et al.* (2011). The Lin28/let-7 axis regulates glucose metabolism. Cell *147*, 81-94.

CURRICULUM VITAE

The Johns Hopkins University School of Medicine

Claudia Roxana Ruiz — March 2014

Educational History

Ph.D. expected 2014	Neuroscience Program	Johns Hopkins School of Medicine
	Mentor: Mollie Meffert M.D. Ph.D	
B.S. 2007	Neuroscience and Behavioral Biology	Emory University

Other Professional Experience

2009	Research Rotation	Laboratory of Alfredo Quinones-Hinojosa M.D. Johns Hopkins School of Medicine
2008	Research Rotation	Laboratory of Ted Dawson M.D. Ph.D. Johns Hopkins School of Medicine
2008	Research Rotation	Laboratory of Seth Blackshaw Ph.D. Johns Hopkins School of Medicine
2008	Research Assistant	Laboratory of David Morgan Ph.D. Alzheimer's Research Laboratory University of South Florida
2007	Research Assistant	Laboratory of Steven Shivers Ph.D. Molecular Staging Laboratory Lakeland Regional Cancer Center
2005-2006	Research Assistant	Laboratory of Philippe Rochat Ph.D. Child Studies Center Emory University

Scholarships and Fellowships

2012-present Ruth L. Kirschstein National Research Service Grant Award (F31) NIMH

2012 Carl Storm Underrepresented Minority Fellowship Award, Gordon Conference

Academic Honors

2013 Richard Goodman Scholars Award, Johns Hopkins Department of Neuroscience
Awarded by the Neuroscience Steering Committee to one student, selected from fourth year and above, who 'has made an outstanding discovery and exemplifies the characteristics that we hope to instill in our students'

2012 Biomedical Scholars Association (BSA) Milestone Achievement Award, Johns Hopkins

2006 Dean's List, Emory University

2004 National Order of Omega, Greek Leadership Honor Society, Emory University

2004 Nu Rho Psi, The National Honor Society in Neuroscience, Emory University

Publications, Peer Reviewed

Ruiz CR, Shi J, & Meffert MK. Transcript specificity in BDNF-induced regulated protein synthesis. *Neuropharmacology* (Invited Review. Special Issue: BDNF regulation of synaptic structure, function, and plasticity), 76; 657-63. January 2014. PMID 23707639

Lee DC, **Ruiz CR,** Lebson, L, Selenica ML, Rizer J, Hunt JB Jr, Rojiani R, Reid P, Kammath S, Nash K, Dickey CA, Gordon M, Morgan D. Aging enhances classical activation but mitigates alternative activation in the central nervous system. *Neurobiology of Aging* 34, 1610-1620, June 2013. PMID 23481567

Huang Y-W A*, **Ruiz CR***, Eyler ECH*, Lin K, & Meffert MK. Dual regulation of miRNA biogenesis generates target specificity in neurotrophin-induced protein synthesis. *Cell 148,* 933-946, March 2, 2012. PMID 22385959

Publications, In-preparation

Ruiz CR*, Amen AM*, Shi J, & Meffert MK. TRBP mediates differential induction of Lin28 paralogs by neurotrophin signaling. *Manuscript in-preparation*.

Posters and Abstracts

Ruiz CR, Huang Y-W A, Eyler ECH, Shi J, & Meffert MK. Dual regulation of miRNA biogenesis generates target specificity in neurotrophin-induced protein synthesis. Presented June 2012 at the Cell Biology of the Neuron Gordon Conference, Waterville Valley, New Hampshire (Poster)

Huang Y-W A, **Ruiz CR**, Eyler ECH, Lin K, Meffert MK. Regulated microRNA biogenesis and P-body mRNA localization determine specificity of BDNF-induced protein synthesis. Presented November 2011 at the Society for Neuroscience Meeting, Washington D.C. (Poster)

Guerrero-Cazares, H., Niranjan, A., **Ruiz, CR.**, Atri, D., Achanta, P., Garzon-Muvdi, T., Mohyeldin, A., Quinones-Hinojosa, A . Migration of human brain tumor stem cells in response to slit proteins. Presented September 2009 at the World Stem Cell Summit, Baltimore, Maryland (Poster)

Lee, D.C., **Ruiz CR,** Lebson, L., Morgan, D., Gordon, M. Age-induced changes in classical and alternatively activated gene expression profiles following polarization of microglia in mouse CNS. Presented November 2008 at the Society for Neuroscience Meeting, Washington D.C. (Poster)

Patents

New Invention Disclosure; Patent-Pending, Filed February 21, 2012. 'Viral expression construct for Lin28-resistant Let-7 Precursor MicroRNA'

Professional Membership

2008-present Society for Neuroscience Member
2008-present American Association for the Advancement of Science

Teaching and Mentoring Experience

2013	Guided the rotation project of a Biological Chemistry Graduate Student
2012	Teaching assistant, Neurobiology Course
2012	Guided the rotation project of a Biochemistry, Cellular, & Molecular Biology (BCMB) Graduate Student
2011	Guided the rotation project of a Neuroscience Graduate Student
2011	Guided the rotation project of a BCMB Graduate Student
2010	Guided the rotation project of a Neuroscience Graduate Student
2010-2014	Guided the research project of an Undergraduate Student (Currently a Neuroscience Masters student)

Service and Leadership

2011-2013	Graduate Student Association (GSA) Neuroscience Representative
2011-2013	Neuroscience Graduate Admissions Committee Member
2010	Neuroscience Department Green Team, Co-Chair
2009-2011	Departmental Retreat Planning Committee, Co-Chair
2008-2013	Leadership Initiative for the Environment (LIFE), Co-Chair

Talks and Seminars

2012	Center for Cell Dynamics Seminar Live Cell Imaging Workshop
2010	Center for Cell Dynamics Seminar Research Talk
2009	Departmental Neuroscience Journal Club Research Talk
2009	Department of Biological Chemistry Evening Research Discussion